1989-12

CW projectile tracking range analysis

Feng, Yen-Chun

Monterey, California. Naval Postgraduate School

NAVAL POSTGRADUATE SCHOOL
Monterey, California

THESIS

CW PROJECTILE TRACKING
RANGE ANALYSIS

by

Yen-Chun Feng

Dec 1989

Thesis Advisor Hung-Mou Lee

classified

rity classification of this page

REPORT DOCUMENTATION PAGE

Report Security Classification Unclassified		1b Restrictive Markings	
Security Classification Authority		3 Distribution Availability of Report	
Declassification Downgrading Schedule		Approved for public release; distribution is unlimited.	
erforming Organization Report Number(s)		5 Monitoring Organization Report Number(s)	
Name of Performing Organization aval Postgraduate School	6b Office Symbol *(if applicable)* 33	7a Name of Monitoring Organization Naval Postgraduate School	
Address *(city, state, and ZIP code)* onterey, CA 93943-5000		7b Address *(city, state, and ZIP code)* Monterey, CA 93943-5000	
Name of Funding Sponsoring Organization	8b Office Symbol *(if applicable)*	9 Procurement Instrument Identification Number	
Address *(city, state, and ZIP code)*		10 Source of Funding Numbers	
		Program Element No	Project No / Task No / Work Unit Accession No

Title *(include security classification)* CW PROJECTILE TRACKING RANGE ANALYSIS

Personal Author(s) Yen-Chun Feng

Type of Report	13b Time Covered	14 Date of Report *(year, month, day)*	15 Page Count
aster's Thesis	From To	Dec 1989	93

Supplementary Notation The views expressed in this thesis are those of the author and do not reflect the official policy or po-on of the Department of Defense or the U.S. Government.

Cosati Codes			18 Subject Terms *(continue on reverse if necessary and identify by block number)*
d	Group	Subgroup	Maximum Tracking Range, Power Requirement

Abstract *(continue on reverse if necessary and identify by block number)*

The conventional low-power CW doppler projectile tracking radar is investigated through simulation. The power re-irement for full range tracking with real-time track data processing stopped within 160 m of the point of impact is obtained. is power can be lowered by a factor of more than 4 if a set of three switchable filters is utilized.

Distribution Availability of Abstract unclassified unlimited ☐ same as report ☐ DTIC users	21 Abstract Security Classification Unclassified	
Name of Responsible Individual ng-Mou Lee	22b Telephone *(include Area code)* (408) 646-2846	22c Office Symbol 62LI

FORM 1473,84 MAR 83 APR edition may be used until exhausted
All other editions are obsolete

security classification of this page

Unclassified

Approved for public release; distribution is unlimited.

CW PROJECTILE TRACKING RANGE ANALYSIS

by

Yen-Chun Feng
Lieutenant Colonel, Taiwan Army
B.S., Chung-Cheng Institute of Technology, 1974

Submitted in partial fulfillment of the
requirements for the degree of

MASTER OF SCIENCE IN ENGINEERING SCIENCE

from the

NAVAL POSTGRADUATE SCHOOL
Dec 1989

ABSTRACT

The conventional low-power CW doppler projectile tracking radar is investigated through simulation. The power requirement for full range tracking with real-time track data processing stopped within 160 m of the point of impact is obtained. This power can be lowered by a factor of more than 4 if a set of three switchable filters is utilized.

TABLE OF CONTENTS

I. INTRODUCTION 1

II. PROPOSED CW RADAR DESIGN 4
A. RADAR SYSTEM SCHEMATICS 4
B. THEORY 5

III. PROJECTILE TRAJECTORY PREDICTION 9
A. THE TRAJECTORY IN A FIXED INERTIAL FRAME 10
B. GROUND-OBSERVED TRAJECTORY 13
1. Trajectory Relative to Radar 13
a. Velocity Transformation 14
b. Projectile Location Relative to the Radar 15
c. Radar Coordinate 16
2. Trajectory Relative to Gun 16

IV. RANGE ANALYSIS AND POWER REQUIREMENT 17
A. RANGE EQUATION 17
1. The Receiver Noise Figure 17
2. System Loss Factor 17
a. Transmission Loss 17
b. Miscellaneous Loss 18
3. Signal-to-Noise Ratio 18
4. Transmitting and Receiving Antenna Gain 22
5. Video Bandwidth and Filters 22
a. First Filter 23
b. Second Filter 24
c. Third Filter 24
B. TRAJECTORY SIMULATION AND RESULTS 25
1. Input and Parameters. 25
a. Earth 25
b. Radar 25

c. Gun 25
d. Projectile 25
e. Environment 25
f. Drag Coefficient 26
2. Results of Simulation 26
a. Radar Observed Trajectory 27
b. Gun Based Trajectory 27
c. Radar Tracking Parameters 30
d. Doppler Frequency and Velocity 33
C. PROJECTILE RADAR CROSS-SECTION 35
1. Case 1 37
2. Case 2 38
D. PROPAGATION EFFECTS 42
1. Computation 43
2. Summary of Results 43
a. Signal Strength Enhancement 43
b. Strong Interference 43
3. Stop-Processing Point 46
E. POWER REQUIREMENT 48

V. CONCLUSIONS 53

APPENDIX A. PROJECTILE TRAJECTORY SIMULATION AND RANGE ANALYSIS 54

APPENDIX B. CROSS-SECTION ANALYSIS 68
A. CASE 1 69
B. CASE 2 69

APPENDIX C. PROPAGATION FACTORS 73

APPENDIX D. MISSED DETECTION AND FALSE ALARM 75

LIST OF REFERENCES 80

INITIAL DISTRIBUTION LIST 82

LIST OF TABLES

Table 1. STOP PROCESSING POINT. 47
Table 2. MULTIPLE FILTERS SWITCH POINTS 52

LIST OF FIGURES

Figure 1. Schematics for Proposed CW Radar Design. 4
Figure 2. Spectra of Received Signals. 6
Figure 3. Measurement Base and Velocity vs. Time. 7
Figure 4. Inertial Coordinate Systems. 13
Figure 5. Missed Detection and Noise Error vs. Threshold-to-Signal Power 10 dB. . 19
Figure 6. Missed Detection and Noise Error vs. Threshold to Signal Power 10.5 dB 20
Figure 7. Missed Detection and Noise Error vs. Threshold to Signal Power 11 dB. 20
Figure 8. Missed Detection and Noise Error vs. Threshold-to-Signal Power 11.5 dB 21
Figure 9. Missed Detection and Noise Error vs. Threshold-to-Signal Power 12 dB. 21
Figure 10. Doppler Frequency vs. Slant Range. 23
Figure 11. Drag Coefficient vs. Mach Number for 155 mm Projectile. 27
Figure 12. Projectile Trajectory: Height vs. Slant Range. 28
Figure 13. Projectile Trajectory: Height vs. Time. 28
Figure 14. Projectile Trajectory: Height vs. Ground Range. 29
Figure 15. Projectile Trajectory: Cross Range vs. Ground Range. 30
Figure 16. Radar Azimuthal Tracking Angle vs. Time. 31
Figure 17. Radar Elevation Angle vs. Time. 31
Figure 18. Radar Azimuthal Tracking Angular Speed vs. Time. 32
Figure 19. Radar Elevation Tracking Angular Speed vs. Time. 32
Figure 20. Servo System Response Time vs. Time. 33
Figure 21. Doppler Frequency vs. Time. 34
Figure 22. Doppler Velocity vs. Time. 34
Figure 23. Radar Cross-Section of the Sphere vs. $\frac{2\pi a}{\lambda}$. 36
Figure 24. Approximate Shape of 155mm Projectile. 37
Figure 25. Radar Cross Section Case 1. 38
Figure 26. Radar Cross Section Case 2. 39
Figure 27. The In-Flight Projectile Radar Cross Section vs. Aspect Angle. 40
Figure 28. In-Flight Projectile Radar Cross Section vs. Slant Range. 41
Figure 29. Reflection and Interference from a Spherical Earth. 42
Figure 30. Waveguide Mode with Ducting Height and Antenna Height. 44
Figure 31. Propagation Factor with 13.1m Duct Height. 45

Figure 32. Propagation Factors vs Ground Range from Impact Point. 45
Figure 33. Narrow Beamwidth Effect on the Spherical Earth Surface. 46
Figure 34. Power Requirement for Full Range Tracking without Multiple Filters. . 48
Figure 35. Doppler Frequency vs. Slant Range. 49
Figure 36. Radar Cross Section vs. Slant Range. 50
Figure 37. Log(Normalized f_d) vs. Log(Normalized R^4/σ). 51
Figure 38. Power Requirement for Trajectory Tracking with Multiple Filters. . . . 52

I. INTRODUCTION

At a proving ground, it is always desirable to record the trajectories of test-fired munitions for later analysis. This is especially true when anomalies occur. Continuous wave (CW) radars have often been adopted for this purpose because of their simplicity. Compared to a pulsed radar of similar range performance, a CW radar has no modulator in its transmitter, hence no range gating is necessary in its receiver. Furthermore, a CW radar has a bandwidth corresponding to the doppler shift, which rarely exceeds 100 kilo-Hertz (kHz) while a pulsed radar has a band width in the mega-Hertz range. Thus a CW radar can be designed to carry out coherent signal integration over a longer time interval. This increases the integration gain and lowers the required transmitter power for the CW radar.

High gain antennas of very narrow beamwidths are also used to reduce the transmitter power requirement. It is important to aim such antennas accurately on the target. To acquire the bearing and elevation angles of a target directly, several receiving feeds together with complicated comparator and multiple data channels are needed. Since the trajectory of a test round can be roughly predicted, an alternative to the actual acquisition of target tracking angles is by steering the antenna according to the predicted trajectory. The directly measurable data will be the doppler shift of the target as a function of flight time. Discrepancies between this data and the doppler shift based on the predicted trajectory should be carefully analyzed and explained. When an anomaly occurs which causes the target to break off track, this recorded data will be valuable for diagnosing the problem.

Many CW radar tracking systems are available. For example, a model DR 582 X-band Instrumentation Radar manufactured by TERMA Elektronik AS of Denmark is being installed at the Ta-Fu Proving Ground in Taiwan. These systems typically track a long-range projectile only up to the summit of the trajectory. Since the point of impact of a long-range projectile is of great interest, it is desirable to extend the range of the radar to cover as large a portion of the trajectory as possible while keeping the system relatively simple. The purposes of this thesis are to investigate the maximum range attainable using a simple CW radar and to determine the required minimum transmitter power.

When tracking a projectile, a CW radar detects only the doppler frequency shift due to the projectile motion. This frequency shift is proportional to the component of the projectile velocity pointing radially away from the radar. By combining this information with the tracking angles, the ground range of the projectile can be deduced through integrating this velocity component. A low-pass filter can be employed to perform this signal integration in real time. The output can be used to update the predicted track if a data filtering mechanism such as the Kalman filter is utilized in real time. Since information on the doppler integrating filter is not provided by any manufacturer, one way to implement this low pass filter is suggested in Chapter 2. The design described therein is consistent with the operational instruction for the aforementioned system. It is needed for tracking simulation required in Chapter IV. The trajectory-updating Kalman filter is a desirable improvement to currently available systems on the market. Its design is outside the scope of this thesis.

As explained above, trajectory estimation is necessary for tracking with a simple CW radar. Since the radar and the gun are moving with the spinning Earth, the familiar reference frame in which the radar and the gun are stationary is an accelerating frame which is difficult to work with. Instead, by ignoring the rotation of the Earth around the sun, the inertial frame of reference having its origin at the center of the Earth and its z-axis along the spin axis of the Earth simplifies the equations of motion of the projectile. The z-x plane can be chosen to contain the radar at $t = 0$ when the projectile is fired. To obtain the familiar ground-based quantities, transformation to the inertial frame in which the radar (or the gun) is passing instantaneously through the z-x plane can be performed. In this frame, the distance and the relative velocity of the projectile from the radar (or the gun) can be found easily.

The projectile will be spinning around its axis if a rifled gun barrel is used. The lift force due to air pressure will rotate the projectile to align its axis along its air velocity vector. The kinematics of the projectile, including its angular momentum, is most easily described in terms of the motion of, and the rotation around, its center of mass [Ref. 1]. The orientation of the projectile, which lies along one of its principal axis of inertia, can be described in terms of two of the three Euler angles [Ref. 2], leaving the third angle for measuring the spin of the projectile.

It can be shown that the effect of gravitational force on the projectile orientation is negligible. The ratio between the gravitational force on the center of mass to the force affecting the angular momentum is of the order of the square of the ratio of projectile size to the Earth radius [Ref. 3]. Thus the change of the orientation of the projectile axis

is due largely to the resistance of air. For a streamlined body, the lift from the air flow is large when there is an angle of attack [Ref. 4]. Furthermore, the rotation of the projectile axis is slow. It is reasonable to assume that the orientation of the axis of the projectile is always along its air velocity. This assumption will be utilized to determine the radar cross-section of the projectile.

It is easily seen in the ground coordinate that the projectile velocity is much greater than the wind velocity so that the latter only introduces small corrections to the projectile axis. Since the wind acts on the projectile over the entire trajectory, a better estimate of the range can be obtained by including the wind velocity profile to trajectory prediction. A less elaborate alternative is to adopt a wind profile model such as the Ekman spiral for wind speed approximation [Ref. 5]. Since the change in the predicted range is not expected to be large, the wind velocity is treated as constant throughout this thesis.

II. PROPOSED CW RADAR DESIGN

A. RADAR SYSTEM SCHEMATICS

The receiver design of a radar is critical to its range performance. Since no specific information for any CW radar tracking system is available, the following receiver configuration is proposed. Here Figure 1 shows the schematics of the radar.

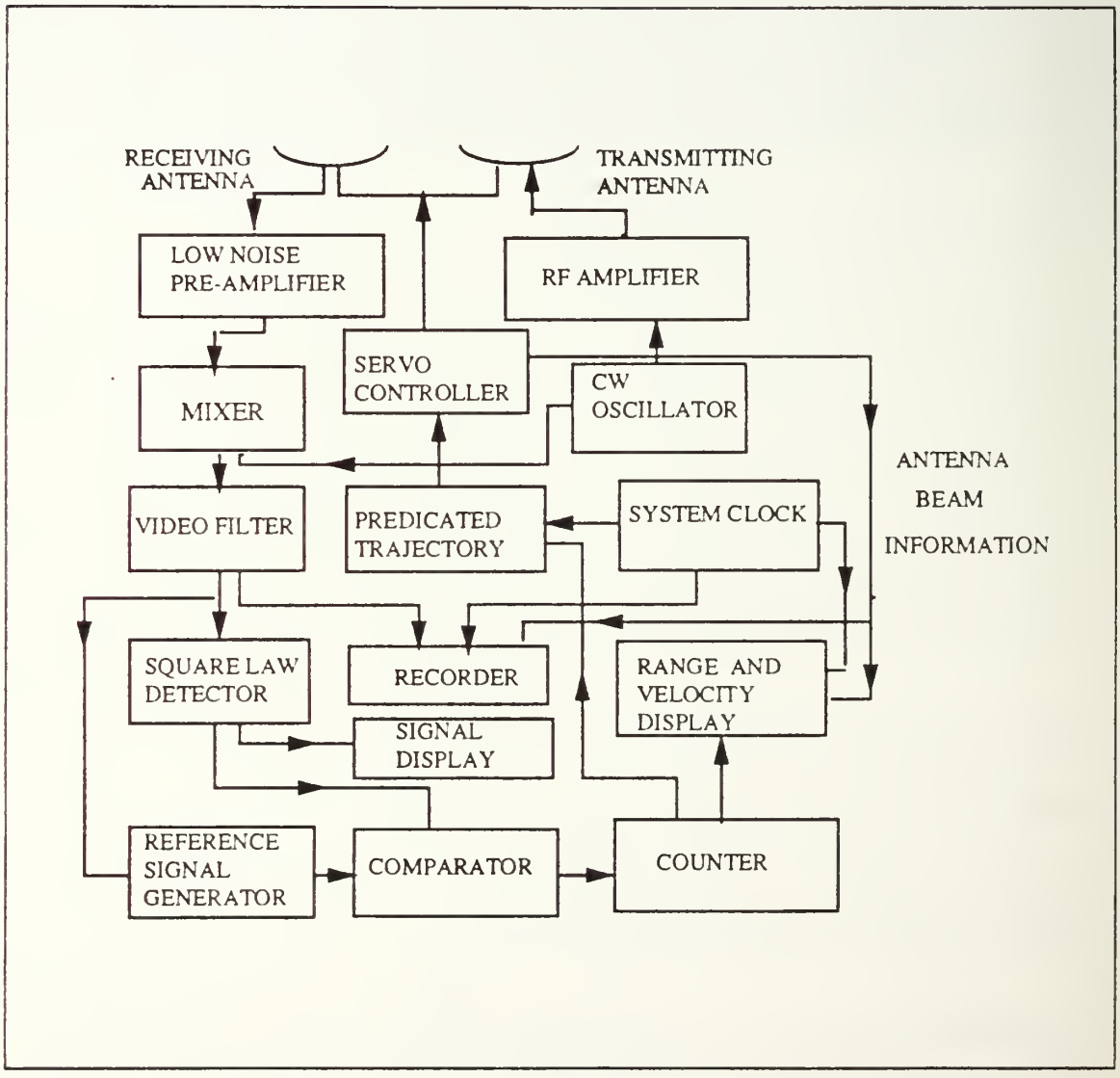

Figure 1. Schematics for Proposed CW Radar Design.

The received signal at the frequency $(f_t + f_d)$ from the receiving antenna is fed to a narrow-band, low-noise RF pre-amplifier with a bandwidth of 1 MHz centered at 10.475 GHz. The noise figure of such a pre-amplifier can be as low as 1.5 to 2 dB, with a minimum gain of 28 dB [Ref. 6]. This low-noise pre-amplifier can limit the receiver noise figure (F_n) to about 2 dB. The 1 MHz bandwidth is chosen according to the estimated maximum doppler frequency (f_{dmax}) and the fact that the target is always flying away from the radar. The output signal from the low-noise pre-amplifier is reduced to the base band at the mixer, and then passed through the video filter of bandwidth B_v. The filter output, at the doppler frequency f_d, can be recorded either with an analog or a digital recorder. The bandwidth of this recorder should be wider than f_{dmax} to allow truthful recording of the raw data for later analysis. The doppler signal is then fed into the square-law detector.

The output of the square-law detector oscillates at a frequency of $2f_d$. Since this frequency is proportional to the velocity of the projectile receding away from the radar, it can be integrated to obtain the projectile range information.

The integration is most easily accomplished by counting the number of cross-over points of a pre-determined level by the square-law detector output. As to be explained later, this number, denoted by MN, is the displacement of the projectile away from the radar measured in half the transmitter wavelengths.

The square-law detector, a counter, and a clock will be adequate for measuring the range and the velocity of the projectile receding from the radar. First, a measurement base, MB, is set in terms of the number MN of transmitter half wavelengths. Then the time T_n for the output of the square-low detector to run through MN pre-set level crossings is measured. Here MB is the radial range increase of the projectile and $\frac{MB}{T_n}$ is the radial velocity of the projectile.

As discussed in the introduction, the trajectory of the projectile is predicted beforehand. The elevation and bearing angles of the radar are updated at the end of every T_n interval. This information is sent to the servo control system to keep the antenna on the projectile.

B. THEORY

The theory of operation for the proposed CW radar system will be described. The doppler effect is used in a CW radar for moving target detection. This effect was found by Christian Doppler in 1842. It states that the frequency of a harmonic signal will shift when reflected by a moving target. The change in frequency is proportional to the ve-

locity of the target. Let f_d denote the doppler shift, V_r the radial velocity of the target with respect to the radar, c the velocity of light, and f_t the transmitted carrier frequency. The doppler frequency shift is

$$f_d = 2\frac{V_r}{\lambda} \tag{2.1}$$

$$= 2V_r\frac{f_t}{c} \tag{2.2}$$

The doppler is zero when the trajectory of the projectile is perpendicular to the radar line of sight. It is positive for an approaching target (see Figure 2).

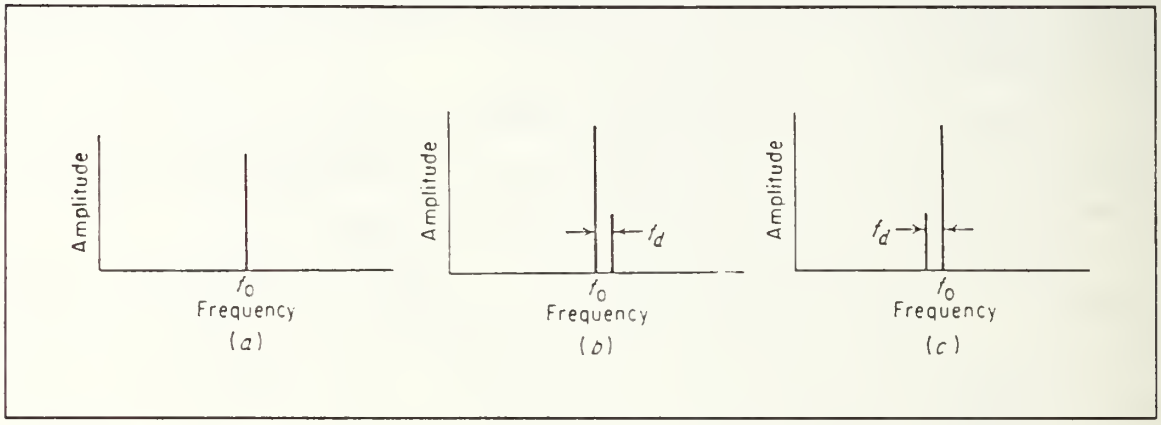

Figure 2. **Spectra of Received Signals: (a) no doppler shift, no relative** motion (b) approaching target (c) receding target.

The frequency of the signal out of the square-law detector is $2f_d$. Thus the number of crossings, MN, of this signal over a pre-set level within a time interval T_n is :

$$MN = T_n \times \frac{2f_d}{2} \tag{2.3}$$

$$= T_n \times 2\frac{V_r}{\lambda} \tag{2.4}$$

According to equation (2.1), the radial displacement of the projectile over this period (Figure 3 on page 7) is :

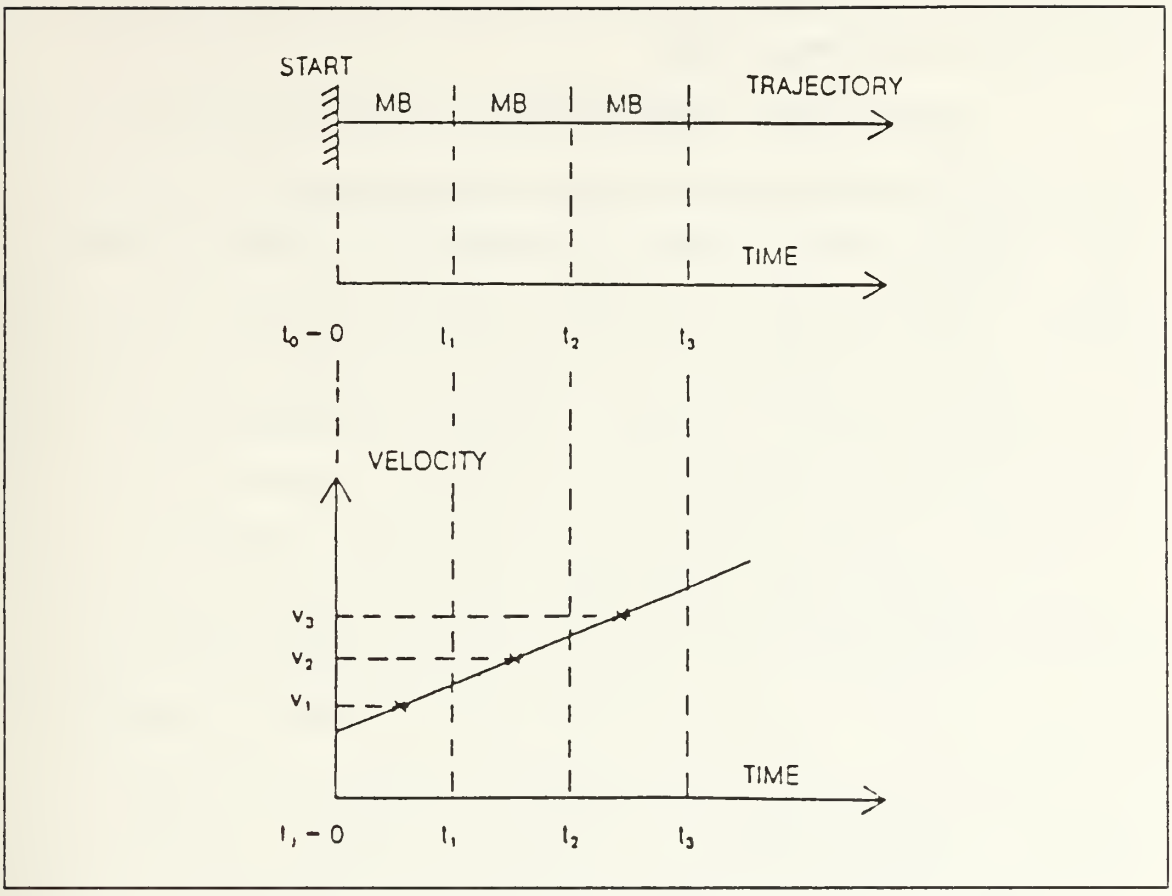

Figure 3. Measurement Base and Velocity vs. Time.

$$MB = T_n \times V_r \tag{2.5}$$

$$= MN \times \frac{\lambda}{2} \tag{2.6}$$

For example, if the transmitting frequency f_r of interest is 10525 MHz, we can set the number MN to 100. Then

$$MB = \frac{100 \times 2.997 \times 10^8}{2 \times 10525 \times 10^6} \tag{2.7}$$

$$= 1.4234\,\text{m} \tag{2.8}$$

This is a small change in target location for updating the radar pointing direction. Since MB is the displacement of the target along the radar pointing direction, this dis-

placement can be projected onto the ground. The ground range can be derived by adding up the individual projected ranges.

III. PROJECTILE TRAJECTORY PREDICTION

To analyze the range performance of the radar, information about the trajectory of the projectile is required. There are many factors such as air drag, gravitational force, projectile shape and spin, Earth rotation,...etc., which can affect the trajectory. As discussed in the INTRODUCTION, the projectile spin mainly provides a stabilizing mechanism to the projectile and is assumed to have little effect on its trajectory. The direction of the projectile axis (or heading) is assumed to be along the direction of the air velocity of the projectile. Thus only the motion of the center of mass of the projectile needs to be considered. The projectile center of mass and the center of air pressure are assumed to be the same. The trajectory is thus reduced to that of a particle trajectory.

Wind velocity can increase, decrease or deviate the trajectory through air drag on the projectile. In this thesis, it is assumed that wind velocity is constant over the course of the projectile; it is usually called the ballistic wind.

Drag force depends on the air velocity of the projectile. It points against the projectile heading. Its magnitude is proportional to the square of projectile air speed, the local air density, the projectile cross-section, and the drag coefficient. Air density depends on the temperature profile of the atmosphere. The drag coefficient is very complicated and, in fact, varies with the projectile air speed. Measured data of the drag coefficient are available. The drag force on the in-flight projectile is given below :

$$\vec{f} = -\hat{h}\frac{\rho}{2}AC_D(\vec{V}-\vec{W})^2 \tag{3.1}$$

where $\vec{W}$ is wind velocity, $\vec{V}$ is the velocity of the projectile, C_D is the drag coefficient, A is the cross-section area of the projectile, and ρ is the local air density. Here $\hat{h}$ is the heading of the projectile, which is a unit vector in the direction of $\vec{V}-\vec{W}$.

The gravitational force is the only other factor affecting the trajectory in an inertial frame of reference. In the accelerating reference frame fixed on the surface of the Earth, there is the fictitious Coriolis force. It causes an apparent trajectory drift. As observed on the ground, this drift can reach 3.1 km for a trajectory of 27.4 km ground range.

A. THE TRAJECTORY IN A FIXED INERTIAL FRAME

In order to simplify the equation of motion, the Earth-centered inertial frame (r, θ, ϕ) is used. The plane containing the radar and the spin axis of the Earth when the projectile is fired at t = 0 is the z-x plane. The radar is moving with the Earth at an angular velocity of Ω . Its location in this inertial frame is $(r_R, \theta_R, \Omega t)$.

The components of the projectile velocity in this reference frame are :

$$\dot{r} = V_r \tag{3.2}$$

$$r\dot{\theta} = V_\theta \tag{3.3}$$

$$r(\sin\theta)\dot{\phi} = V_\phi \tag{3.4}$$

The Lagrangian formulation of the principle of least action is convenient for deriving the equations of motion of the projectile [Ref. 7]. The Lagrangian of the projectile in the inertial spherical coordinate system [Ref. 1 , 8] (r, θ, ϕ), without considering the drag force, can be expressed as :

$$L = T(r, \theta, \phi, \dot{r}, \dot{\theta}, \dot{\phi}) - U(r, \theta, \phi) \tag{3.5}$$

$$L = \frac{m}{2}(\dot{r}^2 + r^2\dot{\theta}^2 + r^2\dot{\phi}^2 \sin^2\theta) - mga(1 - \frac{a}{r}) \tag{3.6}$$

where g is the gravitational acceleration at ground level. For the r component, the equation of motion is :

$$\frac{d}{dt}\frac{\partial L}{\partial \dot{r}} = \frac{\partial L}{\partial r} \tag{3.7}$$

$$\ddot{r} = -\frac{a^2}{r^2}g + r\dot{\theta}^2 + r\dot{\phi}^2 \sin^2\theta \tag{3.8}$$

For the θ component :

$$\frac{d}{dt}\frac{\partial L}{\partial \dot{\theta}} = \frac{\partial L}{\partial \theta} \tag{3.9}$$

$$\frac{d}{dt}(r^2\dot{\theta}) = r^2\dot{\phi}^2 \sin\theta\cos\theta \tag{3.10}$$

and, for the ϕ component:

$$\frac{d}{dt}\frac{\hat{c}L}{\dot{\phi}} = \frac{\hat{c}L}{\hat{c}\phi} \tag{3.11}$$

$$\frac{d}{dt}\left(\frac{r^2}{a}\dot{\phi}\sin^2\theta\right) = 0 \tag{3.12}$$

The nonlinear drag force can be included. The complete equations of motion become :

$$\frac{d}{dt}V_r = -\left(\frac{a}{r}\right)^2 g + \frac{V_\theta^2 + V_\phi^2}{r} + f_r \tag{3.13}$$

$$\frac{d}{dt}\left(\frac{r}{a}V_\theta\right) = \cot\theta V_\phi^2 + r f_\theta \tag{3.14}$$

$$\frac{d}{dt}(r\sin\theta V_\phi) = r\sin\theta f_\phi \tag{3.15}$$

$$r = a + h \tag{3.16}$$

where h is the height from the Earth surface and a is the radius of the Earth. The ratio of projectile height to the Earth radius can be expressed as :

$$\frac{r}{a} = 1 + \frac{h}{a} \tag{3.17}$$

The projectile velocity is :

$$\vec{V} = V_r\hat{r} + V_\theta\hat{\theta} + V_\phi\hat{\phi} \tag{3.18}$$

$$= \dot{r}\hat{r} + r\dot{\theta}\hat{\theta} + r\sin\theta\dot{\phi}\hat{\phi} \tag{3.19}$$

and the wind velocity is :

$$\vec{W} = W_\theta\hat{\theta} + W_\phi\hat{\phi} + W_r\hat{r} \tag{3.20}$$

Note that f_r, f_θ, f_ϕ are the components of the drag force divided by the mass of the projectile :

$$\vec{f} = -\hat{h}\frac{\rho}{2m}AC_D|\vec{V} - \vec{W}|^2 \tag{3.21}$$

$$= f_r\hat{r} + f_\theta\hat{\theta} + f_\phi\hat{\phi} \tag{3.22}$$

The equations of motion can be discretized. Assume that the gravitational and the drag force acceleration are approximately constant over the period T_n when the projectile moves from $\vec{r}_n$ to $\vec{r}_{n-1}$, the equations of motion are approximately :

$$\frac{\dot{r}_{n+1} - \dot{r}_n}{T_n} = -g\frac{a^2}{r_n^2} + r_n\dot{\theta}_n{}^2 + r_n\sin^2\theta_n\phi_n^2 + f_{rn} \tag{3.23}$$

$$\frac{r_{n+1}^2\dot{\theta}_{n+1} - r_n^2\dot{\theta}}{T_n} = r_n^2\sin\theta_n\cos\theta_n\dot{\phi}_n^2 + r_n f_{\theta n} \tag{3.24}$$

$$\frac{r_{n+1}^2\sin^2\theta_{n+1}\dot{\phi}_{n+1} - r_n^2\sin^2\theta_n\dot{\phi}_n}{T_n} = r_n\sin\theta_n f_{\phi n} \tag{3.25}$$

From the above equations, if r_n, θ_n, ϕ_n and $\dot{r}_n$, $\dot{\theta}_n$, $\dot{\phi}_n$ are known, then r_{n-1}, θ_{n-1}, ϕ_{n-1}, $\dot{r}_{n-1}$, $\dot{\theta}_{n-1}$, and $\dot{\theta}_{n-1}$ can be derived as follows :

With measured T_n, equation (1) provides r_{n-1} , then

$$r_{n+1} = r_n + \frac{\dot{r}_n + \dot{r}_{n+1}}{2}T_n \tag{3.26}$$

Equations (3.26) and (3.24) give $\dot{\theta}_{n-1}$, then

$$\theta_{n+1} = \theta_n + \frac{\dot{\theta}_n + \dot{\theta}_{n+1}}{2}T_n \tag{3.27}$$

Equations (3.27) and (3.23) give $\dot{\phi}_{n-1}$, then

$$\phi_{n+1} = \phi_n + \frac{\dot{\phi}_n + \dot{\phi}_{n+1}}{2}T_n \tag{3.28}$$

Note that the muzzle location is $\vec{r}_o$ and the muzzle velocity of the projectile, which is assumed to be known, is $\vec{V}_o$. Through the above procedures, the full trajectory of the projectile can be constructed by computer simulation.

B. GROUND-OBSERVED TRAJECTORY

In order to obtain the trajectory as observed from the ground, the position of the projectile should be converted into its relative location from the radar antenna and from the gun. The necessary coordinate transformation matrices are given below (Figure 4 on page 13).

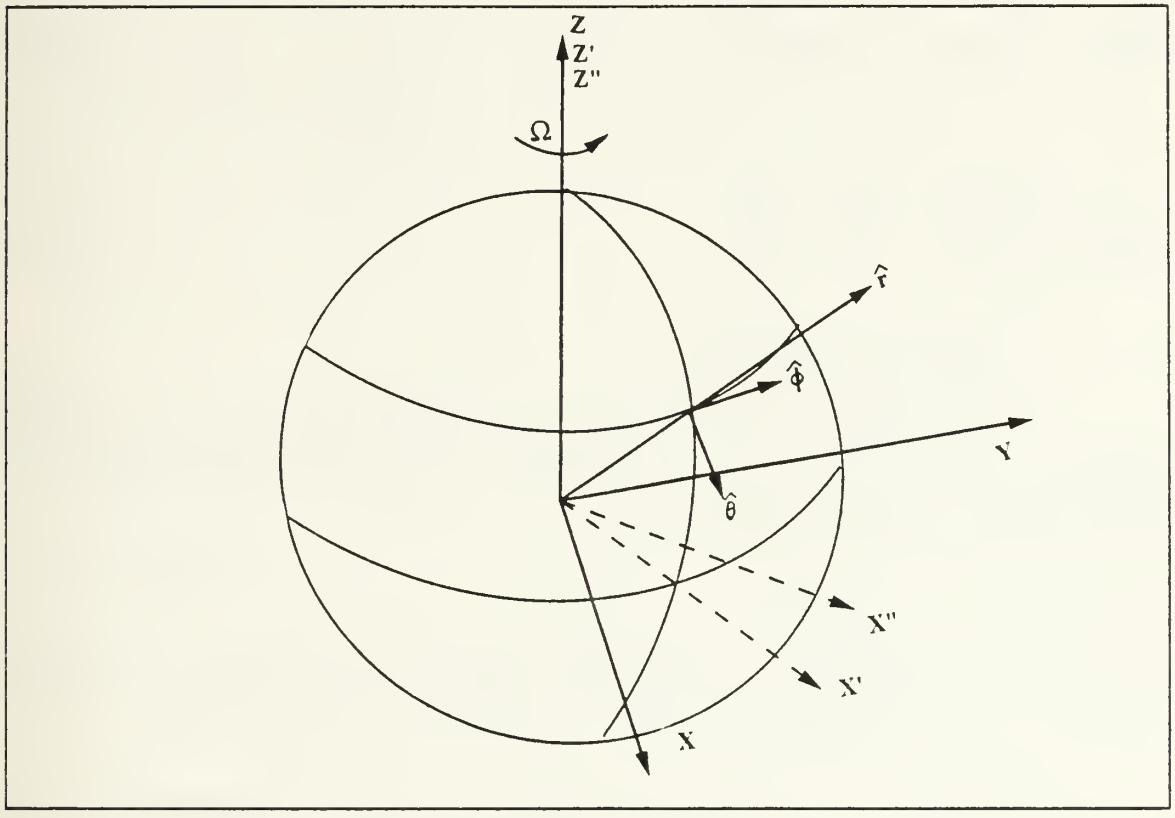

Figure 4. Inertial Coordinate Systems.

1. Trajectory Relative to Radar

To set the elevation and bearing angles for the radar and to estimate the doppler shift, the location and velocity of the projectile relative to the radar as viewed from the ground are needed. On the ground, the projectile motion is most easily described in an inertial frame in which, at time, t, the radar is passing through the $z' - x'$ plane instantaneously. The z' axis is chosen so that it coincides with the z axis. The transformation from the fixed inertial spherical coordinate system to this (x', y' ,z') system can be accomplished through the following rotation matrices R_z, R_{rec} , and R_{cyl} :

$$R_z(\Omega t) = \begin{bmatrix} \cos \Omega t & \sin \Omega t & 0 \\ -\sin \Omega t & \cos \Omega t & 0 \\ 0 & 0 & 1 \end{bmatrix} \tag{3.29}$$

$$R_{rec}(\phi_p) = \begin{bmatrix} \cos \phi_p & 0 & -\sin \phi_p \\ \sin \phi_p & 0 & \cos \phi_p \\ 0 & 1 & 0 \end{bmatrix} \tag{3.30}$$

$$R_{cyl}(\theta_p) = \begin{bmatrix} \sin \theta_p & \cos \theta_p & 0 \\ \cos \theta_p & -\sin \theta_p & 0 \\ 0 & 0 & 1 \end{bmatrix} \tag{3.31}$$

a. Velocity Transformation

The projectile velocity in the (x', y', z') coordinate system can be obtained by first changing the results in section IIIA from the spherical coordinate system into the rectangular coordinate system (x, y, z) :

$$\begin{bmatrix} V'_{px} \\ V'_{py} \\ V'_{pz} \end{bmatrix} = R_{rec}(\phi_p) R_{cyl}(\theta_p) \begin{bmatrix} V'_{pr} \\ V'_{p\theta} \\ V'_{p\phi} \end{bmatrix} \tag{3.32}$$

Since the (x', y', z') coordinate system is obtained by rotating the (x, y, z) coordinate system by an angle Ωt around the z-axis.

$$\begin{bmatrix} V'_{px'} \\ V'_{py'} \\ V'_{pz'} \end{bmatrix} = R_z(\Omega t) \begin{bmatrix} V'_{px} \\ V'_{py} \\ V'_{pz} \end{bmatrix} \tag{3.33}$$

$$= R_{rec}(\phi_p - \Omega t) R_{cyl}(\theta_p) \begin{bmatrix} V'_{pr} \\ V'_{p\theta} \\ V'_{p\phi} \end{bmatrix} \tag{3.34}$$

The velocity of the radar, $\vec{V}_R$, in the (x', y', z') coordinate is :

$$\begin{bmatrix} V_{Rx'} \\ V_{Ry'} \\ V_{Rz'} \end{bmatrix} = R_{rec}(0)R_{cyl}(\theta_R)\begin{bmatrix} 0 \\ 0 \\ V_{R\phi} \end{bmatrix} \tag{3.35}$$

$$= \begin{bmatrix} \sin\theta_R & \cos\theta_R & 0 \\ 0 & 0 & 1 \\ \cos\theta_R & -\sin\theta_R & 0 \end{bmatrix}\begin{bmatrix} 0 \\ 0 \\ V_{R\phi} \end{bmatrix} \tag{3.36}$$

$$= \begin{bmatrix} 0 \\ V_{R\phi} \\ 0 \end{bmatrix} \tag{3.37}$$

Hence

$$\vec{V}_R = V_{Ry'}\hat{y}' \tag{3.38}$$

$$= \Omega(r_R \sin\theta_R)\hat{y}' \tag{3.39}$$

b. Projectile Location Relative to the Radar

The relationship between (x', y', z') and (r, θ, ϕ) is given by :

$$\begin{bmatrix} x \\ y \\ z \end{bmatrix} = \begin{bmatrix} r\sin\theta\cos\phi \\ r\sin\theta\sin\phi \\ r\cos\theta \end{bmatrix} \tag{3.40}$$

$$\begin{bmatrix} x' \\ y' \\ z' \end{bmatrix} = R_z(\Omega t)\begin{bmatrix} x \\ y \\ z \end{bmatrix} \tag{3.41}$$

$$= \begin{bmatrix} r\sin\theta\cos(\phi - \Omega t) \\ r\sin\theta\sin(\phi - \Omega t) \\ r\cos\theta \end{bmatrix} \tag{3.42}$$

c. Radar Coordinate

Substitute $(r_R, \theta_R, \Omega t)$ into equation (3.42),

$$\begin{bmatrix} x_R' \\ y_R' \\ z_R' \end{bmatrix} = \begin{bmatrix} r_R \sin\theta_R \\ 0 \\ r_R \cos\theta_R \end{bmatrix} \tag{3.43}$$

2. Trajectory Relative to Gun

Relative to the gun (muzzle), a similar inertial frame (x'', y'', z'') in which the gun is instantaneously passing through the z'' - x'' plane at time t can be used. The z'' axis coincides with the z-axis. The coordinate transformation is :

$$\begin{bmatrix} x'' \\ y'' \\ z'' \end{bmatrix} = \begin{bmatrix} r\sin\theta\cos(\phi - \phi_G - \Omega t) \\ r\sin\theta\sin(\phi - \phi_G - \Omega t) \\ r\cos\theta \end{bmatrix} \tag{3.44}$$

The firing plane of the gun is the plane containing its barrel and passing through the center of the Earth. For artillery, it is customary to use the coordinate system (x_f, y_f, z_f) in which the gun muzzle is the origin and the $z_f - x_f$ plane is the firing plane. Here z_f is the vertical direction and x_f is along the horizontal from the gun. The relation between (x_f, y_f, z_f) and (x'', y'', z'') depends on the gun bearing angle θ_{AzG}, which is the angle of the x_f axis measured counterclockwise from the East. If the the gun is oriented along θ_{AZG} and is located at r_G , θ_G, ϕ_G, the vector $\vec{r}_p - \vec{r}_G$ in the coordinate (x_f, y_f, z_f) is :

$$\begin{bmatrix} x_f \\ y_f \\ z_f \end{bmatrix} = \begin{bmatrix} 0 & \cos\theta_{AzG} & \sin\theta_{AzG} \\ 0 & -\sin\theta_{AzG} & \cos\theta_{AzG} \\ 1 & 0 & 0 \end{bmatrix} \times \begin{bmatrix} \cos\theta_G & 0 & \sin\theta_G \\ 0 & 1 & 0 \\ -\sin\theta_G & 0 & \cos\theta_G \end{bmatrix} \begin{bmatrix} x'' \\ y'' \\ z'' \end{bmatrix} \tag{3.45}$$

Note that $\vec{r}_p - \vec{r}_G$ is the relative location of the projectile from the gun. Hence its components can replace (x'', y'', z'') directly in equation (3.45).

IV. RANGE ANALYSIS AND POWER REQUIREMENT

A. RANGE EQUATION

The power requirement of the CW radar can be obtained from the radar equation [Ref. 9] :

$$P_t = \frac{(4\pi)^3 k T_s F_n L (\frac{S}{N})_{\min} (B_v R^4)}{G^2 \sigma \lambda^2 F^4} \qquad (4.1)$$

In equation (4.1), the radar cross-section (σ), the maximum range (R), and the propagation factor (F) will be discussed in this chapter in detail. The Boltzman constant k is 287.05 n-m kg-°K. The absolute temperature T_s is 290°K . The wavelength λ is 0.0285m. Other parameters are based on the configuration of the CW radar as proposed in Chapter 2. They are defined as follows.

1. The Receiver Noise Figure

The receiver noise figure (F_n) is the ratio of the signal-to-noise power ratio at the receiver input to the signal-to-noise power ratio at the receiver output, assuming that the receiver temperature is 290°K . The F_n value for the receiver considered is assumed to be 2 dB.

2. System Loss Factor

The loss factor consists of the fractional loss of transmitter power delivered to the transmitting antenna (L_t), the fractional loss of the receiving antenna output power delivered to the receiver input (L_r), and miscellaneous loss (L_m). They are discussed below.

a. Transmission Loss

The transmission loss is the loss in the transmitting or the receiving portion of the transmission line. Since the transmitter is light-weight and is to be mounted very close to the antenna, L_t is estimated to be about 1.2 dB due to the use of narrow bandwidth rotary joints. The receiver pre-amplifier can be mounted directly to the receiving antenna output, followed with the mixer immediately. This arrangement will reduce L_r to about the same level as L_t.

b. Miscellaneous Loss

The miscellaneous loss (L_m) for this CW radar system is mainly due to the quantization loss at the comparator. Since only two-level (crossing) comparison is made, it is not expected to be significant and will be ignored.

Base on the above argument, the total loss is estimated at 2.4 dB.

3. Signal-to-Noise Ratio

For a tracking radar, it is important that the receiver output signal is sufficiently high above the noise level so that information carried by the signal can be extracted reliably. With the proposed receiver configuration, the signal-to-noise ratio (S N) of the output from the video filter is the figure of significance. First of all, this signal is recorded for later analysis. Its minimum S N has to be assured. In real-time, after passing through the square-law detector, this signal generates the timing sequence for updating the radar pointing direction and for evaluating the projectile radial velocity. It drives the gain control to keep the reference signal at a preset level. It is also the input into the comparator following which the number of signal cross-overs is tallied and the elapsed time is clocked as explained in section IIA.

The square-law detector and the comparator perform threshold detection. The reference signal acts as the threshold. The comparator outputs a +1 signal when the detector output is above the reference level; it outputs a -1 signal when the detector output falls below the reference. The reference signal level, which is set at a fraction of the detector output signal, determines the accuracy of the real-time output of the system. In what follows, the minimum S N ratio and the threshold setting in terms of the threshold-to-signal power ratio are discussed.

The signal input to the comparator is oscillating at twice the doppler frequency. Within each cycle of the signal, the portion rising above the threshold level to the peak and back to the threshold level can be considered as a pulse. This pulse is contaminated with noise, which is assumed to be white. The probability of each contaminated pulse falling under a certain threshold level is well-known. This probability of missed detection is the fraction of signal pulses failed to be detected by the comparator. Between two pulses, the number of false alarms is the number of extra cycles counted. These two effects tend to cancel each other so the optimum threshold setting is achieved by equalizing the fraction of missed pulse and the fraction of noise pulses. The program to compute these fractions are listed in Appendix D [Ref. 10].

Figure 5 on page 19, Figure 6 on page 20, Figure 7 on page 20, Figure 8 on page 21, and Figure 9 on page 21 show the fractional errors due to missed pulses and

noise pulses respectively. If the signal-to-noise ratio is 10 dB, the comparator output error is 5.55% when the threshold-to-signal power ratio is set at 0.455. Stronger signal allows the threshold to be set at a lower fractional value with an improved error ratio. For example, for a signal 12 dB above the noise, the threshold setting of 0.38, or -4.2 dB below the signal, will limit the error to 1.15%. In this thesis, the minimum signal-to-noise ratio is chosen to be 10 dB.

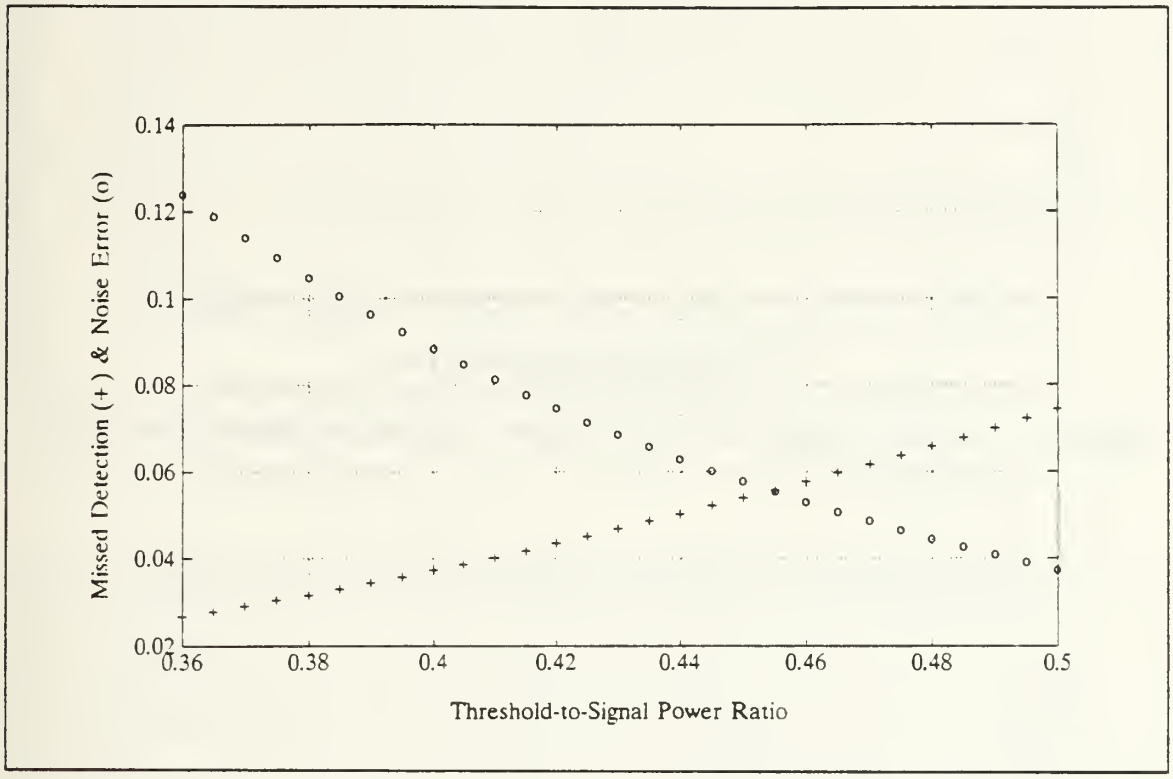

Figure 5. Missed Detection and Noise Error vs. Threshold-to-Signal Power Ratio S/N = 10 dB.

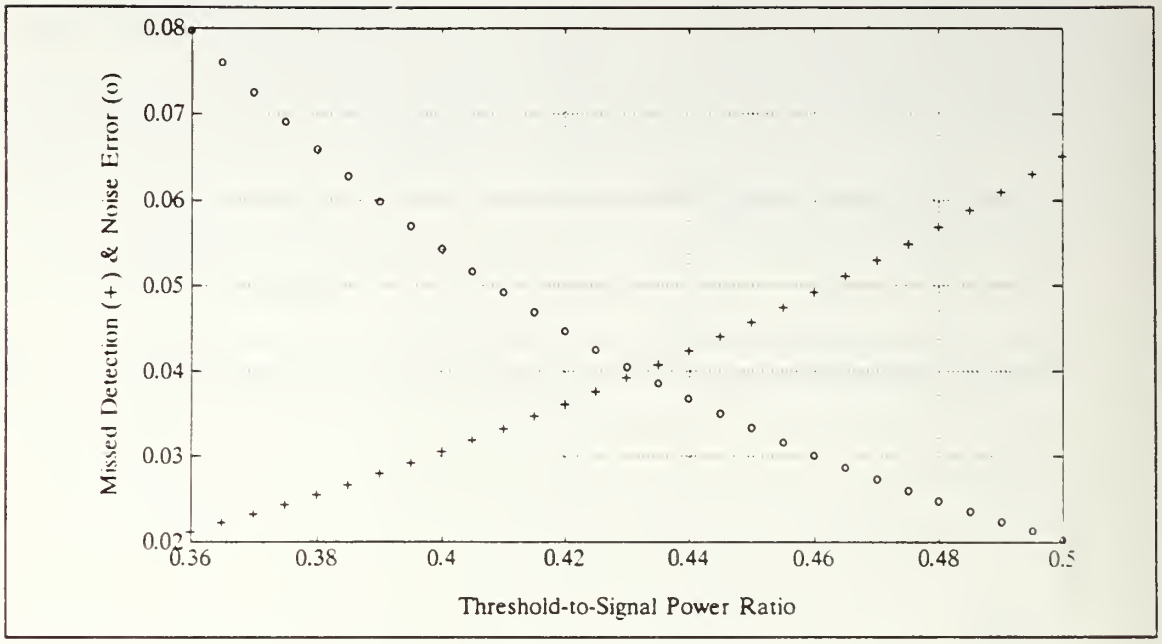

Figure 6. Missed Detection and Noise Error vs. Threshold to Signal Power Ratio S/N = 10.5 dB.

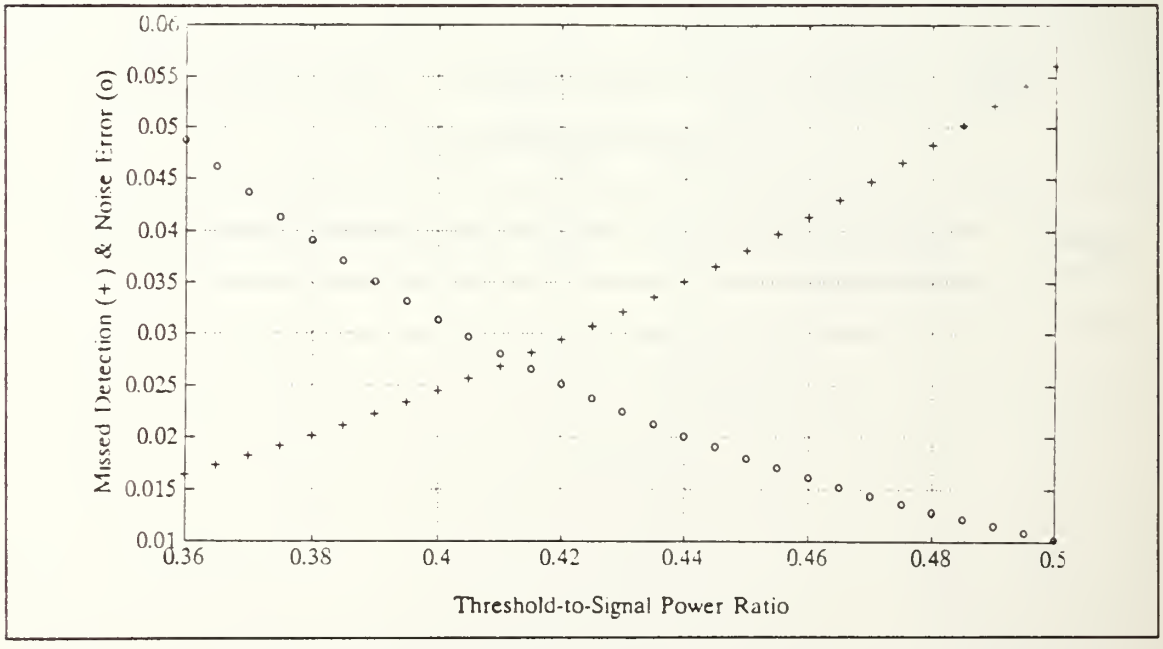

Figure 7. Missed Detection and Noise Error vs. Threshold to Signal Power Ratio S/N = 11 dB.

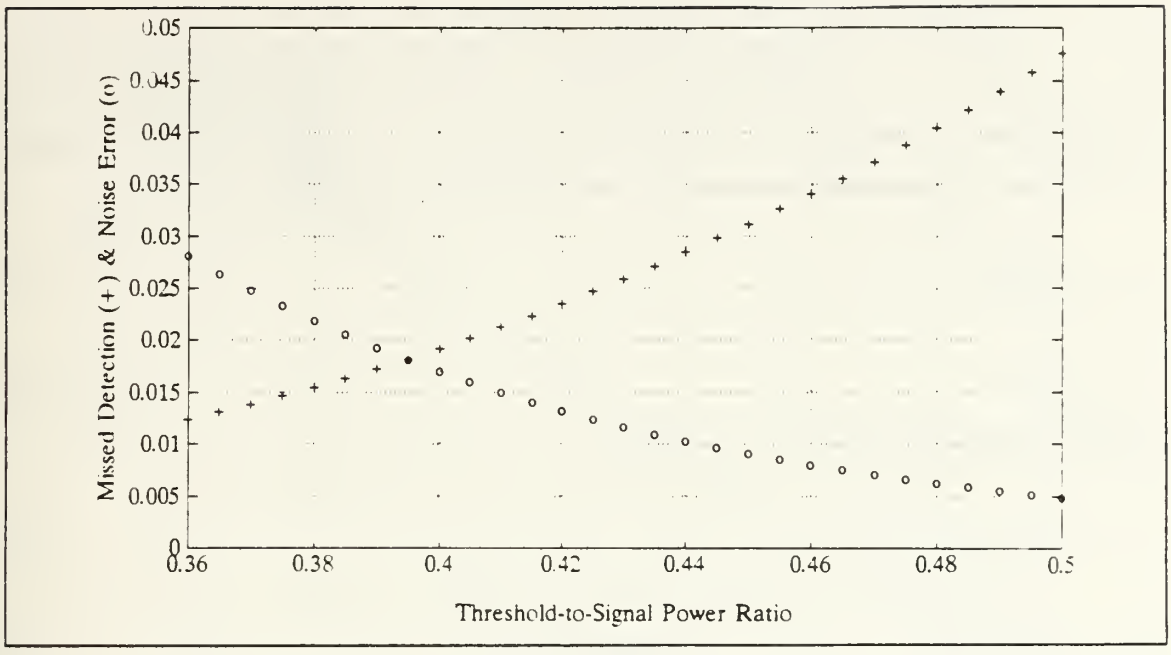

Figure 8. Missed Detection and Noise Error vs. Threshold-to-Signal Power Ratio S/N = 11.5 dB.

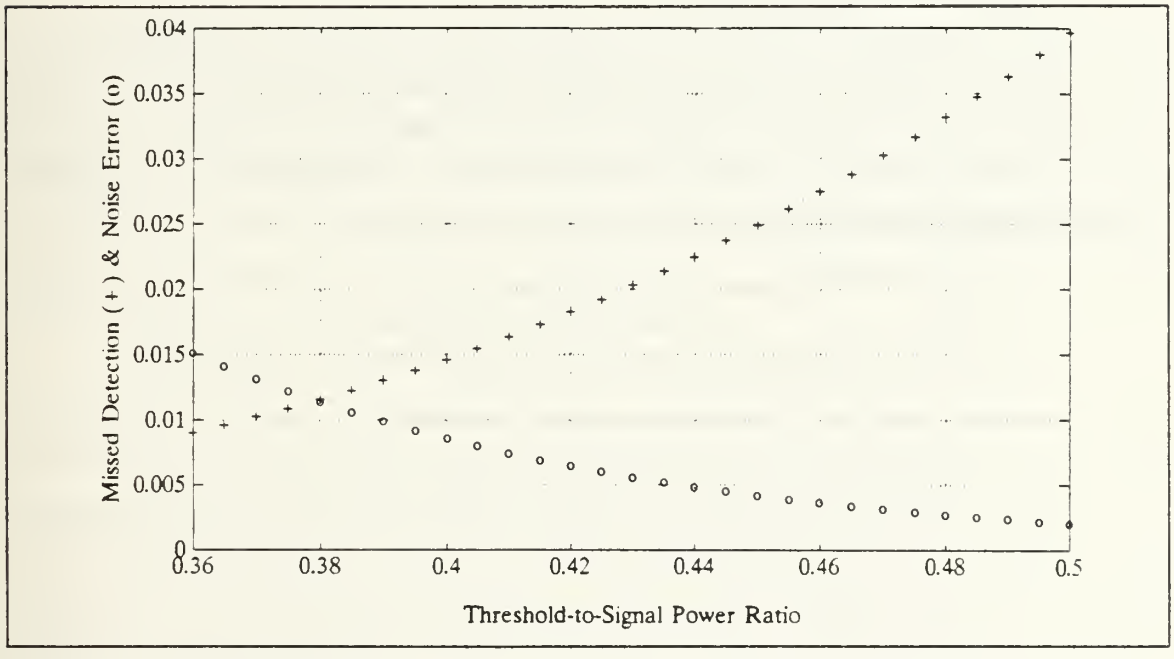

Figure 9. Missed Detection and Noise Error vs. Threshold-to-Signal Power Ratio S/N = 12 dB.

4. Transmitting and Receiving Antenna Gain

Separate but identical transmitting and receiving antennas are used to reduce direct coupling of the transmitter power into the receiver. Since this separation is small, it is neglected in the analysis. In x-band, antennas with one-degree beamwidth are easily achievable. Based on this beamwidth, the antenna gain (G) [Ref. 9] is :

$$G = \frac{27000}{\Delta\theta^2} \tag{4.2}$$

$$= 44.3dB \tag{4.3}$$

and the diameter D of such an antenna is

$$D = 72 \times \frac{\lambda}{\Delta\theta} \tag{4.4}$$

$$= 72 \times \frac{0.0285}{1^\circ} \tag{4.5}$$

$$= 2\,\mathrm{m} \tag{4.6}$$

5. Video Bandwidth and Filters

The required minimum video bandwidth (B_v) is a function of the doppler frequency. As previous mentioned, the bandwidth should be greater than f_{dmax} . Although the doppler frequency f_d of the projectile increases rapidly right after firing, it decreases monotonically afterwards by a factor of more than 4 over its trajectory. An example is shown in Figure 10 on page 23.

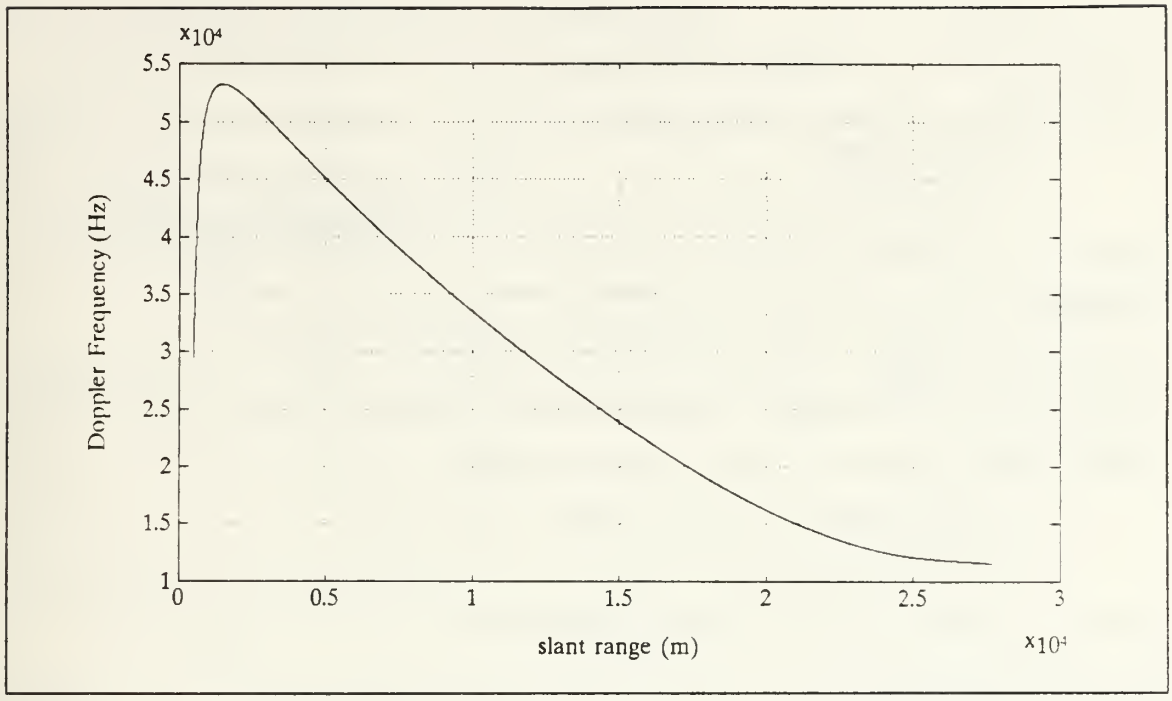

Figure 10. Doppler Frequency vs. Slant Range.

Referring to the range equation (4.1), in order to use the lowest transmitted power possible for full range tracking, the radar range and video bandwidth can be traded off. Note that, assuming a constant radar cross-section, the transmitter power depends on the product R^4B_v. A filter of narrower bandwidth may be employed when the projectile reaches a greater distance. Adoption of a set of three switchable doppler filters is recommended. The following is an example for its implementation based on the doppler frequency of the projectile given in Figure 10.

The maximum doppler shift f_{dmax} from the projectile shown in Figure 10 is a little less than 54 kHz. The maximum range R is about 27 km. Three filters are to be used over three different ranges. Each of the filters will have a bandwidth of 1.2 times the maximum expected doppler frequency over the range in which it is to be used to allow for a 20% estimation error. The transmitter power level will be minimized if the fourth power of the maximum range times the maximum doppler shift in the corresponding range is a constant.

a. First Filter

When the projectile is within 16.06 km slant range, the video bandwidth is chosen to be $1.2 \times f_{dmax}$. Thus :

$$B_v = 1.2 \times f_{dmax} \tag{4.7}$$

$$= 63.9\ kHz \tag{4.8}$$

b. Second Filter

When the projectile moves beyond 16.06 km, but within 23.73 km slant range, the doppler frequency has a maximum value of about 22.03 kHz. The video bandwidth is :

$$B_v = 1.2 \times 22.03\ kHz \tag{4.9}$$

$$= 26.44\ kHz \tag{4.10}$$

c. Third Filter

When the projectile reaches 23.73 km slant range, the maximum doppler frequency is about 12.7 kHz. The video bandwidth is :

$$B_v = 1.2 \times 12.7\ kHz \tag{4.11}$$

$$= 15.2\ kHz \tag{4.12}$$

Since $R^4 f_{dmax}$ is now less than 1/4 of the original value when only one video filter is used, the minimum required transmitter power will be reduced by more than a factor of 4.

B. TRAJECTORY SIMULATION AND RESULTS

Based on the procedures for trajectory estimation presented in Chapter III, a simulation program was written and is included as Appendix A. It was written in PC-Matlab 386. The program is described as follows.

1. Input and Parameters.

a. Earth

The operation is assumed to take place in Taiwan. The radar is located at the longitude of 121°36′27 ″ East and the latitude of 24°36′38 ″ North. The Earth radius is approximately 6.3677225×10^6 m (average value of the artic radius 6.356912×10^6 m and the equator radius 6.378533×10^6 m). The gravitational acceleration at sea level is 9.81 m/ sec^2. The angular velocity of Earth spin is $7.29211844 \times 10^{-5}$ rad sec [Ref. 11].

b. Radar

The transmitting frequency is 10525 MHz. The measurement base MB can be varied to change the update rate of the antenna pointing direction. For both the receiving and the transmitting antenna, the beamwidth is 1° and the gain is 44.3 dB. The antenna height and the distance between the gun and the radar can affect the initial readings of the doppler signal.

c. Gun

The firing elevation angle is assumed to be 45° and the azimuth is counterclockwise from the East and is also assumed to be 45°. Both the elevation angle and the azimuth angle can be varied. The distance between the gun and the radar can be adjusted. (Variations of up to 2000 m are possible at the test site.) The barrel length of the gun under consideration is 7 m.

d. Projectile

The target is a 155 mm calibre artillery projectile. Its weight is 45.4 kg, with a total length of 938 mm. The maximum muzzle velocity is 850 m sec.

e. Environment

(1) Temperature and air density profiles. The temperature T_o at sea surface is assumed to be 288°K and the temperature at the projectile height h is based on the following profile [Ref. 12] :

$$T_h = T_o - a_T h \tag{4.13}$$

where h is the height from sea level, a_T is the temperature lapse rate (-0.0065 °K m). The temperature (T_h) is used for calculating the air density (ρ_h) at the projectile:

$$\rho_h = \rho_o\left(\frac{T_h}{T_o}\right)^{\left[-\left(\frac{g}{a_T R}\right)+1\right]} \tag{4.14}$$

In equation (4.14) ρ_o is the air density at sea level (1.225 kg/m^3), and R is the gas constant (287.05 n-m kg-°K).

(2) Wind profile. The wind is assumed to be constant during the flight time over the projectile trajectory. The value used is the so-called ballistic wind. It can be expressed as :

$$\vec{W} = W_r\hat{r} + W_\theta\hat{\theta} + W_\phi\hat{\phi} \tag{4.15}$$

In this thesis, the wind is 6 m/sec, North-West. It should be noted that the extent to which the estimated trajectory can be modified by the actual wind profile is subject to further study.

(3) Mach number. The Mach number is the ratio of the projectile air speed to local sound speed. The sound speed at the height of the projectile is :

$$a_h = \sqrt{KRT_h} \tag{4.16}$$

where K is 1.4 for idea gas. The Mach number (M) is given by :

$$M = \frac{|\vec{V} - \vec{W}|}{a_h} \tag{4.18}$$

where $|\vec{V} - \vec{W}|$ is the projectile speed with respect to air.

f. Drag Coefficient

The drag coefficient (C_D) is required for calculating the drag force. It depends on the shape of the projectile. The C_D curve is measured experimentally. It is given as a function of Mach number M. For a 155mm projectile, the C_D curve is shown in Figure 11 on page 27.

2. Results of Simulation

The results of trajectory simulation are described below. The variable names used in the program are given in the parentheses when they are first mentioned.

a. Radar Observed Trajectory

The slant range (SRR) is the distance from the radar antenna to the in-flight projectile. The curve showing the projectile height (Height) versus its slant range from the radar is shown in Figure 12 on page 28. The total flight time is 87.4 seconds, and the maximum range is 27.4 km.

b. Gun Based Trajectory

The ground range is measured from the gun to the projectile. The projectile height vs. in-flight time (t) and the projectile height vs. ground range are shown in Figure 13 on page 28 and Figure 14 on page 29. The maximum ground range (Grange) is 27.4 km.

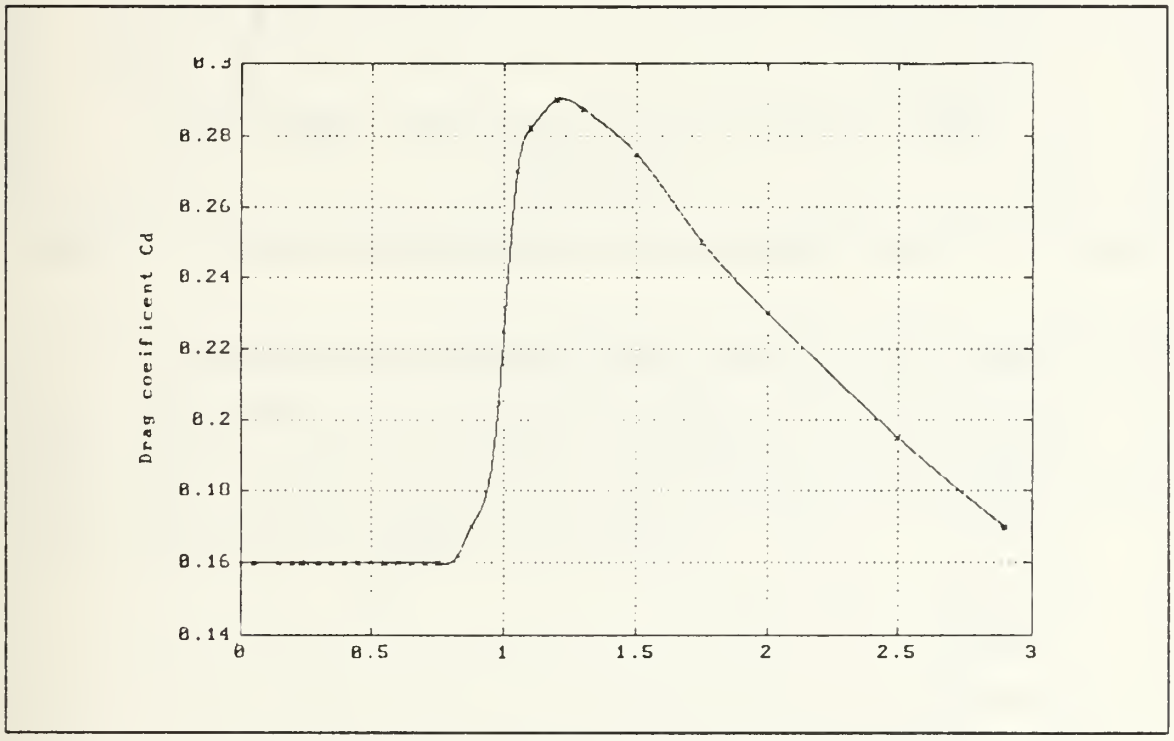

Figure 11. Drag Coefficient vs. Mach Number for 155 mm Projectile.

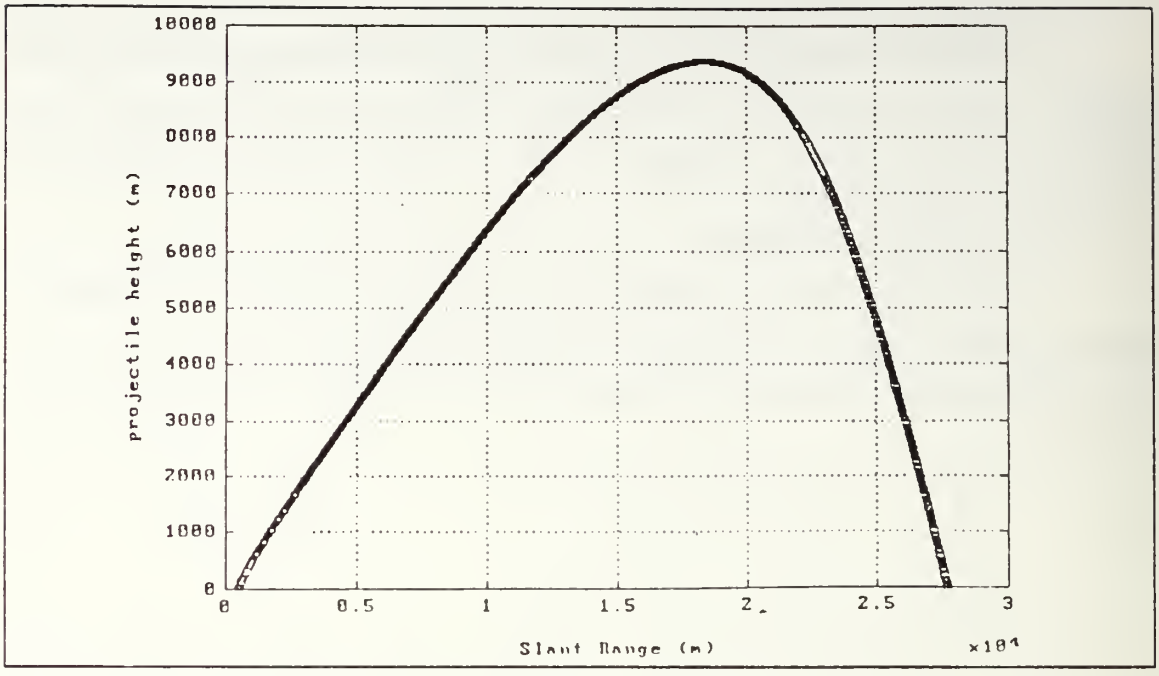

Figure 12. Projectile Trajectory: Height vs. Slant Range.

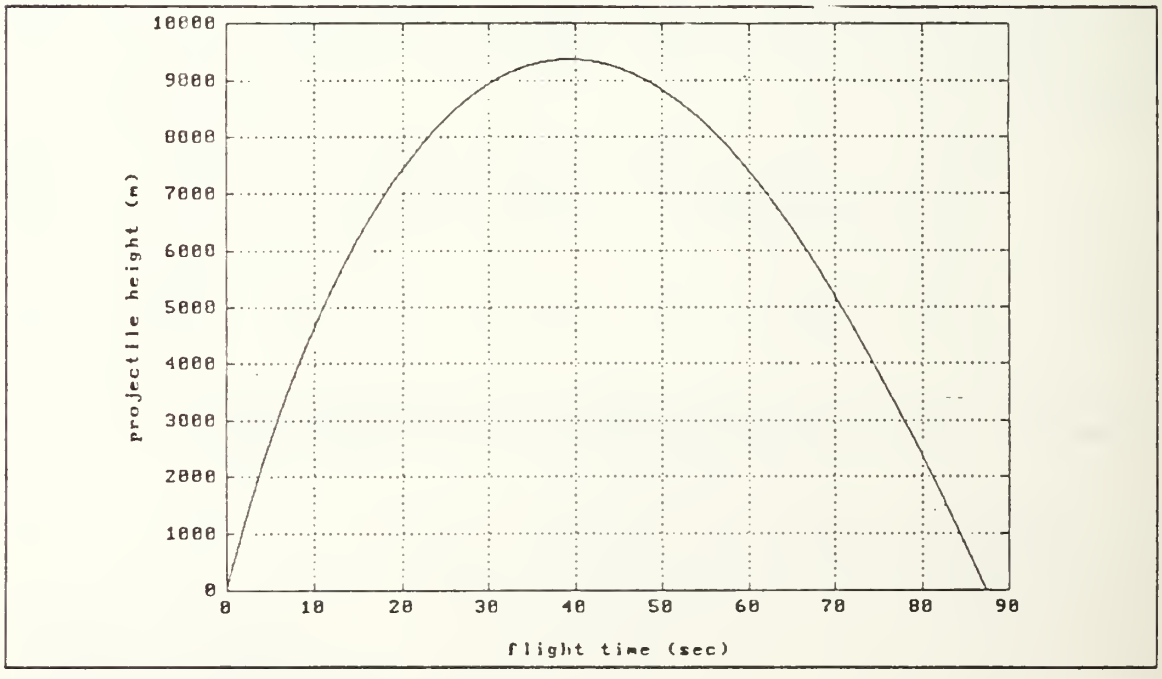

Figure 13. Projectile Trajectory: Height vs. Time.

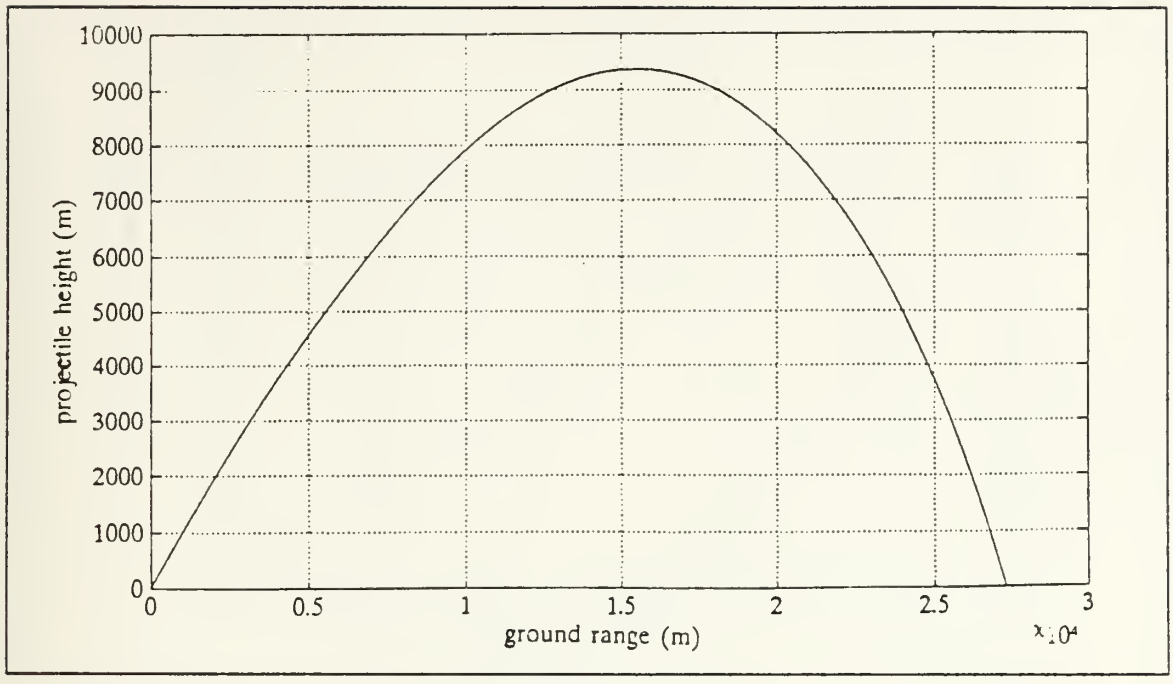

Figure 14. Projectile Trajectory: Height vs. Ground Range.

The cross range (CRange) measures the drift of the projectile from the firing plane. The firing plane is the vertical plane containing the gun barrel. In the case considered, the maximum cross range is about 6.3 km South-East of the firing plane. The point of impact is about 3.14 km away from the firing plane. The curve of cross range vs. ground range is shown in Figure 15 on page 30.

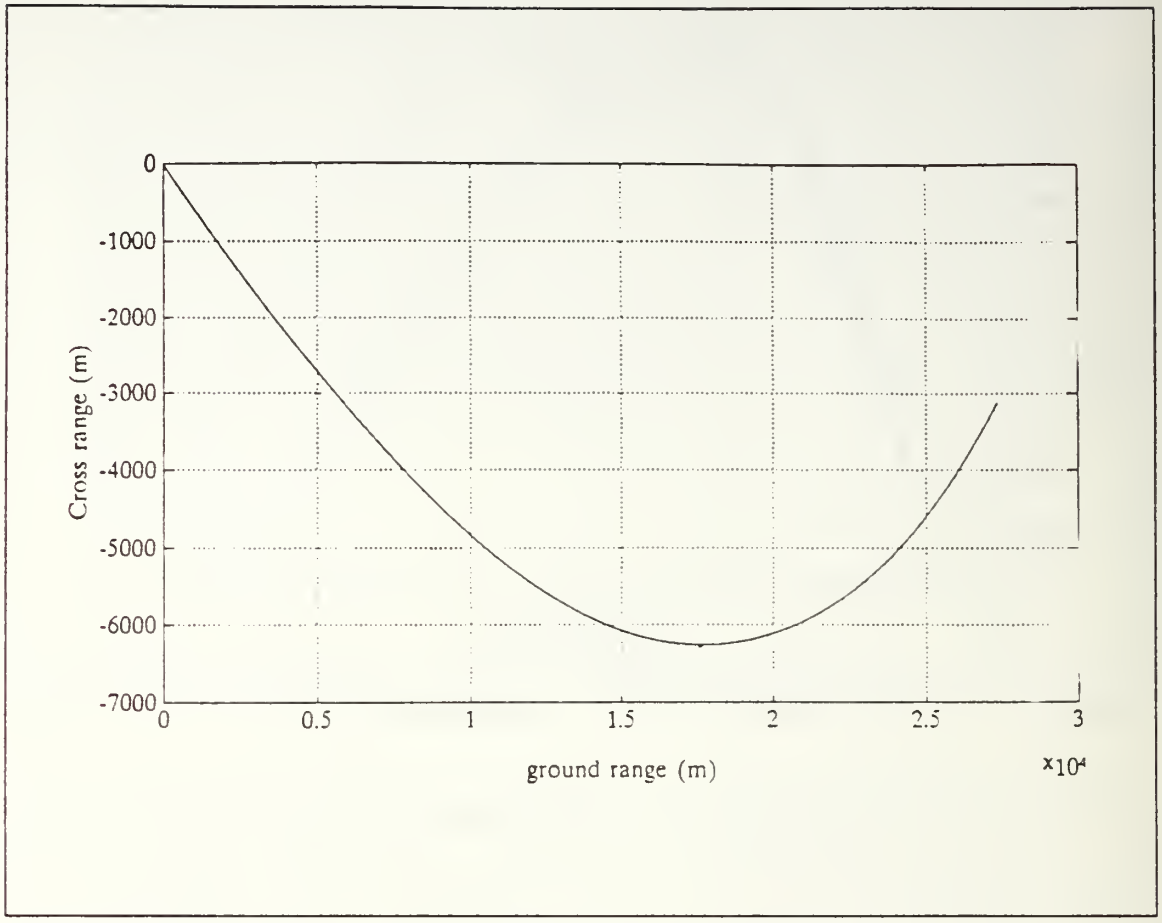

Figure 15. Projectile Trajectory: Cross Range vs. Ground Range.

c. Radar Tracking Parameters

The azimuth (traz) and elevation (trel) antenna pointing angles are required for tracking. The curves of these angles vs. in-flight time when the gun-radar distance is 500 m are shown in Figure 16 on page 31 and Figure 17 on page 31.

The azimuth and elevation angular speeds of the antenna are shown in Figure 18 on page 32, and Figure 19 on page 32.

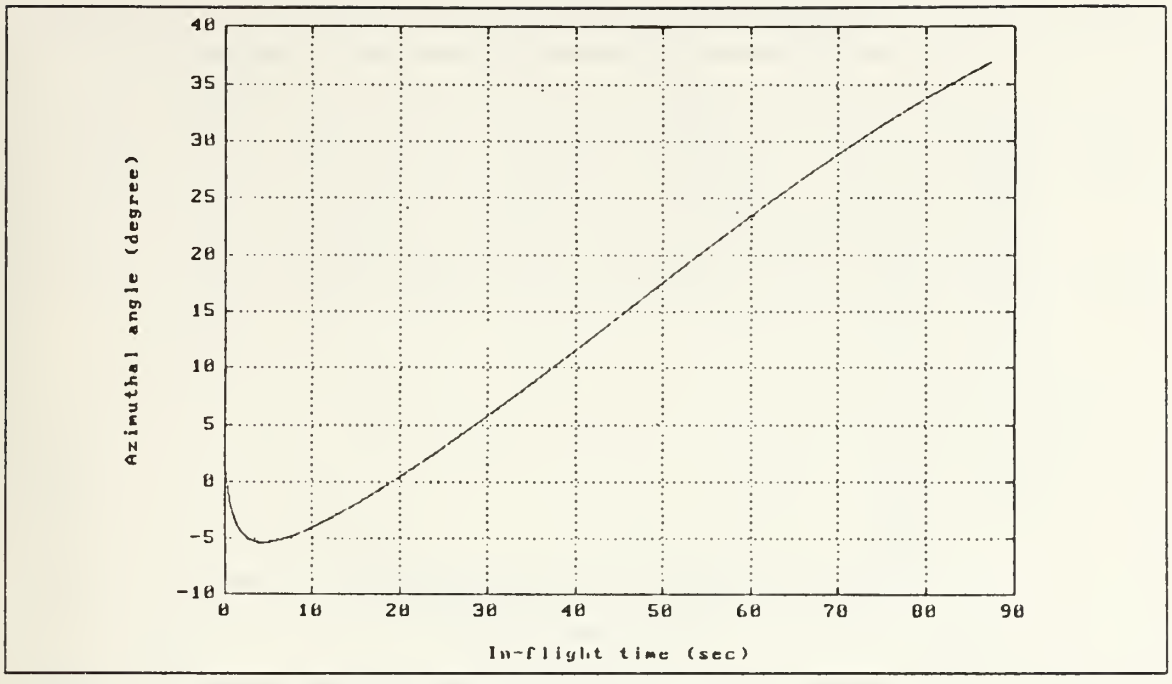

Figure 16. Radar Azimuthal Tracking Angle vs. Time.

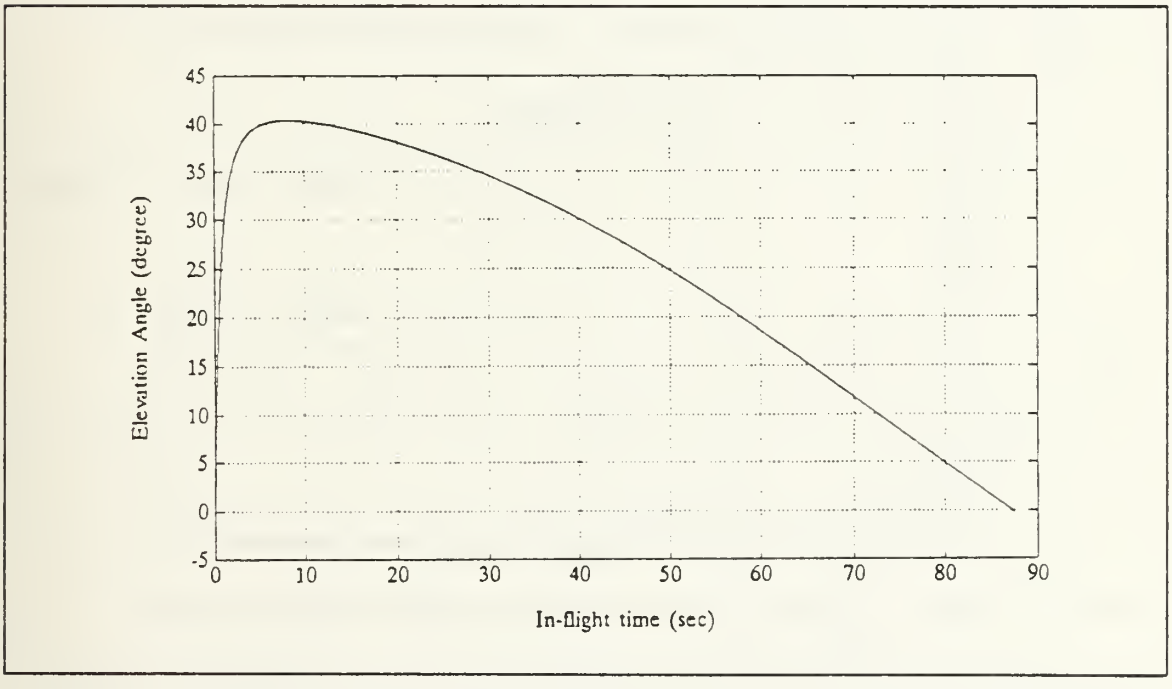

Figure 17. Radar Elevation Angle vs. Time.

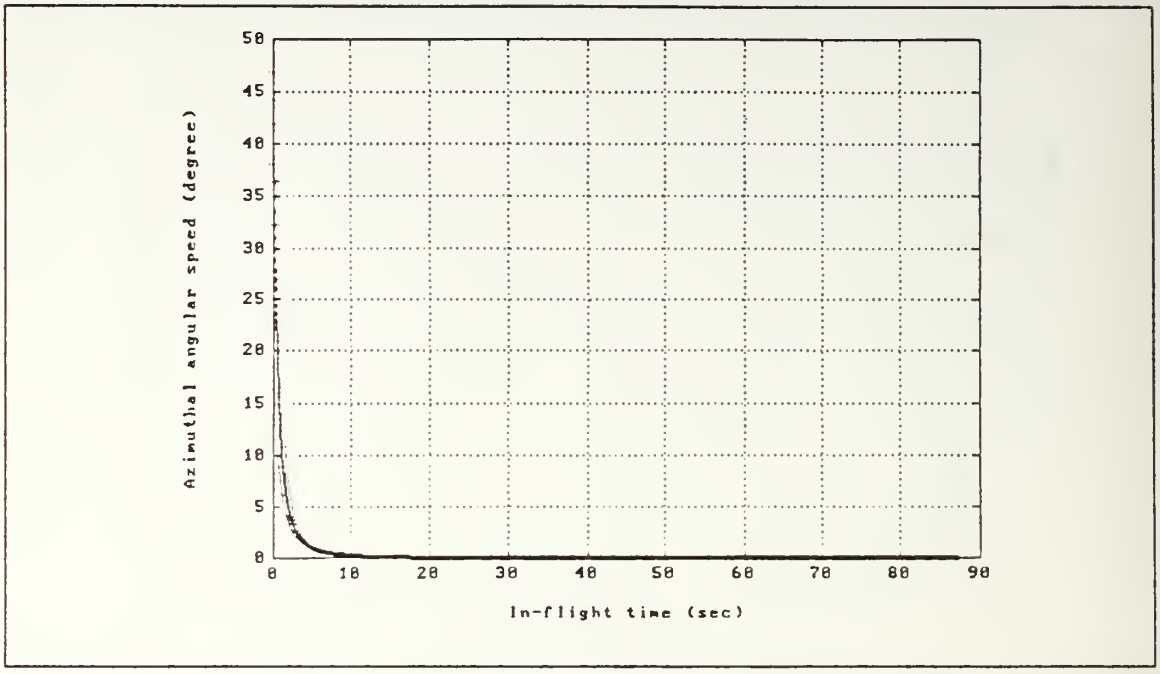

Figure 18. Radar Azimuthal Tracking Angular Speed vs. Time.

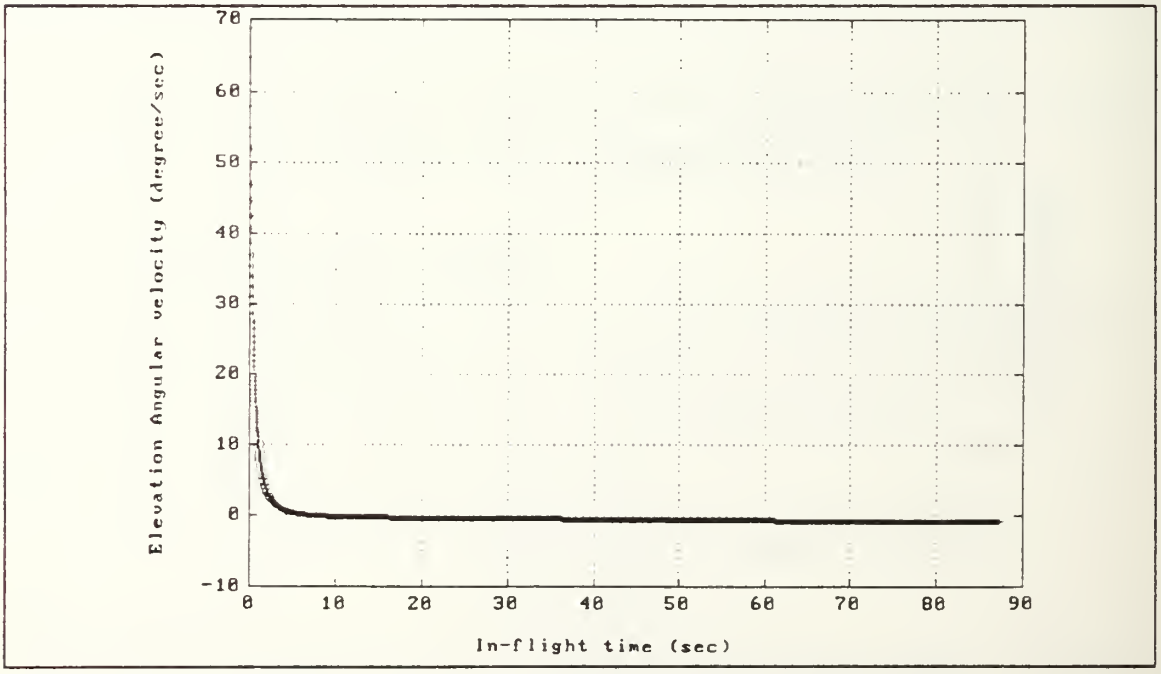

Figure 19. Radar Elevation Tracking Angular Speed vs. Time.

The antenna servo system has to point the antenna to within half a beamwidth in the direction of the projectile. Thus the half beamwidth divided by the angular speed of the antenna is the required response time of the servo system. The servo response time vs. the projectile in-flight time is shown in Figure 20 on page 33. From the above results, it can be seen that over the first few seconds, the elevation angular speed is very high. The distance between the gun and the radar can be increased to reduce this speed.

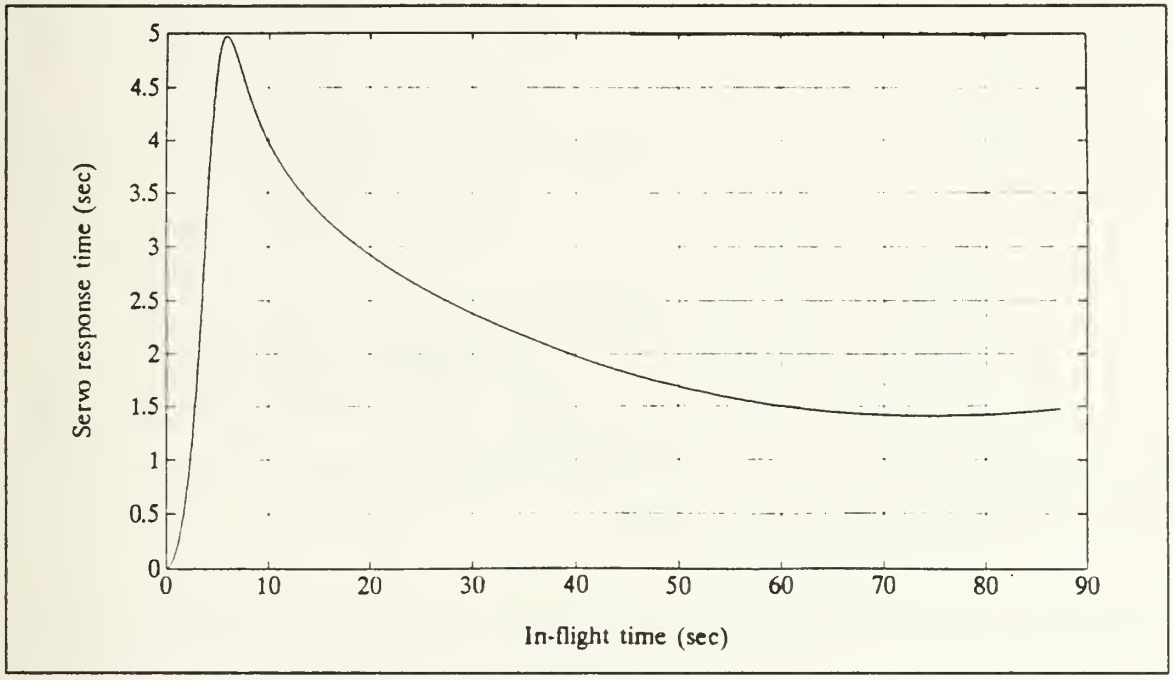

Figure 20. Servo System Response Time vs. Time.

d. Doppler Frequency and Velocity

The doppler frequency (f_d) is a directly measurable data by a CW radar. The doppler cycle can be detected with the square law detector. In the proposed CW radar configuration of this thesis, the doppler cycle is derived from the time interval T_n for each measurement base traveled. This timing sequence has to be simulated in the tracking program. In the simulation program, the doppler velocity (V_{dopp}) is calculated from the projectile velocity relative to the radar and the radar pointing direction. Then T_n is estimated from the time required to travel the distance MB with this doppler velocity. The curves of doppler frequency vs. slant range, doppler frequency vs. time, and doppler velocity vs. time are shown in Figure 10 on page 23, Figure 22 on page 34, and Figure 21 on page 34.

Based on the above results from trajectory simulation, the projectile radar cross section and the transmitter power can be estimated. They will be discussed later.

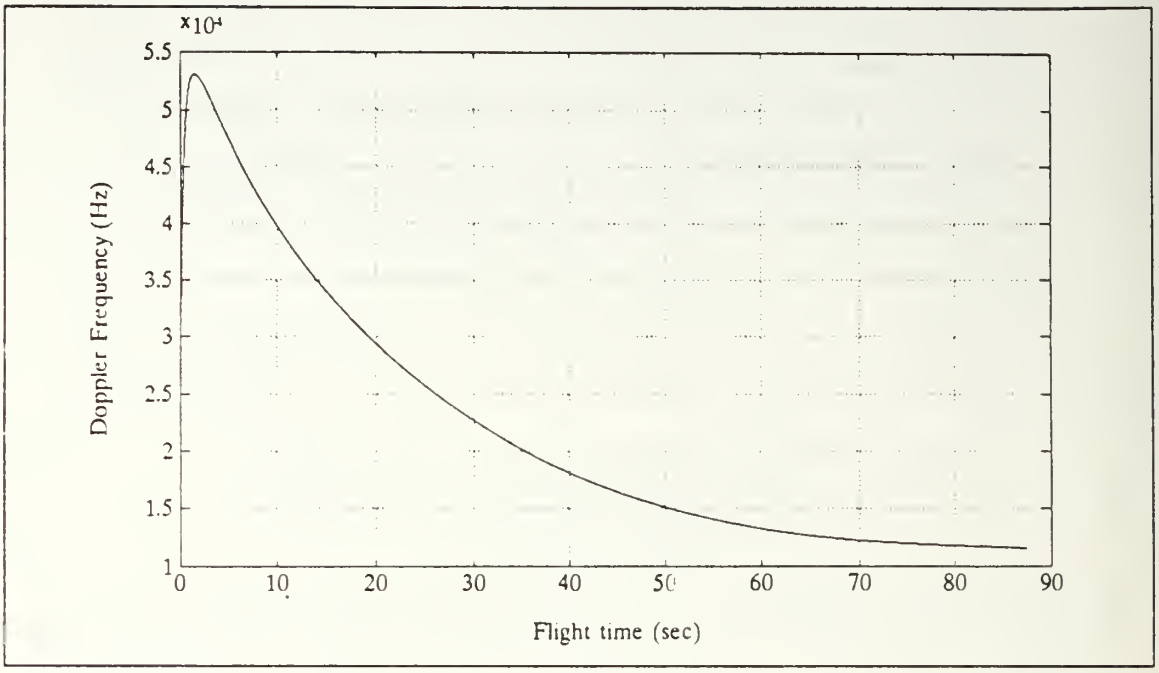

Figure 21. Doppler Frequency vs. Time.

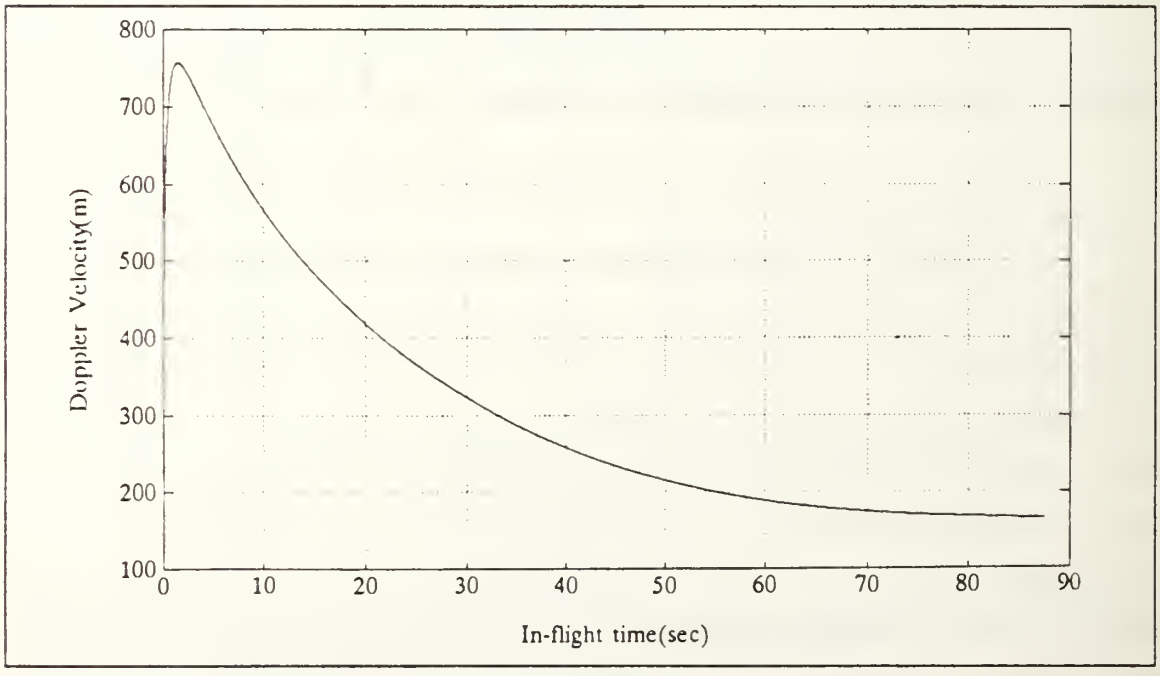

Figure 22. Doppler Velocity vs. Time.

C. PROJECTILE RADAR CROSS-SECTION

The projectile radar cross-section (RCS) is denoted by σ. It is the area intercepting the amount of plane wave power which, when scattered equally in all directions, produces an echo at the radar. In other words, the RCS is given by :

$$\sigma = 4\pi r^2 \left(\frac{E_s}{E_i}\right)^2 \tag{4.18}$$

where E_s is the scattered electric field strength from the target, r is the distance from the target in its far field where the quantity E_s is measured, and E_i is the incident plane wave field strength at the target.

Determination of the RCS of a complex target is difficult. Usually the radar cross-section of a target depends on the following factors: a) target size, b) target shape, c) radar frequency, d) target aspect angle, and e) radar polarization. The RCS is greatly simplified if the target size is large compared to the radar wavelength. Consider the radar cross-section of a simple sphere. The RCS as a function of the circumference of the sphere measured in wavelengths ($2\pi a/\lambda$) is shown in Figure 23 on page 36. The region where the target size is large compared to the radar wavelength, i.e., where $2\pi a/\lambda$ is greater than 10, is called the optical region [Ref. 9]. The RCS in this region is roughly the physical cross-section at area of the target.

The 155 mm projectile is in the optical region at the transmitter frequency (10525 MHz) of interest. Its RCS value will be approximated with its geometrical cross-sectional area. Because of the rotational symmetry of the projectile, the radar cross-section of the projectile is a function of the angle θ_{acp} between the radar pointing direction ($\hat{D}$) and the projectile heading ($\hat{h}$).

The radar pointing direction $\hat{D}$ is given by :

$$\hat{D} = \frac{\vec{r}_P - \vec{r}_R}{|\vec{r}_P - \vec{r}_R|} \tag{4.19}$$

where $\vec{r}_P$ is the projectile position vector, $\vec{r}_R$ is the radar position vector as defined in Chapter III.

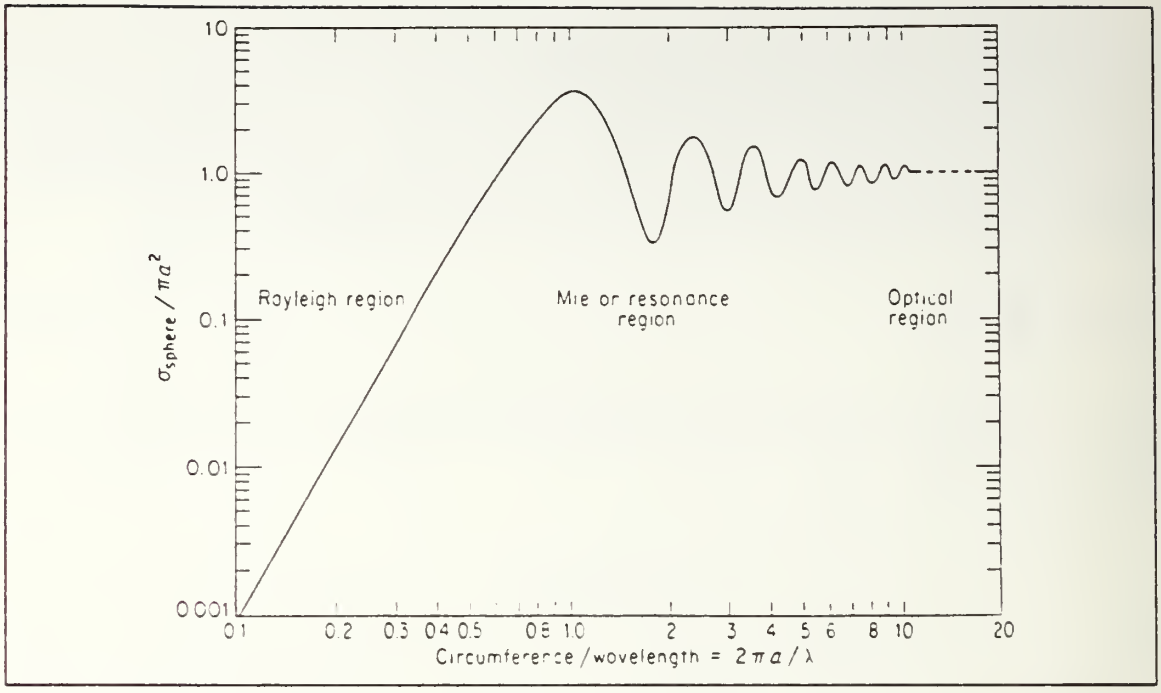

Figure 23. Radar Cross-Section of the Sphere vs. $\frac{2\pi a}{\lambda}$.

The heading of the projectile, $\hat{h}$, is in the direction of its air velocity. It is also defined in ChapterIII:

$$\hat{h} = \frac{(\vec{V} - \vec{W}_v)}{|\vec{V} - \vec{W}_v|} \tag{4.20}$$

In terms of $\hat{h}$ and $\hat{D}$, the aspect angle θ_{asp} of the projectile as seen from the radar is

$$\theta_{asp} = \cos^{-1}(\hat{D} \cdot \hat{h}) \tag{4.21}$$

Note that $0 \leq \theta_{asp} \leq \pi$. For simplicity, the projectile is considered as a circular cone on top of a circular cylinder, as shown in Figure 24 on page 37. The height of the cylinder is 414.4 mm. The height of the cone is 523.6 mm. The diameter of the cylinder and the base of the cone is 155 mm.

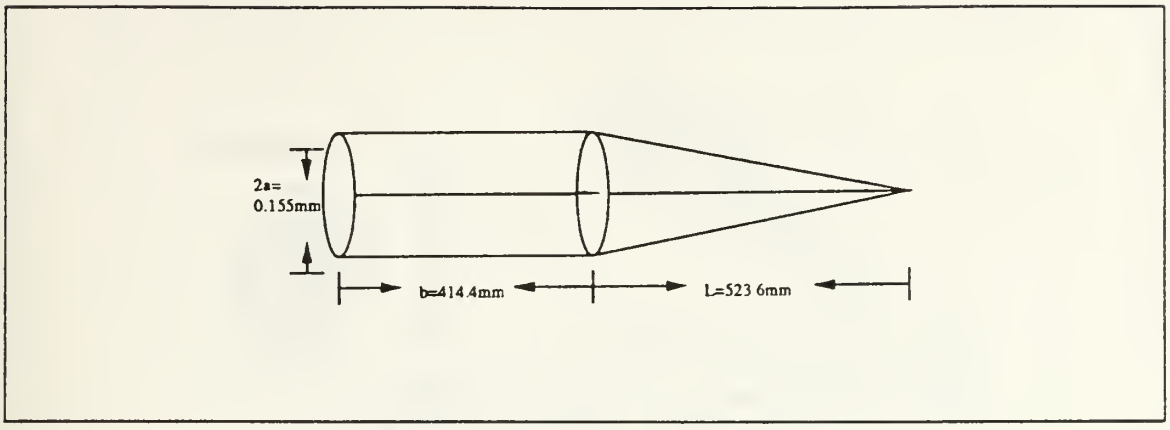

Figure 24. Approximate Shape of 155mm Projectile.

The vertex angle of the cone, 2α, is given by:

$$\alpha = \tan^{-1} \frac{155}{2 \times 523.6} \tag{4.22}$$

$$= 0.1469 \; rad. \tag{4.23}$$

$$= 8.42^{\circ} \tag{4.24}$$

The physical cross-section of the cone is the projected area of the projectile along $\hat{D}$, the radar pointing direction, onto a plane perpendicular to $\hat{D}$. This cross-sectional area will be discussed below according to whether $|\hat{D} \cdot \hat{h}| < \cos\alpha$ or $|\hat{D} \cdot \hat{h}| \geq \cos\alpha$.

1. **Case 1**

As $|\hat{D} \cdot \hat{h}| \geq \cos\alpha$, the projection of the projectile along $\hat{D}$ is shown in Figure 25 on page 38.

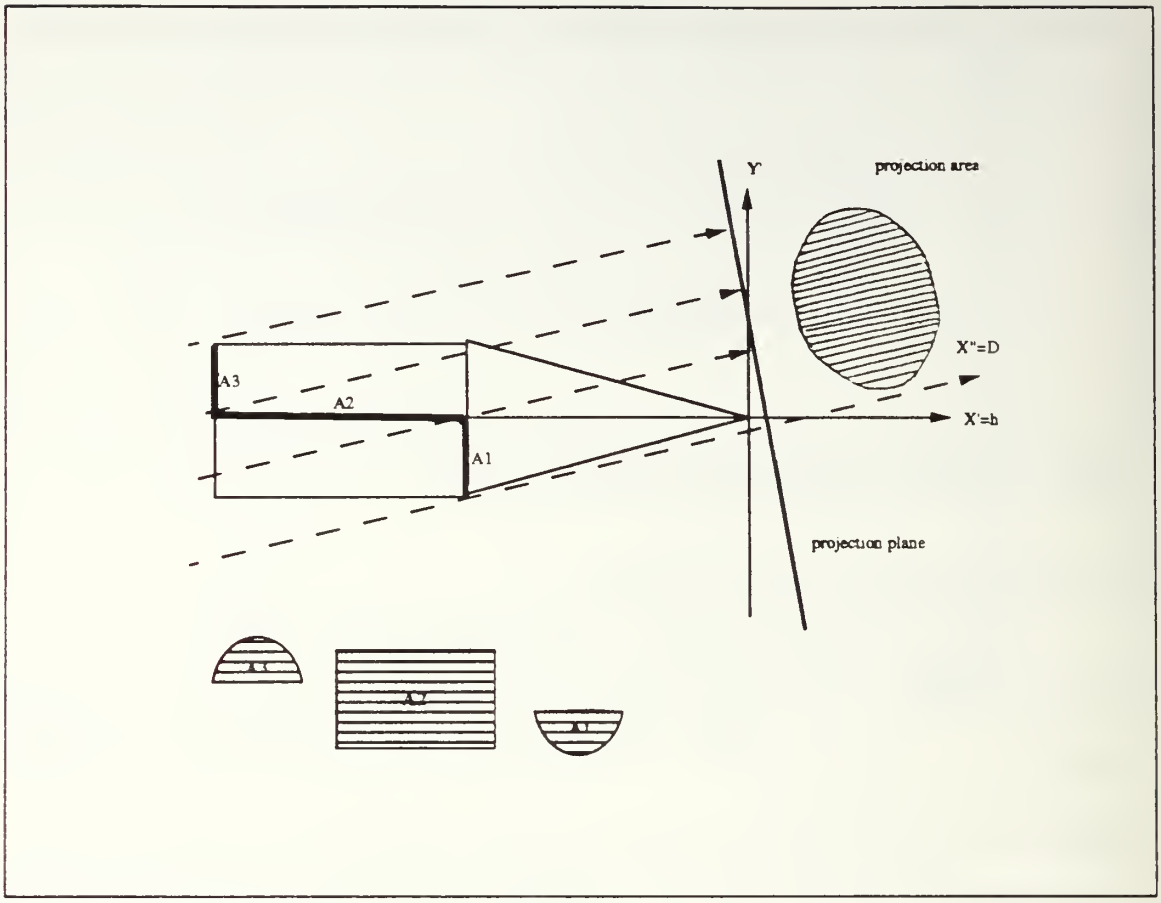

Figure 25. Radar Cross Section Case 1.

The total RCS value is

$$\sigma_t = \pi a^2 \mid \hat{D} \cdot \hat{h} \mid + 2ab \mid \hat{D} \times \hat{h} \mid \tag{4.25}$$

where a in the radius of the cylinder and b is the height of the cylinder.

2. Case 2

As $\mid \hat{D} \cdot \hat{h} \mid < \cos \alpha$, the total RCS is given by equation (4.20) (Figure 26 on page 39).

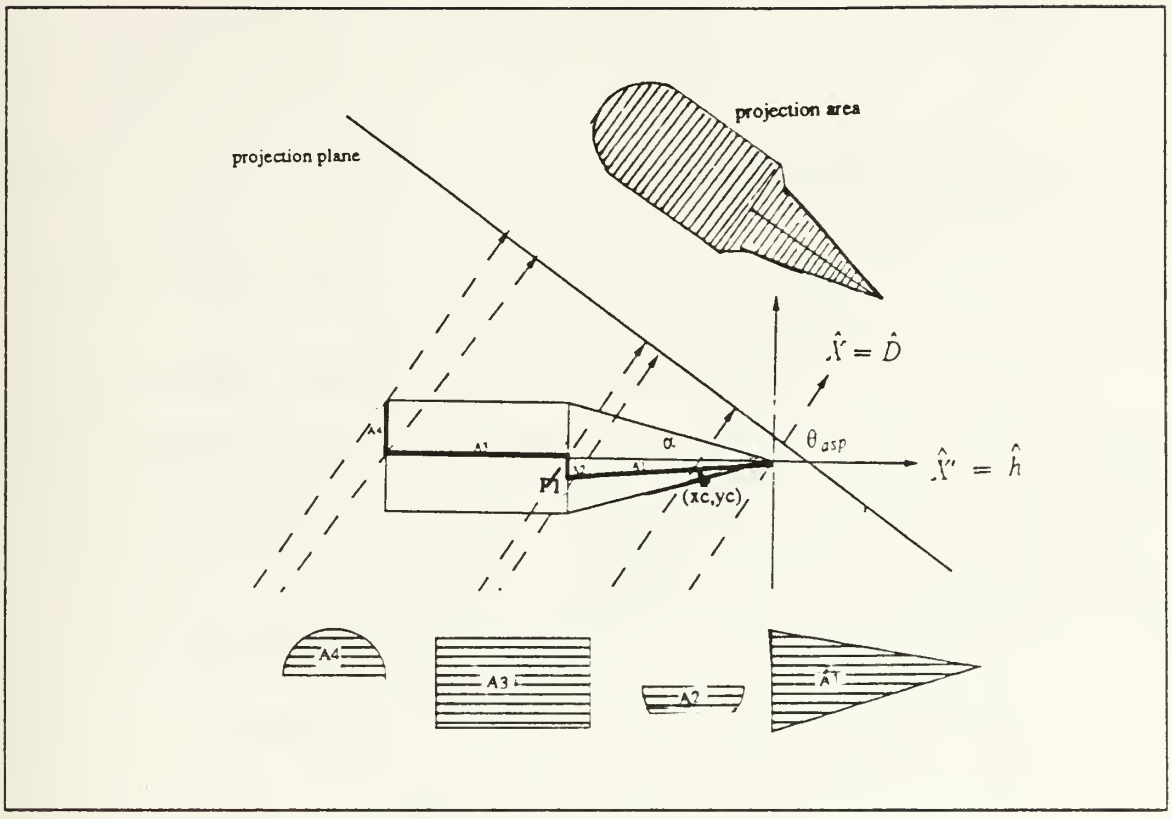

Figure 26. Radar Cross Section Case 2.

$$\sigma_t = \sigma_1 + \sigma_2 + \sigma_3 + \sigma_4 \tag{4.26}$$

$$\sigma_1 = \frac{L^2 \tan\alpha(\tan^2\theta + \tan^4\alpha)^{1/2}(\tan^2\theta - \tan^2\alpha)^{1/2}(\hat{D}\cdot\hat{N})}{\tan^2\theta} \tag{4.27}$$

$$= \frac{aL}{\sin^2\theta_{asp}}\left(1 - \frac{\cos^2\theta_{asp}}{\cos^2\alpha}\right)^{3/2} \tag{4.28}$$

$$\sigma_2 = a^2\left\{\sin^{-1}\left(\frac{\tan\alpha}{|\tan\theta_{asp}|}\right) + \frac{\tan\alpha}{|\tan\theta_{asp}|}\sqrt{1 - \frac{\tan^2\alpha}{\tan^2\theta_{asp}}}\right\}|\hat{D}\cdot\hat{h}| \tag{4.29}$$

$$\sigma_3 = 2ab\,|\hat{D}\times\hat{h}| \tag{4.30}$$

$$\sigma_4 = \pi a^2 \frac{|\hat{D} \cdot \hat{h}|}{2} \tag{4.31}$$

$$\hat{N} = \frac{\hat{D}\cos^2\alpha - \hat{h}\cos\theta_{asp}}{\sqrt{\sin^2\theta_{asp}\cos^4\alpha + \sin^4\alpha\cos^2\theta_{asp}}} \tag{4.32}$$

where L is the height of the cone and $\hat{N}$ is the normal vector of the surface A_1. The detailed derivation of the RCS equations is given in Appendix B.

From the above results, the RCS value of the projectile in-flight can be predicted. It is shown in Figure 27 and Figure 28 on page 41. From above figures, it can be seen that the maximum RCS is about 0.09 m^2 and the minimum RCS is about 0.02 m^2. Since the aspect angle of the projectile changes very fast right after it is fired, the RCS value varies rapidly at the beginning of the trajectory.

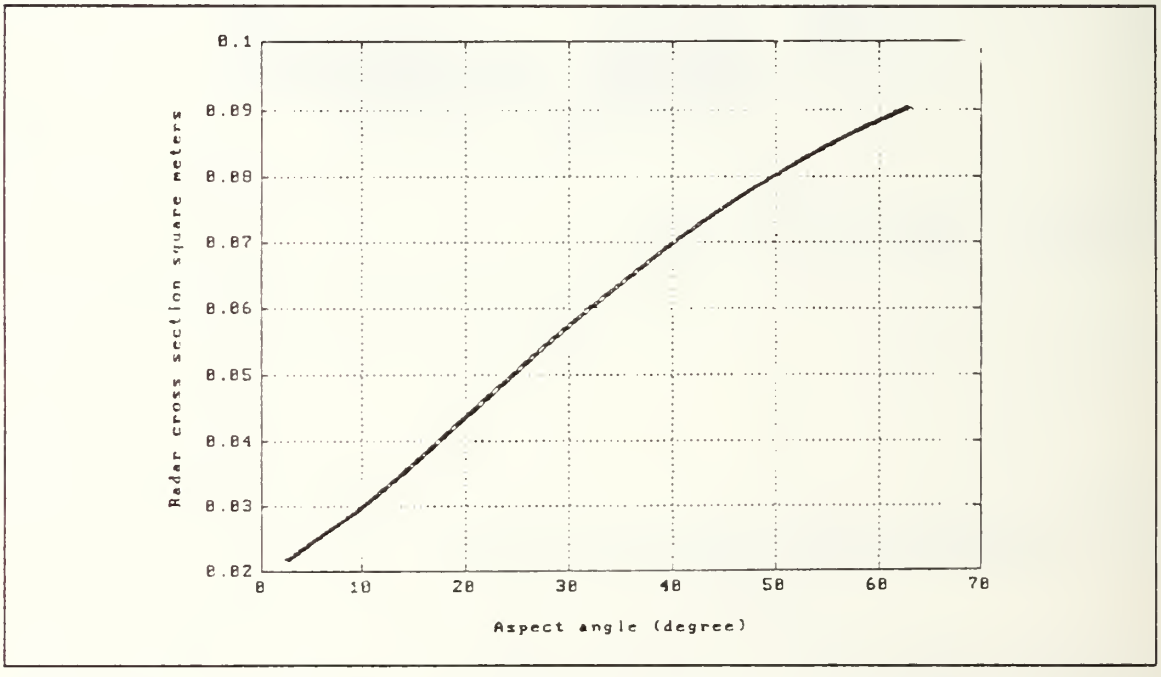

Figure 27. The In-Flight Projectile Radar Cross Section vs. Aspect Angle.

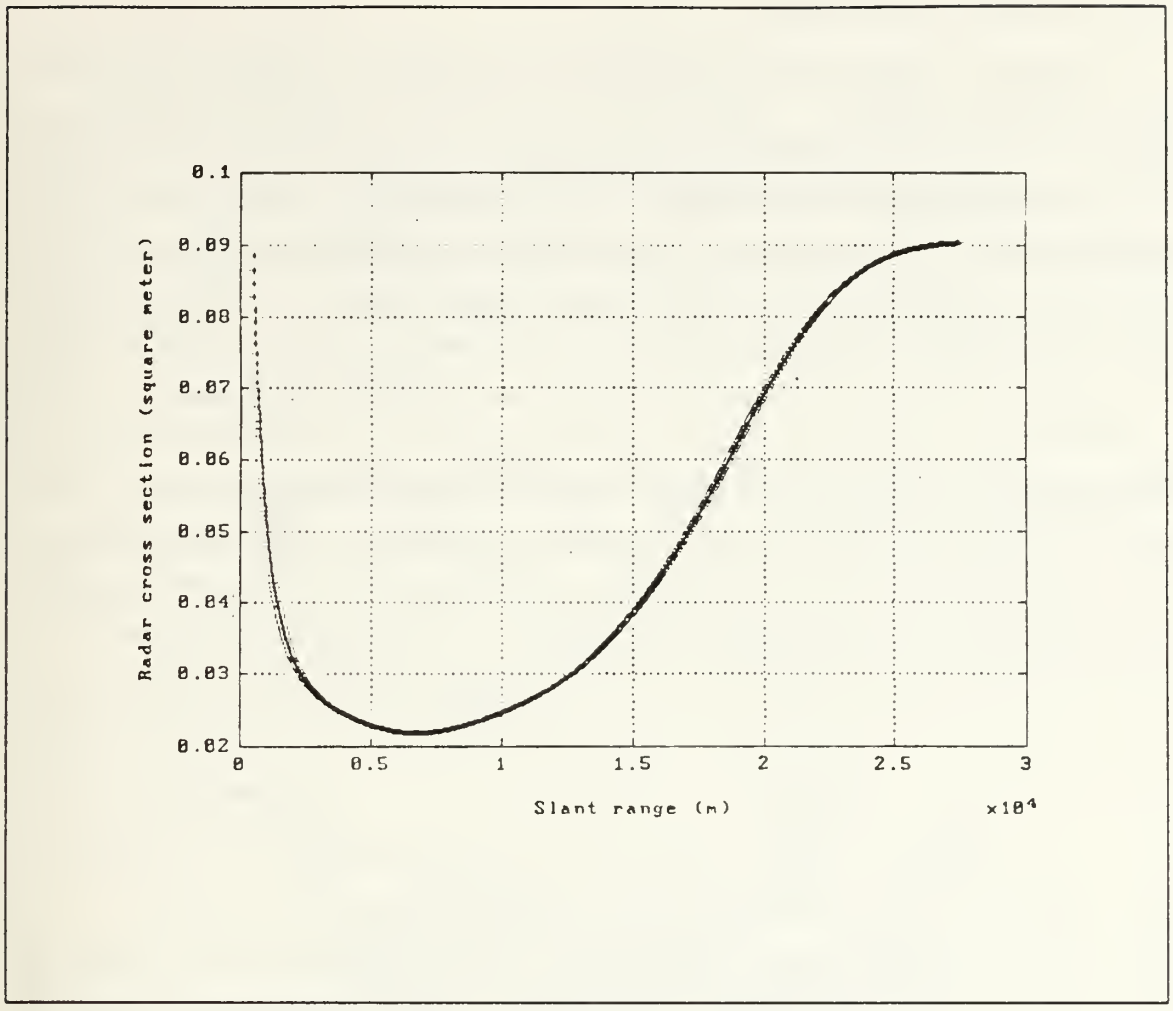

Figure 28. In-Flight Projectile Radar Cross Section vs. Slant Range.

D. PROPAGATION EFFECTS

Propagation of radio waves through the Earth's atmosphere is significantly affected by the propagation medium. The presence of the Earth complicates the situation in three ways: (a) the surface of Earth scatters radiation and produces an interference pattern, (b) the Earth casts a shadow and gives rise to diffraction phenomena, and (c) the Earth's atmosphere is inhomogeneous and produces refraction effects [Ref. 13]. It is customary to group all these factors into a single quantity called the propagation factor (F). In this thesis, the Engineer's Refractive Effects Prediction system (EREPS) [Ref. 14] is utilized to compute the propagation factor based on local environment.

EREPS uses ray tracing for radio wave propagation within the horizon. It includes the bending effect of the refractive index variation of air and the divergence factor when the ray is reflected from the Earth. The field at the target is the sum of the direct ray and the reflected ray, resulting in interference peaks and nulls which become significant when the target falls near the horizon (Figure 29).

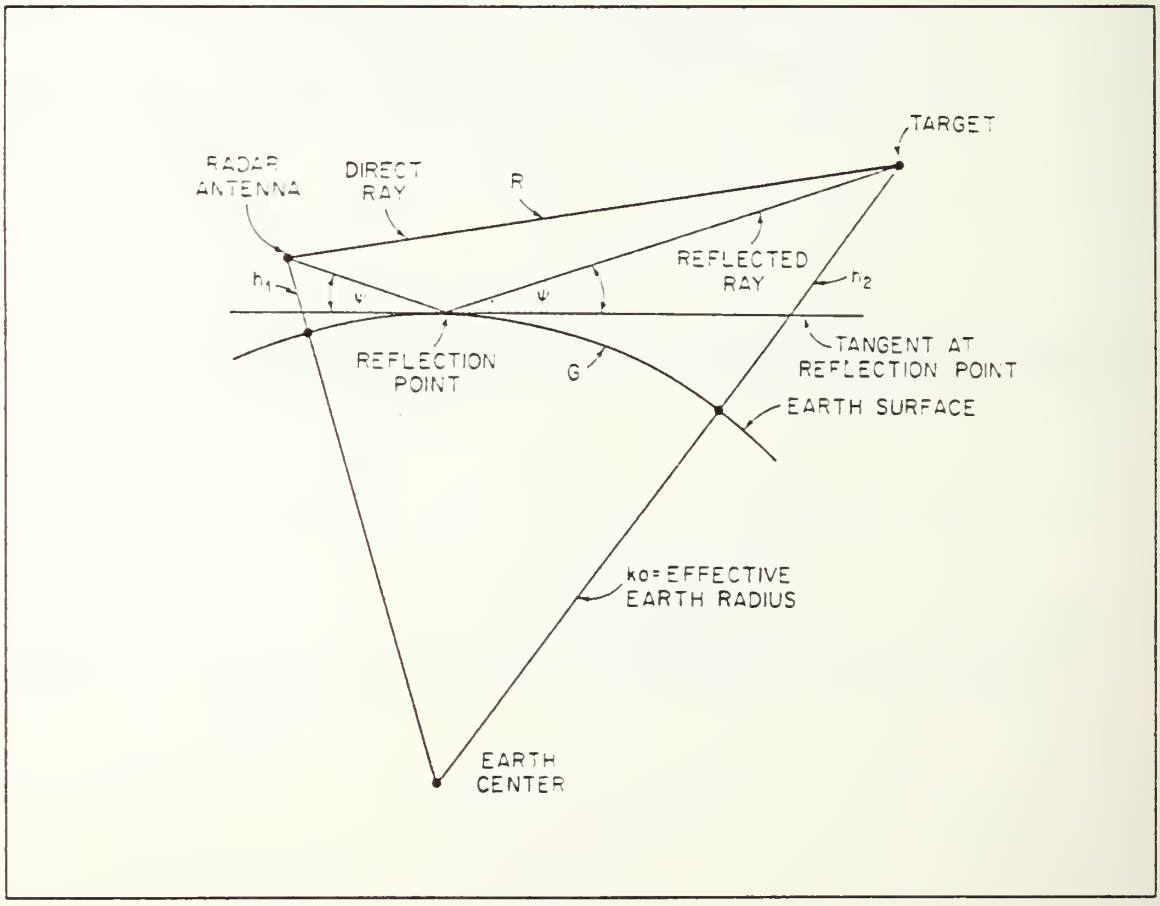

Figure 29. Reflection and Interference from a Spherical Earth.

For the over-the-horizon region, the waveguide mode approach is adopted by EREPS. The Earth's atmosphere is modeled as a leaky waveguide. The Earth's surface is the lower boundary of the guide. Modes of high attenuation along the horizontal direction are called leaky modes. Modes of low attenuation are called trapped modes. In x-band, the effect of the evaporation duct is significant. Trapped modes occur when the evaporation duct height is large or at least comparable to the radar wavelength (see Figure 30 on page 44) [Ref. 15].

1. Computation

A typical EREPS output is given in Figure 30 on page 44. The local annual average meteorological conditions for propagation are available [Ref 13]. The following parameters are used :

1. Evaporation duct height : 13.1m
2. k (effective Earth radius factor) : 1.45
3. Wind speed : 6 m/s
4. Absolute humidity : 10g m^2
5. Surface refractivity : 370.

Note that the projectile is at a particular height when it arrives at a range. This computation has to be repeated for each point along a projectile trajectory. This is done for several trajectories at various ranges (Figure 32 on page 45 and Appendix C). Also note that, in Figure 32 on page 45, the ground range is given a negative sign because it is measured from the point of impact toward the radar.

2. Summary of Results

a. Signal Strength Enhancement

From Figure 32 on page 45, it can be seen that, with ducting, which is present most of the time at the test site, the return signal will be substantially enhanced from the corresponding free space value. (Note that the computation is carried out for a target at 1 m height, i.e., when the projectile is near its point of impact. The applicable range for the projectile of interest lies between 27 to 28 km.) Thus ducting is helpful in enhancing the quality of the recorded full range tracking data.

b. Strong Interference

As shown in Figure 32 on page 45, the return signal will exhibit strong interference when the projectile reaches about 250 m within the point of impact. The more

than ± 15 dB fluctuation makes it difficult to track the projectile in this region using the simple CW system proposed in this thesis. On the other hand, since this strongly fluctuating region is within a few hundred meters from the impact point, this small portion of the trajectory can be estimated with good accuracy. Hence it is desirable to select a 'stop-processing point' at which the CW real-time radial velocity and range computations will be halted. The radar antenna will be guided by the predicted trajectory, and the return video signal will still be recorded.

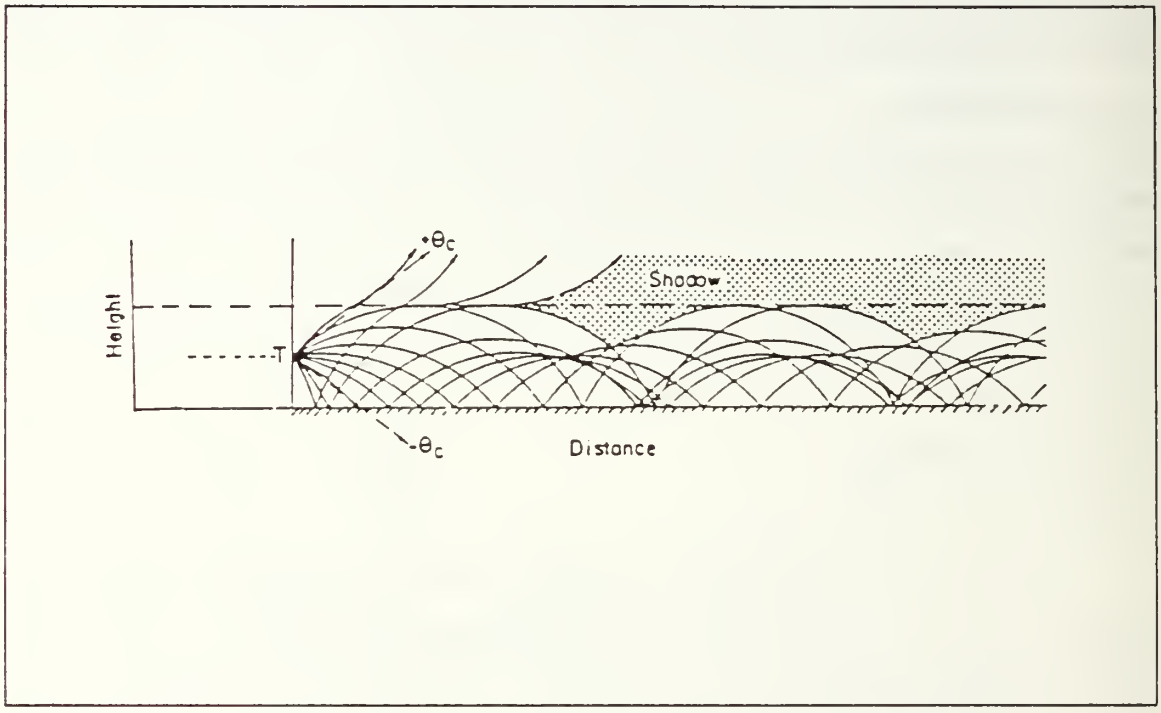

Figure 30. Waveguide Mode with Ducting Height and Antenna Height.

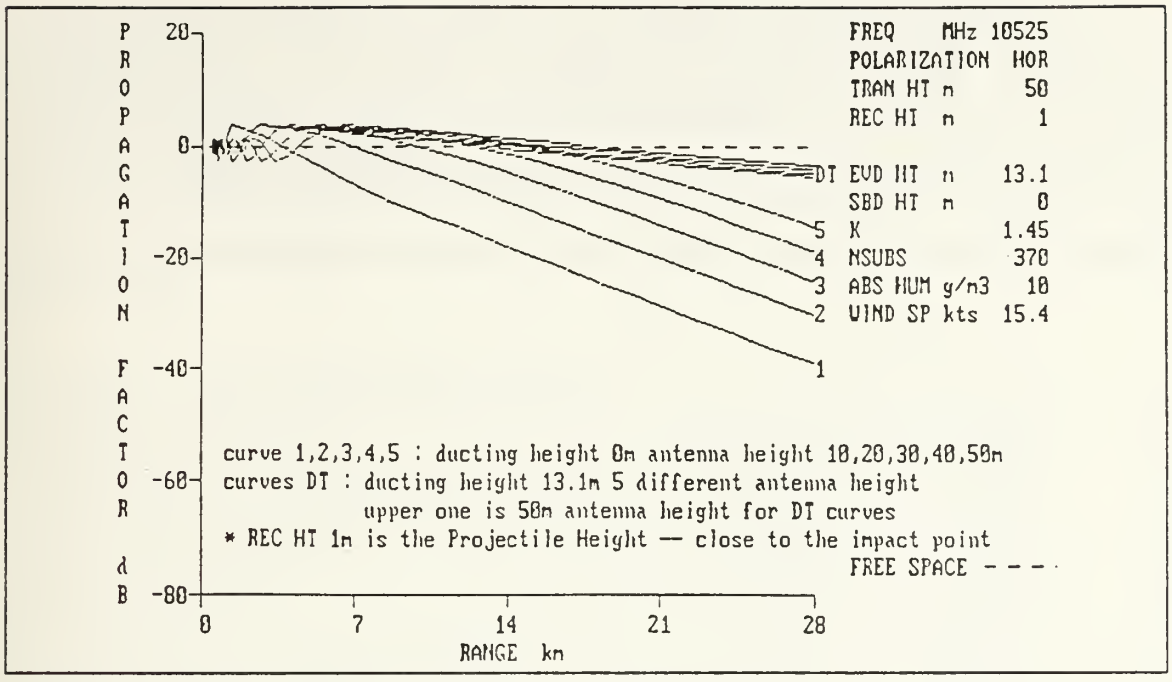

Figure 31. Propagation Factor with 13.1m Duct Height.

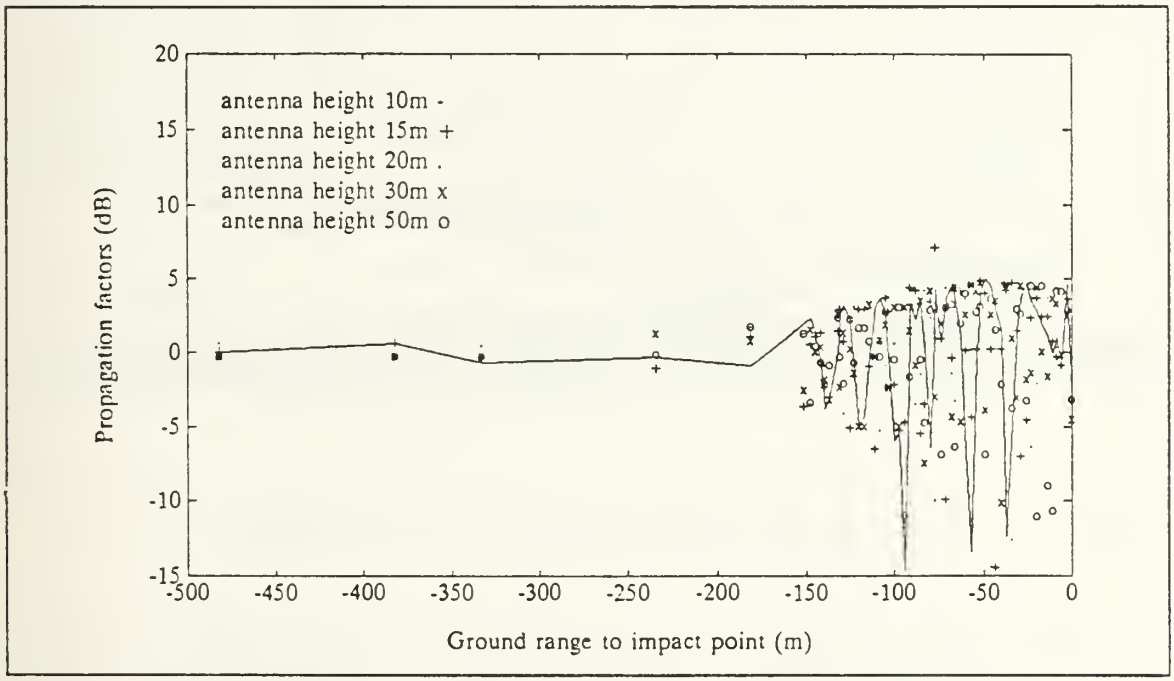

Figure 32. Propagation Factors vs Ground Range from Impact Point.

3. Stop-Processing Point

It should be noted that EREPS does not take into account the antenna radiation pattern. Since the antenna to be used have a beamwidth of 1° only, interference between the direct ray and the reflected ray will not be important until the antenna elevation angle is lowered to within 0.5° above the horizontal direction (Figure 33 on page 46).

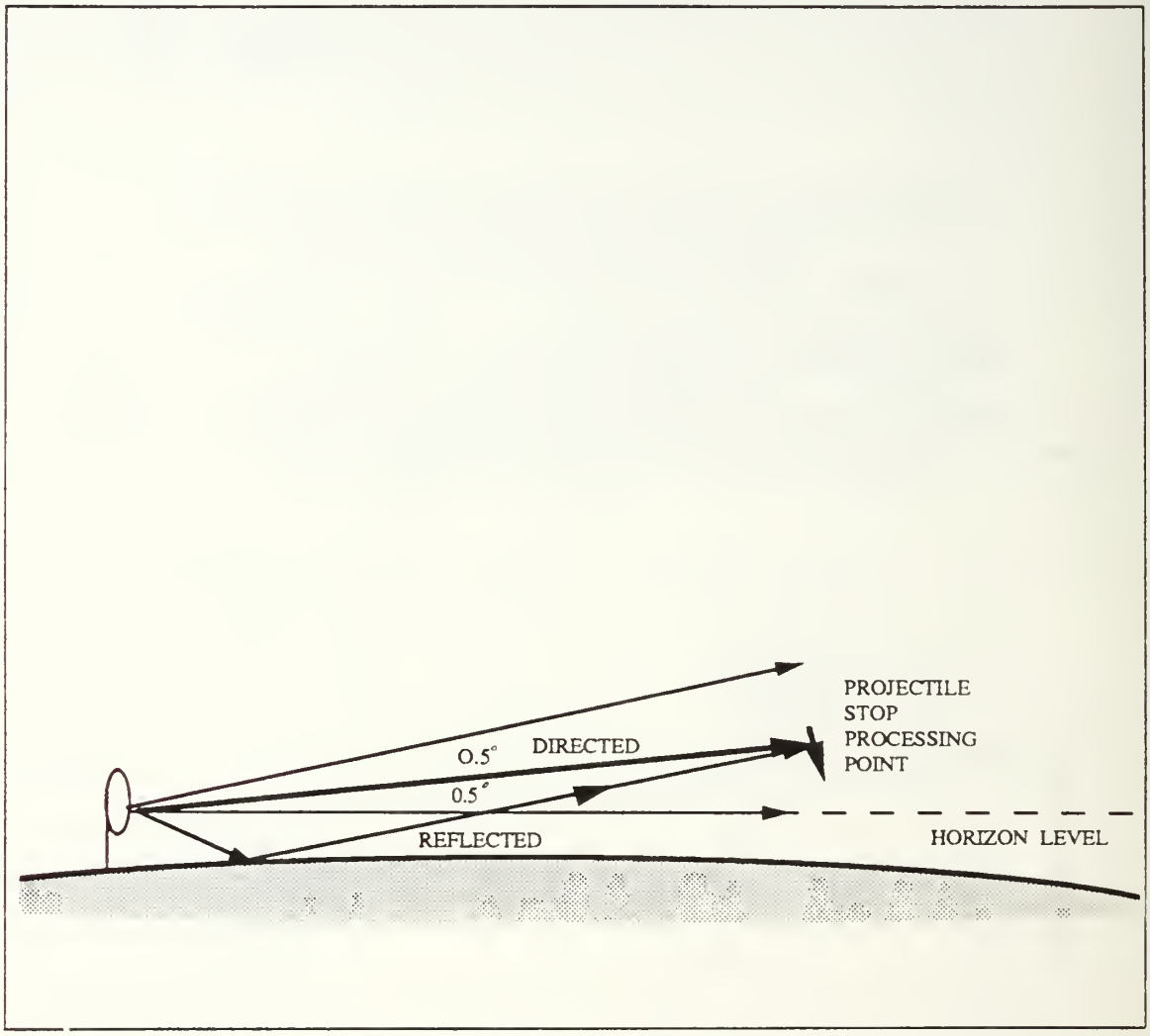

Figure 33. Narrow Beamwidth Effect on the Spherical Earth Surface.

This criterion can be used to determine the stop-processing point as follows: when the system records an antenna elevation angle falling below 0.5°, the square-law detector and the comparator will be switched off. The servo will steer the antenna according to the predicted trajectory smoothly toward the projectile point of impact. Characteristics

for two such stop-processing points for a radar-to-gun distance of 500 m and two different radar heights of 10 m and 30 m respectively are displayed in Table 1 on page 47. Note that these point are close to where the propagation factor starts to fluctuate strongly as predicted by EREPS.

Since the processing of real-time data is stopped before contributions from the reflected ray become important; in what follows, the propagation factor will be considered as unity.

Table 1. STOP PROCESSING POINT.

Antenna height (m)	10	30
Radar to gun distance(m)	500	500
Projectile height (m)	308	305
Slant range (km)	27.53	27.53
Impact range (km)	27.69	27.57
Ground range to impact point (m)	158	157
Elevation angle (degree)	0.49	0.45
Elevation angle at impact point (degree)	-0.15	0.19
Elevation angle difference (degree)	-0.64	-0.64
Azimuth angle (degree)	36.5	36.5
Azimuth angle at impact point(degree)	36.9	36.9
Azimuth angle difference to impact point(degree)	0.39	0.39
In-flight time (sec)	86.48	86.48

E. POWER REQUIREMENT

From equation (4.1), the power requirement for tracking up to the stop-processing point is shown in Figure 34. In order to reduce the required transmitter power requirement, a multiple filter design is proposed for this system.

The multiple filter design is based on the characteristics that, after an initial rise, the doppler frequency decreases with increasing slant range (Figure 35 on page 49). By switching to video filters of narrower bandwidths at longer ranges, the coherent integration time of the radar is increased hence the power requirement can be lowered. Combining the fixed range independent parameters in the radar range equation, the power requirement can be expressed as :

$$P_t = (3.7339 \times 10^{-22}) \times \left(\frac{R^4 B_v}{\sigma}\right)_{\max} \tag{4.33}$$

$$= C \times \left(\frac{R^4}{\sigma}\right)_{\max} f_{dmax} \tag{4.34}$$

$$C = 4.4807 \times 10^{-22} \tag{4.35}$$

where B_v is $1.2 f_d$.

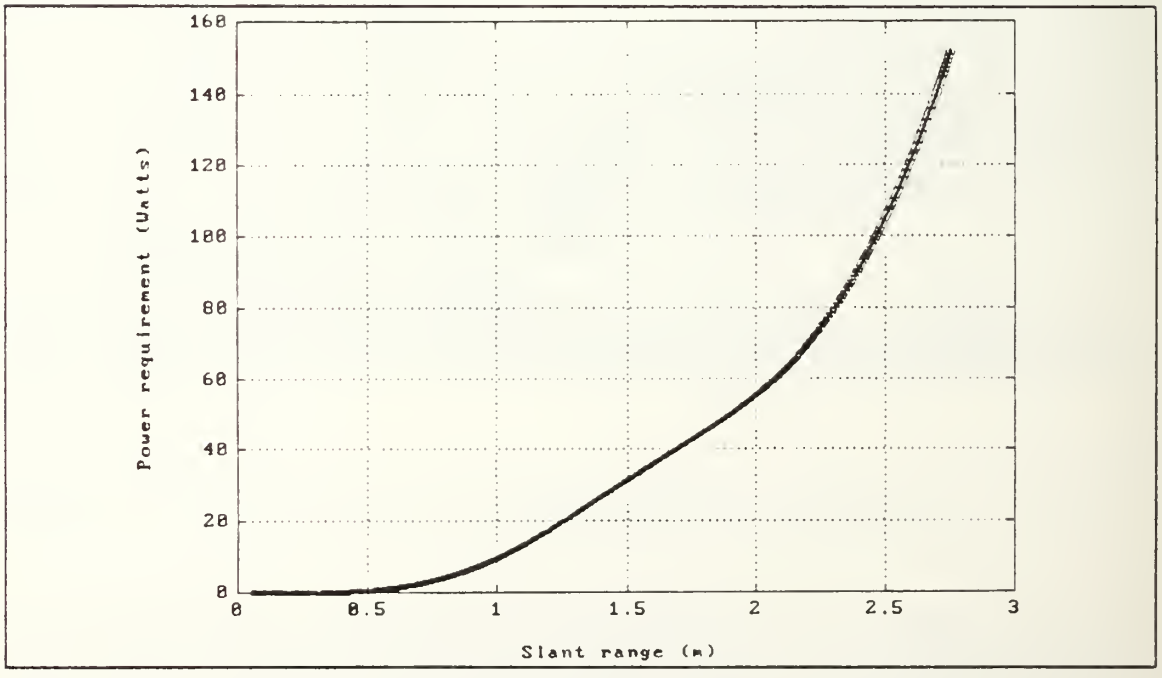

Figure 34. Power Requirement for Full Range Tracking without Multiple Filters.

Since f_d, σ and R are functions of the trajectory (Figure 35 on page 49, and Figure 36 on page 50), if the tracking range is divided into three regions 1, 2, and 3, and one filter is used for each region, the transmitter power requirement becomes :

$$P_t = C(\frac{R^4}{\sigma})_{1,max}(f_d)_{1,max} \tag{4.36}$$

$$= C(\frac{R^4}{\sigma})_{2,max}(f_d)_{2,max} \tag{4.37}$$

$$= C(\frac{R^4}{\sigma})_{3,max}(f_d)_{3,max} \tag{4.38}$$

where the constant C is the same as that of equation (4.34).

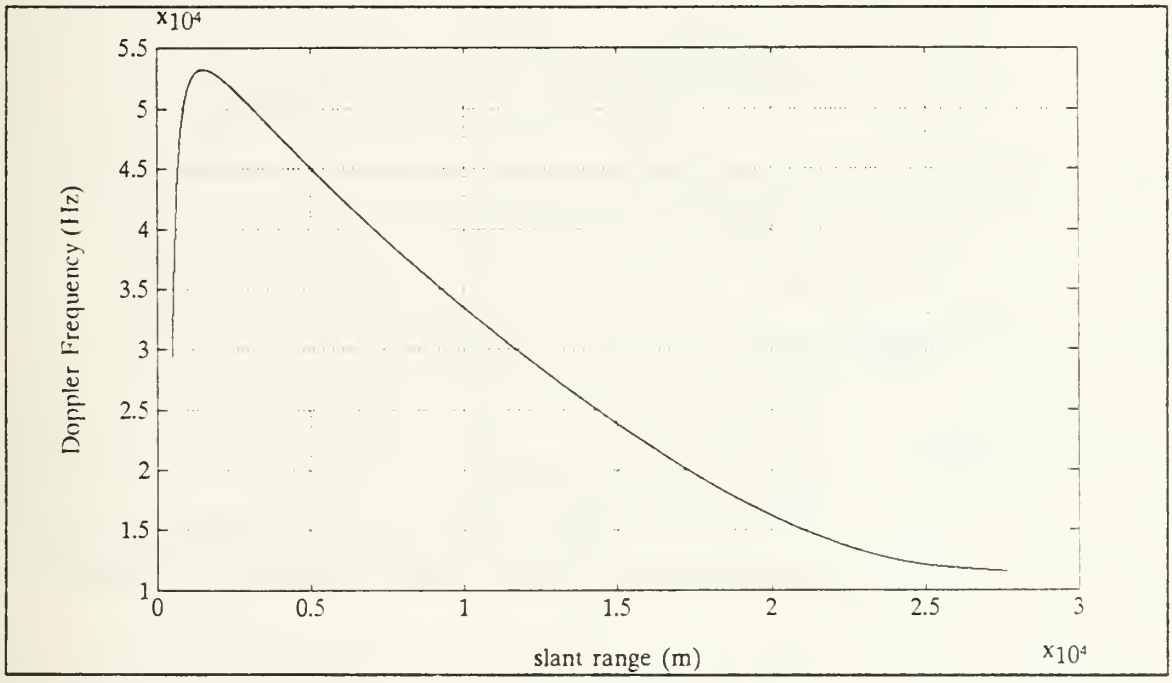

Figure 35. Doppler Frequency vs. Slant Range.

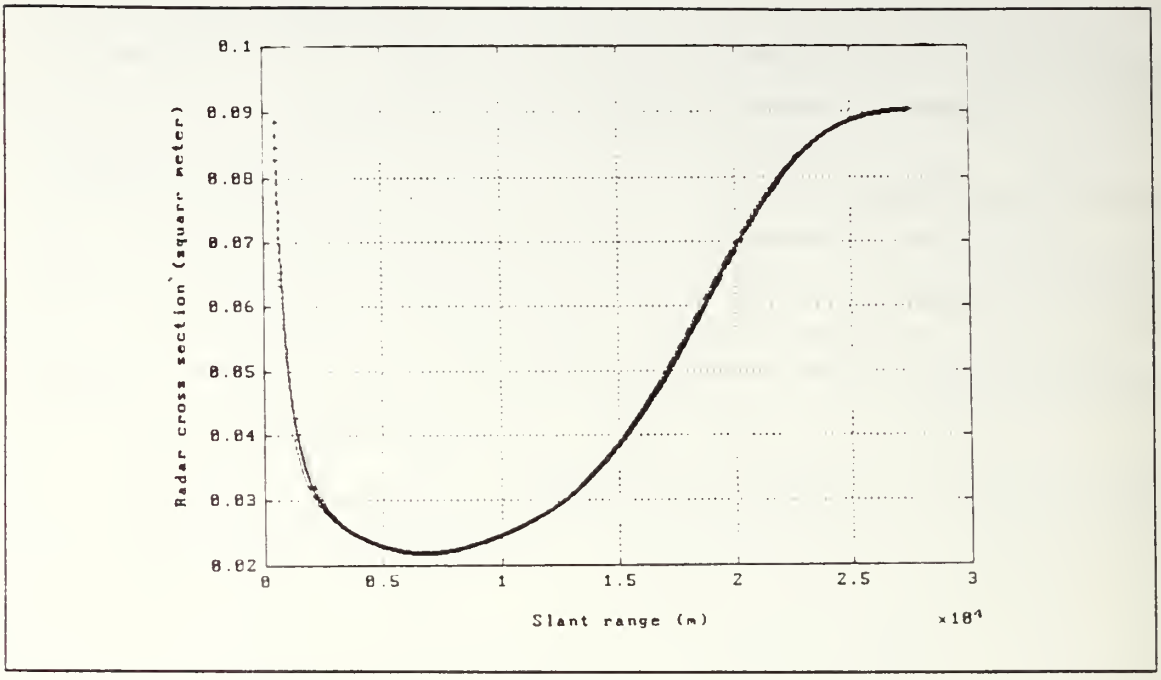

Figure 36. Radar Cross Section vs. Slant Range.

The power requirement written in terms of that of the single filter case is:

$$P_t = \frac{C(\frac{R^4}{\sigma})_{max} f_{dmax}}{C_p} \tag{4.39}$$

where C_p, the power reduction factor, is the factor by which the power requirement is reduced.

In order to find the optimal switch-over points for the filters, the logarithm of f_d versus R^4/σ, normalized to $(f_d)_{max}$ and $(R^4/\sigma)_{max}$ respectively, is plotted (Figure 37 on page 51).

Assume that the first switch-over point is located at (x_1, y_1), and the second one is located at (x_2, y_2). These values can be determined from Figure 37 on page 51 by observing that, at the optimal switch points :

$$x_1 = y_1 + x_2 \tag{4.40}$$

$$= y_2 \tag{4.41}$$

The optimal locations so obtained are listed in Table 2 on page 52. The power reduction factor is $C_p = 10^{0.6218} = 4.186$, as seen from Figure 37 on page 51.

The power requirement as a function of slant range when three filters are used is plotted in Figure 38 on page 52. The antenna height is 10 m and the radar-to-gun distance is 500 m. The required power is 37 Watts. A conventional CW tracking system will track to the summit point only. This point is located at a range of region 1 and requires a transmitter power of 19.5 Watts. Almost full-range tracking is possible by doubling the conventional power through the use of multiple filters.

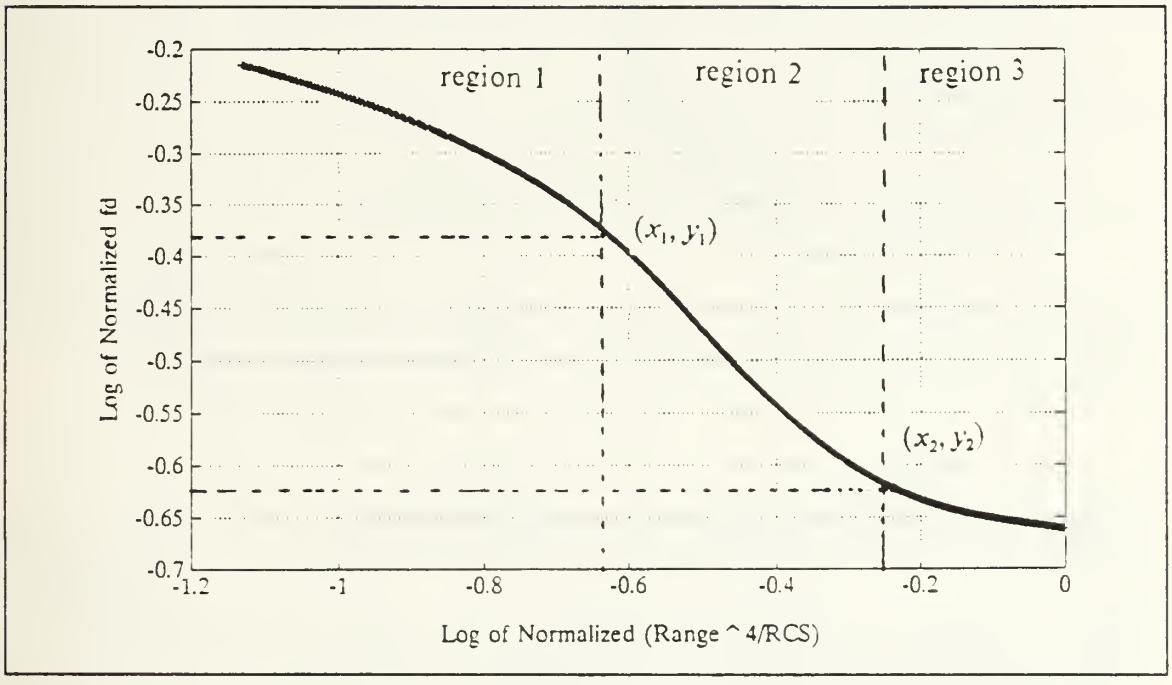

Figure 37. Log(Normalized f_d) vs. Log(Normalized R^4/σ).

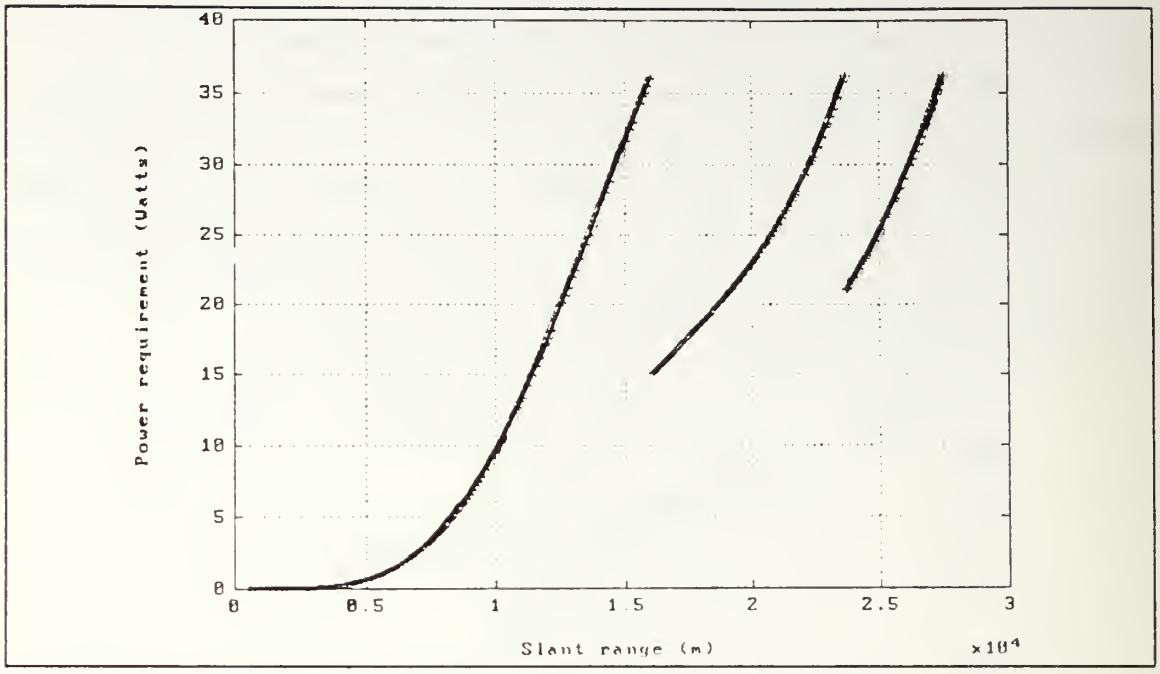

Figure 38. Power Requirement for Trajectory Tracking with Multiple Filters.

Table 2. MULTIPLE FILTERS SWITCH POINTS

Parameters	region 1	region 2	region 3	stop tracking point
Slant range (km)	16.06	23.73	27.53	27.53
Maximum f_d (kHz)	53.25	22.03	12.72	---
Video bandwidth (kHz)	63.90	26.44	15.27	---
Radar cross section (m^2)	0.0385	0.0438	0.0862	0.0903
Required power (Watts)	36.29	36.23	36.29	---

V. CONCLUSIONS

It is demonstrated in this thesis that full-range projectile tracking, with real-time track processing stopped at a range within 160 m of the projectile point of impact, can be achieved if the transmitter output power is 37 watts or higher and a set of three switchable filters are used. If a single filter is used, an output power of 160 watts is required. Either configuration can be implemented with a commercially available, small size, air-cooled RF amplifier which can be mounted near the transmitting antenna.

The tracking relies on the predicated trajectory. Although real-time doppler information is available from the radar, it is used only to confirm that the projectile is on track. A algorithm to utilize this real-time information for updating the predicted trajectory is desired. Kalman filtering appears to be a promising technique which deserves further investigation.

APPENDIX A. PROJECTILE TRAJECTORY SIMULATION AND RANGE ANALYSIS

```
clear
t2=clock;
format long e;
% The first capital letter designations are:  P for the projectile;
 % G for the gun (muzzle); R for the radar.

% The numerals 1, 2, 3 are for the radial, theta and phi components in
 % an inertial spherical coordinate system; 4 is for the radial component
 % in the cylindrical coordinate system associated with the spherical
 % coordinate.  The origin is at the center of the Earth; the polar (z)
 % axis is the axis of spin of the Earth.

% East and South designations are local quantities in a frame rotating
   % with the Earth

% constant declaration
  EarthT=86164.06;                    % sidereal period of Earth spin
  EAV=2*pi/EarthT;                    % Earth angular velocity
  a=(6356912+6378533)/2;              % approximate Earth radius
  g=9.81;                             % gravitational acceleration

  RLATI=24+36/60+38/3600;             % latitude 24o36'38" (radar site)
  RLONGI=121+52/60+27/3600;           % longitude 121o52'27" (radar site)
  f=10525E6;                          % radar transmitted frequency Hz
  lambda=3E8/f;                       % radar transmitted wavelength m
%input parameters
 !del ww
 diary ww
  RB=input('radar to gun base distance(m) =?      ')
% RBaz=input(' radar to gun direction from east=?    ')*pi/180
  RBaz=0;
% MN=input('Measurement base number setting =?     ')
  MN=1000;
  Rh=input('Radar height(m)=?     ')
% Gel=input('firing elevation angle(degree)=?     ')/180*pi
  Gel=45/180*pi;
% Gaz=input('firing azimuth angle(degree)=?      ')/180*pi
  Gaz=45/180*pi;
 diary
    answer=input('If you want reenter parameter please enter 1 else enter');
  if answer==1
     return
     xxa
  end
  B1=5;                               % gun barrel length

  A=pi*(0.155/2)**2;                  % projectile cross section area
  m=45.4;                             % projectile mass (kg)
  FAC=0.5*A/m;                        % coefficient for computing drag
```

```
  MB=MN*(lambda/2);                    % measurement base

% Radar Location at t=0                % the inertial z-x plane
   R1=a+Rh;
   R2=(90-RLATI)*pi/180;
   R3=0;
   R2s=sin(R2);
   R2c=cos(R2);
   R4=R1*R2s;
   Rz=R1*R2c;                          % z-coordinate of radar
   RV=R4*EAV;                          % radar velocity

% Firing Direction and Speed
   PVo=850;                            % muzzle speed of projectile
   Gels=sin(Gel);
   Gelc=cos(Gel);
   Gazs=sin(Gaz);
   Gazc=cos(Gaz);

% Gun (muzzle) Location at t=0
   Gh=Bl*Gels;                         % muzzle height
   Gl=a+Gh;
   Gl=Bl*Gelc;
   RGs=-RB*sin(RBaz)-Gl*Gazs;          % distance, south of radar
   RGe=RB*cos(RBaz)+Gl*Gazc;           % distance, east of radar
   G2=R2+RGs/G1;
   G4=G1*sin(G2);
   G3=R3+RGe/G4;
   Gz=G1*cos(G2);

% Displacement Transformation
   G2c=cos(G2);
   G2s=sin(G2);
   DTG=(0,GAZC,GAZS;0,-GAZS,GAZC;1,0,0-*-G2C,0,G2S;0,1,0;-G2S,0,G2C);

% Projectile Initial Location
   P1=G1;
   P1n=G1;
   P2n=G2;
   P3n=G3;
   P4n=G4;

% Projectile Initial Velocity
   PV1n=PVo*Gels;
   PVg=PVo*Gelc;                       % velocity along ground
   PVe=PVg*Gazc;                       % velocity, east
   PAV2n=-(PVg*Gazs)/G1;               % angular velocity, theta
   PAV3n=PVe/G4+EAV;                   % angular velocity, phi


% Drag Force Considerations

 % Wind Profile:  assumed constant in this program.
  %  The geostrophic wind should be measured and the Ekman spiral
  %  model can be adopted for a better approximation if the true
```

```
 %  wind profile is not available.
% Wind=input('Enter the wind speed m/sec at muzzle height')
  Wind=6;                              % wind velovity at muzzle height
% WindBearing=input('Enter the true wind bearing in degrees')
  WindBearing=135;                     % clockwise from north
  Waz=((90-WindBearing)+180)*pi/180;
  We=Wind*cos(Waz);                    % wind velocity, east
  Ws=-Wind*sin(Waz);                   % wind velocity, south

% Temperature Profile (assumed linear)
 % Th=input('Enter the height (m) at which temperature is measured')
  Th=10;
% TREF=INPUT('ENTER THE MESURED TEMPERATURE IN CELSIUS')
  Tref=15;

  TrefK=273.16+Tref;
  Th1=Th+a;
  S =-0.0065;                          % TEMPERATURE LAPSE RATE K/M
% TP=TREFK+S*(P1-TH1);                 % AIR TEMPERATURE AT THE PROJECTILE

% AIR DENSITY
% DH=INPUT('ENTER THE HEIGHT (M) AT WHICH AIR DENSITY IS MEASURED')
   DH=GH;
% DAO=INPUT('ENTER THE MESURED AIR DENSITY IN KG/CUBIC METER')
  Dao=1.225;                            % air density at sea level
  TDao=TrefK+s*(Dh-Th);
  ss=287.05;                           % gas constant N-m/kg-K
  KC=1.4;                              % Cp/Cv for air
  RAg=-1-g/(s*ss);                     % calculation factor
% DA=DAO*(TP/TDAO)**RAG;               % AIR DENSITY AT PROJECTILE HEIGHT

% Speed of Sound
  KR=KC*ss;
% Vah=sqrt(KR*TP);                     % speed of sound at P1

% curve fitting for Drag coefficient(experimental data input)
 x=(0,0.05,0.15,0.2,0.23,0.25,0.3,0.35,0.4,0.45,0.5,0.55,0.6,...
 0.65,0.7,0.75,0.825,0.875,0.98,1.0,1.05,1.1,1.2,1.3,1.4,1.5,...
 1.75,2,2.5,2.9);
 y=(0.16,0.16,0.16,0.16,0.16,0.16,0.16,0.16,0.16,0.16,0.16,...
 0.16,0.16,0.16,0.16,0.162,0.17,0.205,0.225,0.27,0.282,0.29,...
 0.2875,0.285,0.275,0.25,0.23,0.195,0.17);

 cds=spline(x,y);                      % spline curve fitting function
                                       % get spline coefficient

% Trajectory Computation Begins

  t(1)=0;                              % initial time
  n=0;
%************************  main loop begin ************************************
while P1n>a, n=n+1;

% Update
  P1=P1n;
  P2=P2n;
```

```
  P3=P3n;
  P4=P4n;
  PV1=PV1n;
  PAV2=PAV2n;
  PAV3=PAV3n;
  PV2=PAV2*P1;
  PV3=PAV3*P4;
  PVe=(PAV3-EAV)*P4;
  Height(n)=P1-a;
% velocity transformation matrix
  PR3=P3-EAV*t(n);                    % location relative to radar
  PG3=PR3-G3;                         % location relative to gun
  P2s=sin(P2);
  P2c=cos(P2);
  PR3s=sin(PR3);
  PR3c=cos(PR3);
  PG3s=sin(PG3);
  PG3c=cos(PG3);
  VTR11=P2s*PR3c;
  VTR21=P2s*PR3s;
  VTR31=P2c;
  VTR=(VTR11,P2c*PR3c,-PR3s;VTR21,P2c*PR3s,PR3c;VTR31,-P2s,0);

  VTG11=P2s*PG3c;
  VTG21=P2s*PG3s;
  VTG31=P2c;

% Relative Location
  PRXYZ=(P1*-VTR11; VTR21; VTR31)-(R4; 0; RZ);
  SLR=NORM(PRXYZ);                % SLANT RANGE FROM RADAR
  SRR(n)=SLR;
%*****************************************************************************
 DR(:,n)=PRxyz/SLR;               % direction relative to radar
 Dz=DR(1,n)*R2s+DR(3,n)*R2c;      % tracking direction, elevation
 Dn=DR(3,n)*R2s-DR(1,n)*R2c;      % tracking direction, north comp.
 De=DR(2,n);                      % tracking direction, east component
 traz(n)=atan2(Dn,De)*180/pi;     % azimuthal angle
 trel(n)=asin(Dz)*180/pi;         % elevation angle
%*****************************************************************************
  PGXYZ=DTG*(P1*-VTG11; VTG21; VTG31)-(G4; 0; GZ));
  SL=norm(PGxyz);                     % slant range
  SRange(n)=SL;
  GRange(n)=a*acos((P1**2+G1**2-SL  2)/(2*P1*G1));
                                      % ground range
  PGx=PGxyz(1);
  PGz=PGxyz(3);
  FRange(n)=a*atan(PGx/(G1+PGz));     % range in firing plane
  CRange(n)=PGxyz(2);                 % cross range from firing plane

%Relative Velocity
  PV=(PV1; PV2; PV3);
  PVR=VTR*PV-(0; RV; 0);
  VR(:,n)=PVR;                        % velocity relative to radar
  VRr(n)=PV1;

% Time Interval and Doppler effect Estimation
```

```
  VDopp=PVR'*PRxyz/SLR;                % Doppler velocity
  Vdop1(n)=VDopp;
  fd1(n)=2*VDopp/lambda;                 % Doppler Frequency
  dtn=MB/VDopp;                        % square-law doppler detector
  t(n+1)=t(n)+dtn;
% Frictional Acceleration

  TP=TrefK+s*(P1-Th1);                 % air temperature at the projectile
  Da=Dao*(TP/TDao)**RAg;               % air density at projectile height
  Vah=sqrt(KR*TP);                     % speed of sound at P1
  PVW=(PV1;PV2-WS;PVE-WE);             % PROJECTILE AIR VELOCITY
  PVWM=norm(PVW);
  PVWMM=PVWM/Vah;
  PH=PVW/PVWM;                         % projectile heading
  HeadingR(:,n)=VTR*PH;                % heading as seen from radar
  CD=ppval(cds,PVWMM);
  FA=-FAC*Da*CD*PVWM*PVW;              % drag acceleration

% Location and Velocity Prediction

  PA1=(PV2**2+PV3**2)/P1+FA(1)-g*(a/P1)    2;
  PAA2=P2s*P2c*PAV3**2+FA(2)/P1;
  PAA3=FA(3)/P4;
  PV1n=PA1*dtn+PV1;
  P1n=0.5*(PV1+PV1n)*dtn+P1;
  PAV2n=(PAA2*dtn+PAV2)*(P1/P1n)**2;
  P2n=0.5*(PAV2+PAV2n)*dtn+P2;
  P4n=P1n*sin(P2n);
  PAV3n=(PAA3*dtn+PAV3)*(P4/P4n)**2;
  P3n=0.5*(PAV3+PAV3n)*dtn+P3;
end
%*************** end of main loop ****************
% Estimate Point of Impact
  Ih=P1-a;
  IA=-PA1;
  IV=-PV1;
  dt=(sqrt(IV**2+2*Ih*IA)-IV)/IA;
  N=n+1;
  t(N)=t(n)+dt;
  P1n=a;
  PV1n=PA1*dt+PV1;
  PAV2n=(PAA2*dt+PAV2)*(P1/P1n)**2;
  P2n=0.5*(PAV2+PAV2n)*dt+P2;
  P4n=P1n*sin(P2n);
  PAV3n=(PAA3*dt+PAV3)*(P4/P4n)**2;
  P3N=0.5*(PAV3+PAV3N)*DT+P3;

% Update
  P1=P1n;
  P2=P2n;
  P3=P3n;
  P4=P4n;
  PV1=PV1n;
  PAV2=PAV2n;
  PAV3=PAV3n;
  PV2=PAV2*P1;
```

```
  PV3=PAV3*P4;

  Height(N)=0;

% velocity transformation matrix

  PR3=P3-EAV*t(N);                    % location relative to radar
  PG3=PR3-G3;                         % location relative to gun

  P2s=sin(P2);
  P2c=cos(P2);
  PR3s=sin(PR3);
  PR3c=cos(PR3);
  PG3s=sin(PG3);
  PG3c=cos(PG3);
  VTR11=P2s*PR3c;
  VTR21=P2s*PR3s;
  VTR31=P2c;
  VTR=(VTR11,P2C*PR3C,-PR3S;VTR21,P2C*PR3S,PR3C;VTR31,-P2S,0);

  VTG11=P2s*PG3c;
  VTG21=P2s*PG3s;
  VTG31=P2c;

% Relative Location
  PRXYZ=(P1*-VTR11; VTR21; VTR31)-(-R4; 0; RZ)-;
  SRR(N)=norm(PRxyz);
%************************ Radar parameters registration *********************
  DR(:,N)=PRxyz/SRR(N);            % location relative to radar
  Dz=DR(1,N)*R2s+DR(3,N)*R2c;      % tracking direction, elevation
  DN=DR(3,N)*R2S-DR(1,N)*R2C;      % TRACKING DIRECTION, NORTH COMP.
  De=DR(2,N);                      % tracking direction, east component
  traz(N)=atan2(Dn,De)*180/pi;     % azimuthal angle
  trel(N)=asin(Dz)*180/pi;         % elevation angle
%*****************************************************************************
  PGxyz=DTG*(P1*[VTG11; VTG21; VTG31]-[G4; 0; Gz]);
  SL=norm(PGxyz);                  % slant range
  SRange(N)=SL;
  GRange(N)=a*acos((P1**2+G1**2-SL  2)/(2*P1*G1));
                                   % ground range
  PGx=PGxyz(1);
  PGz=PGxyz(3);
  FRange(N)=a*atan(PGx/(G1+PGz));  % ground range in firing plane
  CRange(N)=PGxyz(2);              % cross range from firing plane

% Relative Velocity
  PV=[PV1; PV2; PV3];
  PVR=VTR*PV-[0; RV; 0];
  VDopp=PVR'*PRxyz/SLR;            % Doppler velocity
  Vdop1(N)=VDopp;
  fd1(N)=2*VDopp/lambda;           % Doppler Frequency
  VR(:,N)=PVR;
  VRr(N)=PV1;
  PVW=(PV1;PV2-WS;PVE-WE);
  HeadingR(:,N)=VTR*(PVW/norm(PVW));
```

```
 for i=1:N;
  VRM(i)=norm(VR(:,i));
  VRrf(i)=VRr(i)/VRM(i);
  VRt(i)=(1-VRrf(i))*VRM(i);
  beamD(i)=1*pi/180*SRR(i);
 end
EXETIME1=etime(clock,t2)
%********************  out put data ********************************
  diary ww
 EXETIME1
  MN=MN
  ng=N
  MB=MB
  tg=t(N)
  r=P1
  dlatitude=(P2-G2)*180/pi
  dlongitude=PG3*180/pi
  Rg=GRange(N)
  FRg=FRange(N)
  CRg=CRange(N)
  CRgmax=max(CRange)
  maxHeight=max(Height)
  maxfd=max(fd1)
  maxrange=SRR(N)
 VDOPmin=min(Vdop1)
 VDOPmax=max(Vdop1)
 diary
%****************************** SAVE AND LOAD DATA FOR NEXT CALCULATION******
!DEL 50010.MAT
SAVE 50010 MAXRANGE EXETIME1 DR HEADINGR SRR HEIGHT T N FD1 MB
!DEL X50010.MAT
SAVE  X50010 TRAZ TREL VDOP1 VRM VRRF VRT VR VRR T SRR BEAMD
%*********************************  Execute other program ***************************
%PR                                    % PRINT OUT TRAJECTORY
%PRTRAK                                % TRACKING PARAMETERS & OUTPUT
%XX0                                   % RCS & RANGE ANALYSIS PROGRAM
%RCSA                                  % RCS SUBFUNCTION
%RANGE3                                % POWER REQUIREMENT
%TDATA                                 % PROPAGATION FACTOR CURVE FITTING
%*************************************************************************************
%*********************************output of trajectory*************************
  !del GH.met
  plot(GRange,Height),grid;
  title('PROJECTILE TRAJECTORY');
  xlabel('ground range (m)');
  ylabel('projectile height (m)');
  meta GH
%prtsc
%pause
  !del GC.met
  plot(GRange,CRange),grid;
  title('PROJECTILE TRAJECTORY');
  xlabel('ground range (m)');
  ylabel('Cross range (m)');
```

```
  meta GC
% pause
% prtsc
  !del RH.met
  plot(SRR,Height,'o'),grid;
  title('PROJECTILE TRAJECTORY');
  xlabel('Slant Range (m)');
  ylabel('projectile height (m)');
   meta RH
% prtsc
pause
 % !del TH.met
  plot(t,Height),grid;
  xlabel('flight time (sec)');
  ylabel('projectile height (m)');
 meta TH
% pause
%prtsc
  !del TSGFC.met
  plot(t,SRange, t,GRange, t,FRange, t,CRange),grid;
  xlabel('flight time (sec)');
  ylabel('slant, ground, firing plane & cross ranges (m)');
  meta TSGFC
%pause
prtsc
  !del SGFCT.met
  plot(SRange,t, GRange,t, FRange,t, CRange,t),grid;
  xlabel('slant, ground, firing plane & cross ranges (m)');
  ylabel('flight time (sec)');
  meta SGFCT
%pause
%prtsc
  !del TVR.met
  plot(t,VRr,'+'),grid;
  xlabel('flight time (sec)');
  ylabel('Vertical Speed');
  meta TVR
%pause
%prtsc
 !del TVH.met
  plot(t,VRt,'+'),grid;
  xlabel('Flight time (sec)');
  ylabel('Horizontal Speed');
  meta TVH
%pause
prtsc
 !del FH.met
  plot(FRange,Height),grid;
  xlabel('ground range in firing plane (m)');
  ylabel('projectile height (m)');
  meta FH
 %pause
 %prtsc
 !del FC.met
  plot(FRange,CRange),grid;
  xlabel('Firing plane Range (m)');
```

```
  ylabel('Cross range (m)');
   meta FC
%pause
prtsc
 !del GV.met
 plot(GRange,VRM),grid;
 xlabel('Ground Range (m)');
 ylabel('Projectile Speed (m/sec)');
 meta GV
%pause
%prtsc
 !del GRV.met
 plot(GRange,VRrf),grid;
 xlabel('Ground range (m)');
 ylabel('Ratio of radial velocity to speed');
 meta GRV
%pause
%prtsc
%********************  TRAKING PARAMETERS CALCULATION AND OUTPUT *******
%********************* Tracking angular velocity ***************
  avel1=diff(trel)./diff(t);
  avaz1=diff(traz)./diff(t);
%************************ PLOT ***********************************
for n=1:N-1
  ta(n)=t(n);
end
  !del AVAEt.met
  plot(ta,avel1,'+'),grid;
  title('RADAR TRACKING ELEVATION ANGULAR SPEED ');
  xlabel('In-flight time (sec)');
  ylabel('Elevation Angular velocity (degree/sec)');
  meta AVAEt
% pause
 prtsc
  !del AVAZt.met
  plot(ta,avaz1,'+'),grid;
  title('RADAR TRACKING AZIMUTHAL ANGULAR SPEED');
  xlabel('In-flight time (sec)');
  ylabel('Azimuthal angular speed (degree)');
  meta AVAZt
%pause
prtsc
%***************************** Radar Tracking Parameter output ************
  !del tret.met
  plot(t,trel),grid;
  title('RADAR TRACKING ELEVATION ANGLE degree');
  xlabel('In-flight time (sec)');
  ylabel('Elevation Angle (degree)');
  meta the1
% pause
% prtsc
  !del traz1.met
  plot(t,traz),grid;
  title('RADAR TRACKING AZIMUTHAL PARAMETER');
  xlabel('In-flight time (sec)');
  ylabel('Azimuthal angle (degree)');
```

```
  meta traz1
%pause
% prtsc
  !del AVAE.met
  plot(avel1,'+'),grid;
  title('RADAR TRACKING ELEVATION ANGULAR VELOCITY ');
  xlabel('MEASUREMENT BASE ');
  ylabel('Elevation Angular velocity (degree/sec)');
  meta AVAE
% pause
% prtsc
  !del AVAZ.met
  plot(avaz1,'+'),grid;
  title('RADAR TRACKING AZIMUTHAL ANGULAR VELOCITY');
  xlabel('MEASUREMENT BASE');
  ylabel('AZIMUTH ANGULAR (degree)');
  meta AVAZ
%pause
%prtsc
EXETIME1=etime(clock,t2)
%*************************  graph ***********************************************
  !del TVD.met
  plot(t,fd1),grid;
  title('DOPPLER FREQUENCY');
  xlabel('Flight time (sec)');
  ylabel('Doppler Frequency (Hz)')
  meta TVD
% pause
 prtsc
  !del treVD.met
  plot(trel,Vdop1),grid;
  title('DOPPLER Velocity');
  xlabel('Radar tracking elevation angle (degree)');
  ylabel('Doppler Velocity(m)')
  meta trehVD
%pause
% prtsc
  !del trazVD.met
  plot(traz,Vdop1),grid;
  title('DOPPLER Velocity');
  xlabel('Radar Tracking azimuthal Angle (degree)');
  ylabel('Doppler Velocity(m)')
  meta trazVD
%pause
%prtsc
  !del RVD1.met
  plot(SRR,Vdop1),grid;
  title('DOPPLER Velocity');
  xlabel('Slant Range(m)');
  ylabel('Doppler Velocity(m)')
  meta RVD1
%pause
 prtsc
  !del tVD1.met
  plot(t,Vdop1),grid;
  title('DOPPLER Velocity');
```

```
  xlabel('In-flight time(sec)')
  ylabel('Doppler Velocity(m)')
  meta tVD1
 prtsc
%***************************** Radar Tracking Parameter output ************
  !del tret.met
  plot(t,trel),grid;
  title('RADAR TRACKING ELEVATION ANGLE degree');
  xlabel('In-flight time (sec)');
  ylabel('Elevation Angle (degree)');
  meta the1
% pause
 prtsc
  !del traz1.met
  plot(t,traz),grid;
  title('RADAR TRACKING AZIMUTHAL PARAMETER');
  xlabel('In-flight time (sec)');
  ylabel('Azimuthal angle (degree)');
  meta traz1
%pause
prtsc
*******************************************************************************
%******** RCS and Power requirement Estimation********
load 50010

t3=clock
Bv1=1.2*max(fd1);                    % video Bandwidth for 1st filter
Bv2=1.2*22031;                       % video Bandwidth for 2nd filter
Bv3=1.2*12721;                       % video Bandwidth for 3rd filter
%********************* radar parameters calculation ***************************
Loss=10**0.24;                       % total loss 2.4dB
KT=4.021E-21;                        % KT=K*T
SN=10;                               % minimum signal to noise ratio 10dB
Lamda=3E8/10525E6;                   % wavelength meter  10525MHz
Fn=10**0.2;                          % noise figure  2dB
G=10**4.43;                          % TX or RX antenna gain 44.3dB
const=((4*pi)**3*KT*Fn*Loss*SN)/((G*Lamda)2);
%******************************************************************************
% Radar cross section & power requirement estimations
 for n=1:N
 if max(Height)==Height(n)           % Summit point data
    ttop=t(n);                       % time at summit
    Ltop=SRR(n);                     % range at summit
  end
 end
%********************** switch 1 power requirement ***********************
  Bcon=Bv1*const;
for n=1:1092
  SRRa(n)=SRR(n);
  ta(n)=t(n);
  uD1=DR(:,n);
  h=HeadingR(:,n);
  ct=h'*uD1;
  rcs=rcsa(ct);              % rcs function
  ct1(n)=ct;
 rcs1(n)=rcs;
```

```
 theta1(n)=acos(ct)*180/pi;
 L1=SRR(n);
 Pt0=L1**4*Bcon/rcs;
 Pt1(n)=Pt0;                  % power requied in free space
 if L1==Ltop                  % required power at summit
  ptop=Pt0;
 end
%********************* switch 2 power requirement ******************
 Bcon=Bv2*const;
for n=1093:1630
  SRRa(n)=SRR(n);
  ta(n)=t(n);
  uD1=DR(:,n);
  h=HeadingR(:,n);
  ct=h'*uD1;
  rcs=rcsa(ct);               % rcs function
  ct1(n)=ct;
 rcs1(n)=rcs;
 theta1(n)=acos(ct)*180/pi;
 L1=SRR(n);
 Pt0=L1**4*Bcon/rcs;
 Pt1(n)=Pt0;                  % power requied in free space
 if L1==Ltop                  % required power at summit
  ptop=Pt0;
 end
switch1=max(Pt1);
end  % end for loop
% ***************************** 3rd filter ****************************
  Bcon=Bv3*const;
for n=1631:1898
  SRRa(n)=SRR(n);
  ta(n)=t(n);
  uD1=DR(:,n);
  h=HeadingR(:,n);
  ct=h'*uD1;
  rcs=rcsa(ct);               % rcs function
  ct1(n)=ct;
 rcs1(n)=rcs;
 theta1(n)=acos(ct)*180/pi;
 L1=SRR(n);
 Pt0=L1**4*Bcon/rcs;
 Pt1(n)=Pt0;                  % power requied in free space
 if L1==Ltop                  % required power at summit
  ptop=Pt0;
 end
switch2=max(Pt1);
end  % end for loop
%************************* output ***************************************
!del ww1
diary ww1
N=N
flighttime=max(t)
stoptime=max(ta)
stoprange=max(SRRa)
stopfd=fd1(1898)
timetop=ttop
```

```
rangetop=Ltop
powertop=ptop
EXETIME2=etime(clock,t3)
TOTALTIME=EXETIME1 + EXETIME2
diary
%************************** graph radar cross section ********************
!del rcs11.met
 plot(SRRa,rcs1,'+'),grid;
 ylabel('Radar cross section square meters');
 xlabel('Slant range');
 meta rcs11
%prtsc
% pause
!del rcsth.met
plot(theta1,rcs1,'+'),grid;
ylabel('Radar cross section square meters');
xlabel('Aspect angle (degree)');
meta rcsth
% pause
%prtsc
!del rasp.met
plot(ta,theta1,'+'),grid;
ylabel('Radar cross section square meters');
xlabel('Aspect angle (degree)');
meta rasp
%pause
%prtsc
!del ras1.met
plot(ct1,'+'),grid;
xlabel('in-flight time (sec)');
ylabel('Aspect angle (degree)');
meta ras1
%prtsc
%pause
%************************ save variable ***************************************
%!del Pw50010.mat
%save Pw50010 pt1max ct1 t fd1 rcs1 L1  N theta1 Pt1 SRR N
%***************************** printout power requirement ********************
  !del power1.met
  plot(SRRa,Pt1,'+'),grid;
  title('RADAR POWER REQUIREMENT ');
  xlabel('Slant range (m) ');
  ylabel('Power requirement (Watts)');
  meta power1
prtsc
%pause
************ RADAR CROSS SECTION CALCULATION **********************
clear
LOAD 50010
for n=1:N
  uD1=DR(:,n);                      % radar to target unit vector
  h=HeadingR(:,n);                  %unit heading vector of projectile
  ct=h'*uD1;                        % antenna beam angle
%function [rcs,ct]=RCS(ct)
% constant declaration
  b=0.155/2;                        % shell base radius
```

```
  l=0.5236;                          % shell cone(nuzzle) height
  i=0.4144;                          % shell cylinder height
  ta=b/l;                           % =atan(b/l) i.e. half shell cone angle
  ta2=ta*ta;
  ca2=1/(1+ta2);
  ca=sqrt(ca2);
  cx=abs(ct);
  cx2=cx*cx;
  sx2=(1-cx2);
  sx=sqrt(sx2);
  rcsc=2*i*b*sx;
  b2=b*b;
  rcsb=pi*b2*cx;
 if cx>=ca
  rcs=rcsc+rcsb;
 else
  rt=ta*cx/sx;
  rt2=rt*rt;
  rcs2=b2*(asin(rt)+rt*sqrt(1-rt2))*cx;
  rcs1=((b*i)/(sx2))*(1-cx2/ca2)**(3/2);
  rcs=rcs1+rcs2+rcsc+rcsb/2;
 end                                    % radar cross section case 2
rcs0(n)=rcs;
ct1(n)=ct;
theta1(n)=acos(ct)*180/pi;
 end
!del rcs11
% plot(SRR,rcs0,'+'),grid;
%ylabel('Radar cross section square meters');
%xlabel('Slant range');
%meta rcs11
%prtsc
%pause
!del rcsth
plot(theta1,rcs0,'+'),grid;
ylabel('Radar cross section square meters');
xlabel('Aspect angle (degree)');
meta rcsth
%pause
!del rasp
plot(t,theta1,'+'),grid;
ylabel('Radar cross section square meters');
xlabel('Aspect angle (degree)');
meta rasp
%pause
!del ras1
plot(ct1,'+'),grid;
xlabel('in-flight time (sec)');
ylabel('Aspect angle (degree)');
meta ras1

%**************** end of program ************************************
```

APPENDIX B. CROSS-SECTION ANALYSIS

The radar cross-section has been discussed in Chapter 4. The derivation of the RCS equations is given below. The radar main beam direction is pointing in the direction $\hat{D}$. The projectile axis (or heading) is pointing along $\hat{h}$. Accordingly, the coordinate system (x,y,z) can be chosen so that $\hat{x} = \hat{D}$ and the y-z plane is the plane on which the physical cross-sectional area of the projectile is to be projected. Another coordinate system (x', y', z') can be chosen so that $\hat{x}' = \hat{h}$ and the projectile is a body of revolution around the $\hat{x}'$ axis. These two coordinate systems can be set up jointly as follows :

$$\hat{x} = \hat{D} \tag{B.1}$$

$$\hat{z} = \frac{\hat{D} \times \hat{h}}{|\hat{D} \times \hat{h}|} \tag{B.2}$$

$$\hat{y} = \hat{z} \times \hat{D} \tag{B.3}$$

$$\hat{x}' = \hat{h} \tag{B.4}$$

$$\hat{z}' = \hat{z} \tag{B.5}$$

$$\hat{y}' = \hat{z}' \times \hat{x}' \tag{B.6}$$

$$= \hat{z} \times \hat{h} \tag{B.7}$$

$$= \frac{[(\hat{h} \times \hat{D})\hat{h} - \hat{D}]}{|\hat{D} \times \hat{h}|} \tag{B.8}$$

$$\hat{D} = \frac{\vec{r}_p - \vec{r}_R}{|\vec{r}_p - \vec{r}_R|} \tag{B.9}$$

Note that the coordinate (x,y,z) are used in this Appendix only and are not related to other parts of the thesis.

The suface of the projectile is given by :

$$y'^2 + z'^2 = f^2(x') \tag{B.10}$$

The RCS is the area enclosed by projecting of this surface on the y-z plane.

A. CASE 1

For $|\hat{D} \cdot \hat{h}| \geq \cos\alpha$, Figure 25 on page 38, the conoid is hidded in the shadow region. The projected areas can be easily seen to be :

$$A_1 = 3.14159 \frac{a^2}{2} \tag{B.11}$$

$$\sigma_1 = A_1 |\hat{D} \cdot \hat{h}| \tag{B.12}$$

$$A_2 = 2ab \tag{B.13}$$

$$\sigma_2 = A_2 |\hat{D} \cdot \hat{h}| \tag{B.14}$$

$$A_3 = A_1 \tag{B.15}$$

$$\sigma_3 = A_3 |\hat{D} \cdot \hat{h}| \tag{B.16}$$

where a is the diameter of the projectile and b is the cylinder height. The total projection area in :

$$\sigma_t = \sigma_1 + \sigma_2 + \sigma_3 \tag{B.17}$$

B. CASE 2

When $|\hat{D} \cdot \hat{h}| < \cos\alpha$, the geometry of the target is shown in Figure 26 on page 39. The RCS value consists of four different parts: A_1 , A_2, A_3, A_4 . Each of them is given below :

For area A_1:

$$y'^2 = c^2 x'^2 \tag{B.18}$$

$$= (x' - x_o')^2 \tan^2\theta_{asp} \tag{B.19}$$

where

$$c = \tan\alpha \tag{B.20}$$

$$(c^2 - \tan^2\theta_{asp})x'^2 + 2x_o' \tan^2\theta_{asp}x' - x_o'^2 \tan^2\theta_{asp} = 0 \qquad (B.21)$$

$$x_c' = \frac{x_o' \tan^2\theta_{asp}}{(\tan^2\theta_{asp} - c^2)} \qquad (B.22)$$

$$y_c' = \frac{x_o' c^2 \tan\theta_{asp}}{(\tan^2\theta_{asp} - c^2)} \qquad (B.23)$$

where x_c', y_c' is the maximum point of the ellipse.

$$\frac{y'}{x'} = \frac{c^2}{\tan\theta_{asp}} \qquad (B.24)$$

$$f(x', y') = y' \tan\theta_{asp} + x' \qquad (B.25)$$

$$N = \nabla f \qquad (B.26)$$

$$= \frac{(c^2x' + y' \tan\theta_{asp})}{(\tan^2\theta_{asp} + c^4)^{1/2}} \qquad (B.27)$$

At a point which is p_1 , $x' = L$, then:

$$y' \tan\theta_{asp} + Lc^2 = 0 \qquad (B.28)$$

or

$$y' = -\frac{Lc^2}{\tan\theta_{asp}} \qquad (B.29)$$

So the coordinate at p_1 is (-L , $\frac{-Lc^2}{\tan\theta_{asp}}$, 0) on the z' axis,

$$\frac{c^4L^2}{\tan^2\theta_{asp}} + z'^2 = c^2L^2 \qquad (B.30)$$

or

$$z' = \frac{cL(\tan^2\theta^{asp} - c^2)^{1/2}}{\tan\theta_{asp}} \qquad (B.31)$$

Hence

$$A_1 = zL\left(\frac{1+c^4}{\tan^2\theta_{asp}}\right)^{1/2} \tag{B.32}$$

$$= L^2 c(\tan^2\theta_{asp} + c^4)^{1/2}\frac{(\tan^2\theta_{asp} - c^2)^{1/2}}{\tan^2\theta_{asp}} \tag{B.33}$$

Let $\hat{N}$ be the normal unit vector of surface A_1:

$$\hat{N} = \frac{\hat{D}\cos^2\alpha - \hat{h}\cos\theta_{asp}}{\sqrt{\sin^2\theta_{asp}\cos^4\alpha + \sin^4\alpha\cos^2\theta_{asp}}} \tag{B.34}$$

then the projection area for A_1 is:

$$\sigma_1 = \frac{L^2\tan\alpha(\tan^2\theta_{asp} + \tan^4\alpha)^{1/2}(\tan^2\theta_{asp} - \tan^2\alpha)^{1/2}(\hat{D}\cdot\hat{N})}{\tan^2\theta_{asp}} \tag{B.35}$$

$$= \frac{aL}{\sin^2\theta_{asp}}\left(1 - \frac{\cos^2\theta_{asp}}{\cos^2\alpha}\right)^{3/2} \tag{B.36}$$

A_2 is part of a semi-circle (Figure 26 on page 39). A straight forward intergration gives:

$$A_2 = a^2\left\{\sin^{-1}\left(\frac{\tan\alpha}{|\tan\theta_{asp}|}\right) + \frac{\tan\alpha}{|\tan\theta_{asp}|}\sqrt{1 - \frac{\tan^2\alpha}{\tan^2\theta_{asp}}}\right\} \tag{B.37}$$

$$\sigma_2 = a^2\left\{\sin^{-1}\left(\frac{\tan\alpha}{|\tan\theta_{asp}|}\right) + \frac{\tan\alpha}{|\tan\theta_{asp}|}\sqrt{1 - \frac{\tan^2\alpha}{\tan^2\theta_{asp}}}\right\}|\hat{D}\cdot\hat{h}| \tag{B.38}$$

A_3 is a rectangle:

$$A_3 = 2ab \tag{B.39}$$

so

$$\sigma_3 = A_3|\hat{D}\times\hat{h}| \tag{B.40}$$

where a is the radius of the projectile base, and b is the height of the cylindrical part of projectile.

A_4 is a semicircle, hence :

$$A_4 = 3.14159 \frac{a^2}{2} \tag{B.41}$$

$$\sigma_4 = A_4 | \hat{D} \cdot \hat{h} | \tag{B.42}$$

The total cross-section σ_t is the sum of upper 4 projection areas.

$$\sigma_t = \sigma_1 + \sigma_2 + \sigma_3 + \sigma_4 \tag{B.43}$$

APPENDIX C. PROPAGATION FACTORS

Projectile Location		Antenna Height				
Ground Range to impact point (m)	Height (m)	10m (dB)	15m (dB)	20m (dB)	30m (dB)	50m (dB)
-482.0000	932.4000	0	0	0.6000	-0.3000	-0.3000
-382.0000	741.2000	0.6000	0.6000	0.6000	-0.3000	-0.3000
-333.0000	647.9000	-0.7000	-0.4000	0.4000	-0.3000	-0.3000
-234.0000	455.2000	-0.3000	-1.1000	1.2000	1.2000	-0.2000
-182.0000	355.7000	-0.9000	1.0000	1.7000	0.7000	1.7000
-152.0000	294.8000	1.9000	-3.7000	1.2000	-2.6000	1.2000
-148.0000	289.2000	2.3000	0.5000	-3.5000	1.5000	-3.4000
-145.0000	283.7000	1.5000	1.0000	0.3000	0	0.4000
-142.0000	278.1000	-0.7000	1.3000	-1.9000	0.3000	-0.7000
-140.0000	272.6000	-3.8000	-2.4000	-1.0000	-1.9000	-2.1000
-137.0000	267.0000	-3.0000	-3.0000	-3.0000	-3.2000	-0.9000
-132.0000	261.5000	0	1.4000	2.3000	2.6000	2.3000
-131.0000	256.0000	2.3000	2.9000	1.5000	-2.4000	-0.3000
-129.0000	250.4000	3.2000	0.7000	-4.1000	1.3000	-2.1000
-125.0000	244.8000	2.2000	-5.1000	0.2000	0.2000	2.2000
-123.0000	239.3000	-0.8000	-1.6000	3.1000	-1.4000	-0.7000
-120.0000	233.7000	-5.0000	2.9000	-4.0000	-5.0000	1.6000
-117.0000	228.2000	-4.2000	2.9000	-4.0000	-5.0000	1.6000
-114.0000	222.6000	-0.1000	-1.0000	2.9000	3.2000	0.7000
-111.0000	217.1000	3.0000	-6.5000	2.7000	-0.3000	-0.3000
-108.0000	211.5000	3.7000	0.7000	-5.3000	0.8000	-0.3000
-105.0000	206.0000	2.7000	3.7000	-0.9000	1.8000	2.7000
-103.0000	200.4000	-0.3000	2.7000	3.8000	-2.4000	-2.4000
-100.0000	194.9000	-6.0000	-2.2000	0.6000	3.0000	-0.5000
-97.0000	189.3000	-5.3000	-5.3000	-5.3000	-5.0000	3.0000
-94.0000	183.8000	-14.7000	-4.7000	-12.5000	3.0000	-11.0000
-91.0000	178.2000	3.4000	4.4000	3.2000	1.4000	-1.7000
-88.0000	172.6000	2.2000	4.2000	-3.5000	-0.9000	3.1000
-85.0000	167.1000	3.5000	-5.5000	-1.5000	3.5000	-0.5000
-83.0000	161.5000	0.5000	-3.5000	4.2000	-7.5000	-4.8000
-80.0000	156.0000	-6.4000	3.4000	2.3000	4.1000	2.8000
-77.0000	150.4000	4.3000	7.1000	-10.0000	-3.0000	3.0000
-74.0000	144.8000	0.7000	0.9000	2.3000	1.9000	-6.9000
-71.0000	139.3000	3.7000	-9.9000	4.4000	3.0000	3.0000
-68.0000	133.7000	4.6000	-0.4000	-1.4000	-4.4000	3.2000
-66.0000	128.1000	3.8000	4.4000	-3.3000	4.4000	-6.4000
-63.0000	122.5000	1.1000	4.1000	4.1000	-4.7000	1.9000
-60.0000	117.0000	-6.7000	0.1000	3.6000	2.5000	4.0000
-57.0000	114.4000	-13.4000	-4.4000	0.2000	4.6000	4.6000
-54.0000	105.9000	-0.2000	0.2000	0.2000	4.1000	2.7000
-52.0000	100.3000	4.0000	4.8000	4.7000	4.7000	3.1000
-49.0000	94.7000	5.0000	4.0000	2.4000	-3.9000	-6.9000
-46.0000	89.2000	4.5000	0.2000	-14.4000	2.5000	3.6000
-43.0000	83.6000	2.8000	-14.5000	1.5000	3.5000	1.5000
-40.0000	78.0000	1.4000	0.2000	4.7000	-10.2000	-2.2000

-37.0000	72.5000	-12.4000	4.2000	16.0000	4.6000	4.6000
-34.0000	66.9000	-4.8000	4.7000	-12.6000	0.9000	-3.8000
-31.0000	61.3000	1.4000	1.4000	1.4000	-3.1000	2.9000
-29.0000	55.7000	3.7000	-7.0000	4.3000	4.5000	2.6000
-26.0000	50.2000	4.7000	-4.6000	2.3000	-1.9000	-3.3000
-23.0000	44.6000	3.5000	2.3000	-6.4000	-1.4000	4.5000
-20.0000	39.0000	2.7000	3.7000	-2.1000	4.4000	-11.1000
-17.0000	33.4000	1,8000	2.4000	2.4000	0	4.5000
-14.0000	27.9000	1.1000	2.4000	3.7000	-1.7000	-9.0000
-11.0000	22.3000	-0.1000	0.7000	2.2000	3.6000	-10.7000
-9.0000	16.7000	1.0000	-0.3000	0.3000	3.3000	4.1000
-6.0000	11.1000	-0.6000	-0.9000	-0.2000	-0.2000	4.1000
-3.0000	5.5000	4.7000	3.6000	2.7000	2.4000	2.8000
0	0	-2.6000	-4.8000	-5.0000	-4.6000	-3.2000

APPENDIX D. MISSED DETECTION AND FALSE ALARM

```
clear
MN=1000;
Npeak=MN/2;
dtmax=0.08650;
Bv1=63900;
FNnoise=Bv1*dtmax/Npeak;
SNR0=10.0;
step=0.5;
Nf=5;
Mf=29;
thshstep=0.005;
thsh0=0.355;
for m=1:Mf
thsh=m*thshstep+thsh0;
thresh(m)=thsh;
FNEnoise(m)=FNnoise*2*asin(sqrt(thsh))/pi;
end
x=SNR0-step;
for n=1:Nf
x=x+step;
SNR(n)=x;
sgnr=10**(0.1*x);

% transfer the signal-to-noise parameter to be used in fdetect.m
snr=sgnr
!del hm tempsnr.mat
save hm tempsnr snr

        for m=1:Mf
        thsh=thresh(m);
        pfan=exp(-thsh*sgnr);
        Pfa(n,m)=pfan;
        FNerror(n,m)=pfan*FNEnoise(m);
        end
        Pmiss(n,1)=Pmissdct(sgnr,0,thresh(1));
        for m=2:Mf
        Pmissd=Pmissdct(sgnr,thresh(m-1),thresh(m));
        Pmiss(n,m)=Pmiss(n,m-1)+Pmissd;
        end
end

!del hm pfaulse.mat
save hm pfaulse Nf Mf thresh FNEnoise SNR Pmiss FNerror Pfa

!del hm pfaulse
diary hm pfaulse
disp(' Threshold   Missed      Noise     Faulse')
disp('            Detection    Error      Alarm  ')
for n=1:Nf
SN_ratio=SNR(n)
(thresh; Pmiss(n,:); FNerror(n,:); Pfa(n,:))';
```

```
end
diary
pause

!del hm pfaulse.met

plot (thresh, Pmiss(1,:),'+', thresh, FNerror(1,:),'o'),grid;
title('Signal-to-Noise Ratio = 10.0 db')
xlabel('Threshold-to-Signal Power Ratio');
ylabel('Missed Detection (+) & Noise Error (o)')
meta hm pfaulse
pause

plot (thresh, Pmiss(2,:),'+', thresh, FNerror(2,:),'o'),grid;
title('Signal-to-Noise Ratio = 10.5 db')
xlabel('Threshold-to-Signal Power Ratio');
ylabel('Missed Detection (+) & Noise Error (o)')
meta hm pfaulse
pause

plot (thresh, Pmiss(3,:),'+', thresh, FNerror(3,:),'o'),grid;
title('Signal-to-Noise Ratio = 11.0 db')
xlabel('Threshold-to-Signal Power Ratio');
ylabel('Missed Detection (+) & Noise Error (o)')
meta hm pfaulse
pause

plot (thresh, Pmiss(4,:),'+', thresh, FNerror(4,:),'o'),grid;
title('Signal-to-Noise Ratio = 11.5 db')
xlabel('Threshold-to-Signal Power Ratio');
ylabel('Missed Detection (+) & Noise Error (o)')
meta hm pfaulse
pause

plot (thresh, Pmiss(5,:),'+', thresh, FNerror(5,:),'o'),grid;
title('Signal-to-Noise Ratio = 12.0 db')
xlabel('Threshold-to-Signal Power Ratio');
ylabel('Missed Detection (+) & Noise Error (o)')
meta hm pfaulse
pause

*****************************************************************************************
function pmsd = Pmissdct(snr, thsha, thshb)
% The parameter snr for the singal-to-noise ratio (NOT in db) should
%  have been saved to hm tempsnr.mat.
%!del hm tempsnr mat
%save hm tempsnr snr
pmsd=quad('fdetect',thsha,thshb,0.0001);

*****************************************************************************************
% The parameter sgnr has to be specified in the program.
function pdens = fdetect(v)
load hm tempsnr
ziv=2*snr*sqrt(v)*i;
LIoz=log(BESSELN(0,ziv));
Lpdens=LIoz+log(snr)-snr*(v+1);
```

```
pdens=exp(Lpdens);
%************************ end of program ***********************************
%************************ output data ***********************************
```

Threshold	Missed Detection	Noise Error	Faulse Alarm
S/N = 10.0 db			
0.3600	0.0266	0.1237	0.0273
0.3650	0.0278	0.1187	0.0260
0.3700	0.0290	0.1138	0.0247
0.3750	0.0303	0.1091	0.0235
0.3800	0.0316	0.1046	0.0224
0.3850	0.0329	0.1002	0.0213
0.3900	0.0343	0.0961	0.0202
0.3950	0.0357	0.0921	0.0193
0.4000	0.0371	0.0883	0.0183
0.4050	0.0386	0.0846	0.0174
0.4100	0.0401	0.0810	0.0166
0.4150	0.0417	0.0777	0.0158
0.4200	0.0433	0.0744	0.0150
0.4250	0.0449	0.0713	0.0143
0.4300	0.0466	0.0683	0.0136
0.4350	0.0483	0.0654	0.0129
0.4400	0.0501	0.0627	0.0123
0.4450	0.0519	0.0600	0.0117
0.4500	0.0537	0.0575	0.0111
0.4550	0.0556	0.0551	0.0106
0.4600	0.0575	0.0527	0.0101
0.4650	0.0595	0.0505	0.0096
0.4700	0.0615	0.0484	0.0091
0.4750	0.0636	0.0463	0.0087
0.4800	0.0656	0.0443	0.0082
0.4850	0.0678	0.0424	0.0078
0.4900	0.0699	0.0406	0.0074
0.4950	0.0721	0.0389	0.0071
0.5000	0.0744	0.0372	0.0067
S/N = 10.5 db			
0.3600	0.0211	0.0798	0.0176
0.3650	0.0221	0.0760	0.0166
0.3700	0.0232	0.0724	0.0157
0.3750	0.0243	0.0690	0.0149
0.3800	0.0255	0.0658	0.0141
0.3850	0.0267	0.0627	0.0133
0.3900	0.0279	0.0597	0.0126
0.3950	0.0291	0.0569	0.0119
0.4000	0.0304	0.0542	0.0112
0.4050	0.0318	0.0516	0.0106
0.4100	0.0332	0.0491	0.0100
0.4150	0.0346	0.0468	0.0095
0.4200	0.0360	0.0446	0.0090
0.4250	0.0375	0.0424	0.0085
0.4300	0.0391	0.0404	0.0080
0.4350	0.0406	0.0385	0.0076

0.4400	0.0423	0.0366	0.0072
0.4450	0.0439	0.0349	0.0068
0.4500	0.0456	0.0332	0.0064
0.4550	0.0474	0.0316	0.0061
0.4600	0.0492	0.0301	0.0057
0.4650	0.0510	0.0286	0.0054
0.4700	0.0529	0.0272	0.0051
0.4750	0.0548	0.0259	0.0048
0.4800	0.0567	0.0247	0.0046
0.4850	0.0588	0.0235	0.0043
0.4900	0.0608	0.0223	0.0041
0.4950	0.0629	0.0213	0.0039
0.5000	0.0650	0.0202	0.0037

S/N = 11.0 db

0.3600	0.0163	0.0487	0.0108
0.3650	0.0172	0.0461	0.0101
0.3700	0.0181	0.0436	0.0095
0.3750	0.0191	0.0413	0.0089
0.3800	0.0201	0.0391	0.0084
0.3850	0.0211	0.0370	0.0079
0.3900	0.0222	0.0350	0.0074
0.3950	0.0233	0.0331	0.0069
0.4000	0.0244	0.0313	0.0065
0.4050	0.0256	0.0296	0.0061
0.4100	0.0268	0.0280	0.0057
0.4150	0.0281	0.0265	0.0054
0.4200	0.0294	0.0251	0.0051
0.4250	0.0307	0.0237	0.0047
0.4300	0.0321	0.0224	0.0045
0.4350	0.0335	0.0212	0.0042
0.4400	0.0350	0.0201	0.0039
0.4450	0.0365	0.0190	0.0037
0.4500	0.0380	0.0179	0.0035
0.4550	0.0396	0.0170	0.0033
0.4600	0.0413	0.0160	0.0031
0.4650	0.0430	0.0151	0.0029
0.4700	0.0447	0.0143	0.0027
0.4750	0.0465	0.0135	0.0025
0.4800	0.0483	0.0128	0.0024
0.4850	0.0502	0.0121	0.0022
0.4900	0.0521	0.0114	0.0021
0.4950	0.0540	0.0108	0.0020
0.5000	0.0561	0.0102	0.0018

S/N = 11.5 db

0.3600	0.0123	0.0280	0.0062
0.3650	0.0130	0.0263	0.0058
0.3700	0.0138	0.0247	0.0054
0.3750	0.0146	0.0232	0.0050
0.3800	0.0154	0.0218	0.0047
0.3850	0.0163	0.0205	0.0043
0.3900	0.0172	0.0192	0.0041
0.3950	0.0182	0.0181	0.0038

0.4000	0.0191	0.0169	0.0035
0.4050	0.0201	0.0159	0.0033
0.4100	0.0212	0.0149	0.0031
0.4150	0.0223	0.0140	0.0028
0.4200	0.0234	0.0132	0.0027
0.4250	0.0246	0.0123	0.0025
0.4300	0.0258	0.0116	0.0023
0.4350	0.0271	0.0109	0.0021
0.4400	0.0284	0.0102	0.0020
0.4450	0.0297	0.0096	0.0019
0.4500	0.0311	0.0090	0.0017
0.4550	0.0325	0.0084	0.0016
0.4600	0.0340	0.0079	0.0015
0.4650	0.0355	0.0074	0.0014
0.4700	0.0371	0.0070	0.0013
0.4750	0.0387	0.0065	0.0012
0.4800	0.0404	0.0061	0.0011
0.4850	0.0421	0.0057	0.0011
0.4900	0.0439	0.0054	0.0010
0.4950	0.0457	0.0050	0.0009
0.5000	0.0476	0.0047	0.0009

S/N = 12.0 db

0.3600	0.0090	0.0151	0.0033
0.3650	0.0096	0.0140	0.0031
0.3700	0.0102	0.0131	0.0028
0.3750	0.0108	0.0122	0.0026
0.3800	0.0115	0.0113	0.0024
0.3850	0.0122	0.0105	0.0022
0.3900	0.0130	0.0098	0.0021
0.3950	0.0138	0.0091	0.0019
0.4000	0.0146	0.0085	0.0018
0.4050	0.0154	0.0079	0.0016
0.4100	0.0163	0.0074	0.0015
0.4150	0.0173	0.0069	0.0014
0.4200	0.0182	0.0064	0.0013
0.4250	0.0192	0.0059	0.0012
0.4300	0.0203	0.0055	0.0011
0.4350	0.0214	0.0051	0.0010
0.4400	0.0225	0.0048	0.0009
0.4450	0.0237	0.0044	0.0009
0.4500	0.0249	0.0041	0.0008
0.4550	0.0261	0.0038	0.0007
0.4600	0.0275	0.0036	0.0007
0.4650	0.0288	0.0033	0.0006
0.4700	0.0302	0.0031	0.0006
0.4750	0.0317	0.0029	0.0005
0.4800	0.0331	0.0027	0.0005
0.4850	0.0347	0.0025	0.0005
0.4900	0.0363	0.0023	0.0004
0.4950	0.0379	0.0022	0.0004
0.5000	0.0396	0.0020	0.0004

%********** end of data **********

LIST OF REFERENCES

1. L. D. Landau and E. M. Lifshitz, *Mechanics*, 3rd ed, Pergamon Press, New York, 1976, reprinted with correction, 1988.

2. G. Baym, *Lectures on Quantum Mechanics*, Benjamin, New York, 1969.

3. H. M. Lee, private communication.

4. L. D. Landau and E. M. Lifshitz, *Fluid Mechanics*, Pergamon Press, New York, 1959.

5. R. G. Fleagle and J. A. Businger, *An Introduction to Atmospheric Physics*, 2nd ed., Academic Press, New York, 1980.

6. AVANTEK, *Solid State Microwave Components Product Guide*, Jan 1988.

7. R. P. Feynmen and M. Sands, *The Feynman Lectures on Physics*, Vol. 2, Addison Wesley, Reading, Mass., 1964.

8. V.I. Arnold, *Mathematical Methods of Classical Mechanics*, Springer-Verlag, pp. 60-68, 1978.

9. Merrill I. Skolnik, *Radar Handbook*, McGraw-Hill Book Inc., 1970.

10. John N. Little and Loren Shure, *Signal Processing Toolbox for use with MATLAB*, The Math Works, Inc., Aug 29, 1989.

11. *Handbook of Chemistry and Physics*, 54th ed., The Chemical Rubber Company, 1973-1974.

12. Richard S. Shsvell, Stanford University, *Fumdamentals of Flight*, 2nd ed., pp. 66-76, Prentice Hall, Inc., 1989.

13. Donald E. Kerr, *Propagation of Short Radio Waves*, IEE Electromagnetic Waves series 24, Peter Peregrinus Ltd., 1987.

14. EREPS: *Computer Program for Evaporation Propagation*, Naval Ocean Systems Center. Patent 4,125.893. 1987.

15. Hall M. P. M., *Effects of the Troposphere on Radio Communication*. Peter Peregrinus Ltd, 1979.

INITIAL DISTRIBUTION LIST

		No. Copies
1.	Defense Technical Information Center Cameron Station Alexandria, VA 22304-6145	2
2.	Library, Code 0142 Naval Postgraduate School Monterey, CA 93943-5002	2
3.	Chairman, Code 62 Department of Electrical and Computer Engineering Naval Postgraduate School Monterey, CA 93943-5000	1
4.	Professor R.W. Adler, Code 62Ab Naval Postgraduate School Monterey, CA 93943-5000	1
5.	Professor Hung-Mou Lee, Code 62LH Naval Postgraduate School Monterey, CA 93943-5000	10
6.	Materiel Evaluation & Test Serivce Library P.O.Box 90502, Nan-Kan Taipei, Taiwan, R.O.C..	2
7.	Ta-Fu Proving Ground Library P.O. Box 90502-1, Ta-Fu, I-Lan Taiwan, R.O.C.	2
8.	Chung-Cheng Institute of Technology, Main Library P.O. Box 8243, Ta-Hsi, 33500, Tao-Yuan Taiwan, R.O.C.	1
9.	Yen-Chun Feng 7, Lane 72, Tzu-Lin, Chin-Tan, 23180 Sin-Tien County, Taipei, Taiwan, R.O.C.	3
10.	Yan-Huang Wu SMC 4805 Naval Postgraduate School Monterey, CA 93943-5000	5

Thesis
F25466 Feng
c.1 CW projectile tracking
range analysis.